EFFECT OF WATER TEMPERATURE ON THE IMMUNE RESPONSE OF AMERICAN LOBSTER (*HOMARUS AMERICANUS*) EXPERIMENTALLY INFECTED WITH WHITE SPOT SYNDROME VIRUS

A Thesis

Submitted to the Graduate Faculty

In Partial Fulfillment of the Requirements

For the Degree of

Master of Science

In the Department of Biomedical Sciences

Faculty of Veterinary Medicine

University of Prince Edward Island

Louise-Marie Roux

Charlottetown, P.E.I.

April 2017

THESIS/DISSERTATION NON-EXCLUSIVE LICENSE

Family Name: **Roux**	Given Name, Middle Name (if applicable): **Louise-Marie, Danielle**
Full Name of University: **University of Prince Edward Island**	
Faculty, Department, School: **Faculty of Veterinary Medicine, Department of Biomedical Sciences, UPEI**	
Degree for which thesis/dissertation was presented: **Master of Science**	Date Degree Awarded: **May 2017**
Thesis/dissertation Title: **Effect of water temperature on the immune response of American lobster (*Homarus americanus*) experimentally infected with white spot syndrome virus**	

In consideration of my University making my thesis/dissertation available to interested persons, I, Louise-Marie Roux, hereby grant a non-exclusive, for the full term of copyright protection, license to my University, University of Prince Edward Island:

(a) to archive, preserve, produce, reproduce, publish, communicate, convert into any format, and to make available in print or online by telecommunication to the public for non-commercial purposes;
(b) to sub-license to Library and Archives Canada any of the acts mentioned in paragraph (a).

I undertake to submit my thesis/dissertation, through my University, to Library and Archives Canada. Any abstract submitted with the thesis/dissertation will be considered to form part of the thesis/dissertation.

I represent that my thesis/dissertation is my original work, does not infringe any rights of others, including privacy rights, and that I have the right to make the grant conferred by this non-exclusive license.

If third party copyrighted material was included in my thesis/dissertation for which, under the terms of the *Copyright Act*, written permission from the copyright owners is required I have obtained such permission from the copyright owners to do the acts mentioned in paragraph (a) above for the full term of copyright protection

I retain copyright ownership and moral rights in my thesis/dissertation, and may deal with the copyright in my thesis/dissertation, in any way consistent with rights granted by me to my University in this non-exclusive license.

I further promise to inform any person to whom I may hereafter assign or license my copyright in my thesis/dissertation of the rights granted by me to my University in this non-exclusive license.

Signature:	**Date: April 11th 2017**

University of Prince Edward Island
Faculty of Veterinary Medicine
Charlottetown

CERTIFICATION OF THESIS WORK

We, the undersigned, certify that Louise-Marie Roux, candidate for the degree of Master of Science has presented his/her thesis with the following title:

EFFECT OF WATER TEMPERATURE ON THE IMMUNE RESPONSE OF AMERICAN LOBSTER (*Homarus americanus*) EXPERIMENTALLY INFECTED WITH WHITE SPOT SYNDROME VIRUS

that the thesis is acceptable in form and content, and that a satisfactory knowledge of the field covered by the thesis was demonstrated by the candidate through an oral examination held on: April 11th 2017.

Examiners

Dr. Luis Bate (Chair) _____

Dr. Spencer Greenwood _____

Dr. Glenda Wright _____

Dr. Mark Fast _____

Dr. Andy Tasker _____

Date:

Abstract

Water temperature influences basic life history traits of the American lobster (*Homarus americanus*) such as survival, growth and reproduction. Yet, relatively little is known about the effects of water temperature on the immune response of *H. americanus*. White spot syndrome virus (WSSV) is currently one of the largest impediments to the shrimp aquaculture industry worldwide. The World Organization for Animal Health (Office International de Epizootic; OIE) lists WSSV as a notifiable disease with the potential to infect all crustacean decapods. This project investigates the constraints imposed by a range of temperatures (10 ^{o}C, 15 ^{o}C, 17.5 ^{o}C, 20 ^{o}C) on the clinical, tissue and molecular immune responses of *H. americanus* experimentally infected with WSSV. Haemocyte concentration and qPCR testing of haemolymph were used to monitor the host's clinical response over time and to determine presence of viral infection, respectively. A decrease in clinical condition of *H. americanus* was observed at 17.5 ^{o}C and 20 ^{o}C but not at 10 ^{o}C and 15 ^{o}C. WSSV-qPCR revealed viral amplification was associated with higher ambient temperature. A combination of light and electron microscopy, as well as qPCR testing of various tissues was used to elucidate changes within infected *H. americanus* at the various temperatures. Of the 11 host tissues examined, hypertrophied nuclei (indicative of WSSV infection) were most easily identifiable within the antennal gland and intestine of infected animals at warmer temperatures (17.5 ^{o}C and 20 ^{o}C). At colder temperatures (10 ^{o}C) no WSSV associated histopathological changes were identified in any of the examined tissues. Electron microscopy was used to explore the general ultrastructure of the antennal gland and the confirmed presence of WSSV rod-shaped and enveloped virions. In infected animals the two main regions of the antennal gland, the coelomosac and labyrinth, contained randomly distributed infected nuclei with marginated host chromatin and WSSV virions in various stages of replication. In marine decapods, the antennal gland is involved in osmoregulation and excretion suggesting that the antennal gland may be a preferred site for WSSV viral replication and inclusion within the excretory product. Lastly, a lobster specific microarray was used to monitor transcriptomic changes across 14,592 genes during viral infection at the different temperatures. Using one-way ANOVA analyses, a total of 717 genes were identified as significantly differentially expressed between infected and control *H. americanus* at the various temperatures. Differentially expressed genes included, ribosomal proteins (L27a, L13, L11, and L39), mitogen-activated protein kinase organizer 1, prolyl-4-hydroxylase-alpha, laminin subunit gamma-3, short-chain dehydrogenase and acute phase serum amyloid A. Microarray results were verified using RT-qPCR. Clinical, tissue and molecular immune results from this study provide a thorough assessment of the impact of temperature and WSSV in *H. americanus*. The use of a range of approaches and experimental temperatures is critical for broadening our understanding of how temperature influences host pathogen interactions in the economically important American lobster *H. americanus*.

Acknowledgements

This project could not have been completed without the help of many individuals.

First and foremost, I thank my co-supervisors Spencer Greenwood and Phil Byrne. Thank you Phil for starting things off, for introducing me to the world of government research and seeing the potential within me as a new researcher. You carry a wealth of information and I am honoured to have learned a small piece of it. Spencer, thank you for always being invested in my personal and professional success, for providing me with ample opportunities to discuss my research and for the light heartedness that accompanied rock star Fridays. I thank you both immensely for being incredibly patient, understanding and supportive as I worked towards completing my degree. It was not an easy journey. As co-supervisors and mentors, you both inspire me to be the most articulate, meticulous and professional researcher that I can be.

I also thank my committee members Glenda Wright, Fraser Clark and Mark Fast for their patience, guidance and technical assistance. You have been wonderful professors, mentors and colleagues and I am grateful to have worked alongside, and learned from all of you.

I would also like to thank the AVC Lobster Science Centre and the Gulf Biocontainment Unit for supporting this collaboration and allowing me to use both facilities. Thank you to the wonderful staff in each facility (Haili Wang, Phyllis Dixon and Greg McCallum). Thank you also the AVC Electron Microscopy laboratory and Dorota Wadowska for all your technical training and assistance.

Lastly, I would like to thank my friends. Those who I have met in PEI (Ari, Laura, Ellen, Ryan, Marc, Alden, Dan), those who supported me from afar (Meghan, Becky, Maddie, Jess, Katie), my fellow graduate students (Denise, Bob, Laura, Logan) and my biggest supporters (members of the LMR fan club), Kevin Hodgson, Katie O'Hanley, and Matt MacFarlane.

I am truly grateful for all of you.

Dedication

My greatest achievements have been the result of Mama and Papa Roux instilling in me the belief that I can do anything.

For that, I dedicate this thesis to them.

Table of Contents

List of Tables

List of Figures

List of Abbreviations

α2-m	α2-macroglobulin
ALF	Anti-lipopolysaccharide factor
AMP	Antimicrobial peptide
ANOVA	Analysis of variance
AQC3	Aquatic containment level 3
aRNA	Reference antisense RNA
ASW	Artificial seawater
BGBP	β-1,3-glucan binding protein
cDNA	Complementary deoxyribonucleic acid
CFIA	Canadian Food Inspection Agency
CO_2	Carbon Dioxide
CpG	5'-C-phosphate-G-3'
C_T	Cycle threshold
dFADD	*Drosophila* Fas-associated death domain-containing protein
Dif	Dorsal-related immunity factor
DMSO	Dimethyl sulfoxide
DNA	Deoxyribonucleic acid
Dome	Domeless
DOPA	3,4,-dihydroxy-L-phenylalanine
DSCAM	Down syndrome cell adhesion molecules
EIPE75	Ecdysone-inducible protein E75
ESD	Epizootic shell disease
EST	Expressed Sequence Tag
EtOH	Ethyl alcohol
FOM	Figure of merit
GAC	Granular activated charcoal
GBU-AAHL	Gulf Biocontainment Unit-Aquatic Animal Health Laboratory
GFP	Green Fluorescent Protein
GNBP	Gram-negative binding protein
Hop	Hopscotch
HSP	Heat shock protein
ie1	Immediate early 1
Imd	Immune deficiency
IPCC	Intergovernmental Panel on Climate Change
Iκ-B	Inhibitor of κ-B
JAK-STAT	Janus kinase-signal transducer and activator of transcription
LC50	Lethal Concentration Required to Kill 50% of Population
LFA	Lobster-fishing area

LGBP	Lipopolysaccharide and glucan binding protein
LOWESS	Locally weighted linear regression
LPS	Lipopolysaccharides
LTA	Lipoteichoic acid
MIH	Moult-inhibiting hormone
miRNA	MicroRNA
MMAM	Modified marine axenic medium
MyD88	Myeloid differentiation primary response gene 88
NAAHP	National Aquatic Animal Health Program (Canada)
NBF	Neutral buffered formalin
NF-κB	Nuclear factor kappa-light-chain-enhancer of activated B cells
NRQ	Normalized relative quantities
NRTC	No reverse transcriptase control
NTC	No template control
OIE	World Organization for Animal Health (Office International des Epizooties)
PAMP	Pathogen-associated molecular pattern
PaV1	*Panulirus argus* virus 1
PBS	Phosphate buffered saline
pCO_2	Partial pressure of carbon dioxide
PEA	Phenylethyl alcohol media
PGN	Peptidoglycans
PGRP	Peptidoglycan recognition protein
PI	Post inoculation
PMT	Photo multiplier tube
PO	Phenoloxidase
PO	Propylene oxide
PPAE	Prophenoloxidase activating enzyme
ppt	Parts per thousand
ProPO	Prophenoloxidase
PRP	Pattern recognition proteins
PstDNV	*Penaeus stylirostris Brevidensovirus*
qPCR	Quantitative Polymerase Chain Reaction
RGD	Arg-Gly-Asp
RNA	Ribonucleic acid
RNAi	Interfering RNA
RT-qPCR	Real Time-quantitative Polymerase Chain Reaction
SAA	Acute phase serum amyloid A
SH2	SRC homology 2
siRNA	Small interfering RNA
SPF	Specific pathogen free

SPH	Serine proteinase homologues
TAB2	TAK1-binding protein 2
TAK1	Transforming growth factor beta-activated kinase 1
TGase	Transglutaminase
THC	Total haemocyte concentration
Tiff	Tagged information file format
TLR	Toll-like receptor
TPS	Trehalose-phosphate synthase
TSB	Trypticase soy broth
WAP	Whey-acidic-protein
WSSV	White spot syndrome virus
YO	Y-Organ/Moulting gland

1.0 GENERAL INTRODUCTION

1.1 The Canadian Lobster Fishing Industry

The American lobster, *Homarus americanus*, is one of Canada's most profitable marine commodities. *H. americanus* inhabits coastal waters that span from North Carolina, USA increasing in latitude to Northern Newfoundland, Canada (Aiken and Waddy, 1986). The Canadian lobster fishery is situated over much of the lobster's northern geographic range, but is primarily based in Nova Scotia, New Brunswick and Prince Edward Island with smaller fisheries also existing in Quebec and Newfoundland and Labrador. In 2014, 92 000 metric tonnes of live *H. americanus* was harvested from Atlantic Canada (Fisheries and Oceans Canada, 2016). The majority (78%) of harvested *H. americanus* is sold within Canada and exported to the US, however it is also shipped to over 50 countries worldwide (Fisheries and Oceans Canada, 2015). *H. americanus* exports average approximately one billion dollars per year (Fisheries and Oceans Canada, 2015).

Exploitation of the fishery is of major concern for the Canadian government (Fisheries and Oceans Canada, 2013). *H. americanus* population parameters such as health, age distribution, and natural mortality rates are difficult to acquire, which makes forecasting trends in abundance a formidable endeavour (Wahle et al., 2004). In an attempt to offset this, Fisheries and Oceans Canada regulates the fishery through "input control," placing limits on fishing efforts. The fishery is divided into 45 distinct lobster-fishing areas (LFA's) each with a tailored integrated fisheries management plan governing fishing seasons, fishing licenses, trap allocation and harvest size (Fisheries and Oceans Canada, 2013).

1.2 Lobster Biology

H. americanus is a member of the largest crustacean order, Decapoda (Barker and Gibson, 1977). It has a segmented body comprised of a head, thorax, and abdomen (Factor, 1995). The head and thorax region are fused together forming a cephalothorax, which is covered by the carapace. The cephalothorax contains the animal's sensory, feeding and locomotory appendages such as the antennae (antennae and antennules), mouthparts (mandibles, maxillae and maxillipeds), and walking legs (pereiopods), respectively (Factor, 1995). The abdomen bears locomotory and reproductive appendages, such as the swimmerets (pleopods) and the tail fan (Factor, 1995).

1.2.1 Mating and Spawning

H. americanus is dioecious (Talbot and Helluy, 1995). Gross external features of morphology, such as position of gonopores, form of first pleopods, carapace size, and shape of sternal spines can be used to distinguish the sexes (Talbot and Helluy, 1995). In *H. americanus,* mating typically occurs during the late summer months, following the female moult, when a male transfers his spermatophore to a female who stores it within the seminal receptacle until it is required for fertilization (Talbot and Helluy, 1995). During fertilization the females eggs are extruded and adhere to the underside of the abdomen, where they incubate over winter for nine to twelve months (Helluy and Beltz, 1991; Templeman, 1940). The eggs undergo embryonic development into nauplii while attached to the female (Helluy and Beltz, 1991). Females tend to moult and mate one summer, with fertilization occurring the following summer (Aiken and Waddy, 1986).

1.2.2 Life Cycle

H. americanus exhibit a complex life cycle that is divided into a series of pelagic and benthic phases (Factor, 1995). Nauplii are hatched from mid-May through early September as free-swimming, pre-larvae (Ennis, 1995). Pre-larvae rapidly undergo development into the first of three larval stages. The three larval stages of *H. americanus* (Stage I, II, III) are free-swimming, planktonic and inhabit warmer (15 ^{o}C - 25 ^{o}C) pelagic zones of the ocean (Factor, 1995). During the final larval stage, stage III, larvae undergo a metamorphosis into post-larval stage IV marking an ecological transition from the planktonic water column to the benthic environment (Ennis, 1995). Duration of pelagic larval stages can vary from two to eight weeks depending on environmental conditions (Aiken and Waddy, 1986). The moult following post-larval stage IV yields the first of three juvenile stages. Juveniles are small in size but resemble adults in form and are entirely benthic, relying heavily on their shelter for protection (Factor, 1995). As the animal increases in size, it becomes better equipped to defend itself from predators and decreases its shelter dependence (Lawton and Lavalli, 1995). The onset of physiological but not functional sexual maturity marks adolescence whereas completion of a successful mating event marks the adult phase (Lawton and Lavalli, 1995). The *H. americanus* life cycle typically requires 5-8 years before the animal is of legal minimum size to be commercially harvested (Waddy et al., 1995).

1.2.3 Growth and Moulting

H. americanus are indeterminate growers since they continue moulting throughout their entire lifespan. Moulting is divided into a series of inter-moult, pre-

moult, ecdysis and post-moult phases, that are further subdivided into stages A, B, C1-3, C4, D, E (Wahle and Fogarty, 2006). Stage E, is ecdysis, where ecdysial sutures break and the exoskeleton is shed (Wahle and Fogarty, 2006). Stage A, B, and C1-3, define the post-moult phase when the soft lobster uses calcium stores (gastroliths) to harden critical appendages (Wahle and Fogarty, 2006). Stage C4 marks the beginning of the inter-moult phase, when the new exoskeleton is at maximum rigidity (Wahle and Fogarty, 2006). Inter-moult lasts until physiological changes associated with the next moult begin. The pre-moult period, stage D, occurs when the new cuticle begins to form under the exoskeleton. During pre-moult the shell is decalcified and shell constituents are absorbed and stored for later reabsorption (Ahearn et al., 2004). Stage D is also when the lobster begins ingesting water in preparation of the final stage, ecdysis (Waddy et al., 1995; Wahle and Fogarty, 2006). During moulting *H. americanus* can increase its volume up to 50% (Waddy et al., 1995). Moulting occurs frequently (several times per year) in the first 5-7 years of the lobsters' life. After which, *H. americanus* tend to moult once per year (males) or every two years (female) typically during the summer months (Waddy et al., 1995).

Ecdysteroid, a hormone synthesized from cholesterol and produced in the moulting gland (Y-organ or YO), is largely responsible for initiating the moulting sequence (Devaraj and Natarajan, 2006). Ecdysteroid levels are negatively regulated by the presence of the moult-inhibiting hormone (MIH) (Mykles, 2011). MIH peaks in haemolymph during the inter-moult phase and decreases during pre-moult, in turn increasing ecdysteroid levels, transitioning the animal to moult (Chang and Mykles,

2011).

1.2.4 Genomics

Genomic resources for *H. americanus* are slowly growing (Clark and Greenwood, 2016; McGrath et al., 2016). However, *H. americanus* still lacks a whole published genome, with the exception of the mitochondrial genome which has been sequenced (Kim et al., 2011). Sequencing of crustacean genomes remains a daunting endeavour given that many new crustacean sequences are not found in public DNA sequence databases and that there exists large evolutionary distance between species whose genomes have been sequenced (other insects) and crustaceans (Richards, 2015). Clark and Greenwood (2016) recently annotated a significant number of crustacean immune genes (with an emphasis on *H. americanus*) which forms the basis for the immune processes described later in this thesis. While the Clark and Greenwood (2016) paper functions as a great resource it is worth noting that the transcript number in total is likely over estimated given that the total number of genes is still unknown.

1.3 Environmental Variables

The geographical range of *H. americanus* presents the animal with a wide array of environmental conditions (Aiken and Waddy, 1986). The interactions between these environmental variables, whether in combination or individually, and the biological processes of *H. americanus* are complex (Aiken and Waddy, 1986).

1.3.1 Salinity

H. americanus are considered osmoconformers in ideal environments but weak osmoregulators near salinity extremes (Dall, 1970; Jury, 1994; McMahon, 1995). *H. americanus* are typically limited to coastal waters where salinities remain above 25 parts per thousand (ppt); however, spring run-off and heavy rainfall events can expose them to varying salinities (Dall, 1970; Jury, 1994). The lethal salinity limit for *H. americanus* is dependent on temperature and dissolved oxygen (McMahon, 1995). At cold temperatures (5 °C) and increased dissolved oxygen concentrations (6.4 mg O_2/L) a lethal salinity of 6 ppt has been recorded (McLeese, 1956). Warmer water temperatures and low salinities (below 15 ppt) are metabolically stressful and energetically costly to *H. americanus* likely resulting in death (Mercaldo-Allen and Kuropat, 1994). The favoured salinity of *H. americanus* is 30-31 ppt (McMahon, 1995).

1.3.2 Dissolved Oxygen

Atmospheric exchange, upwelling, respiration, photosynthesis, temperature and salinity can all affect the availability of dissolved oxygen in the environment (Davis, 1975). *H. americanus* are surprisingly tolerant of low oxygen concentrations; with the exception of when the animal is approaching moulting, as this is when oxygen consumption peaks (Mercaldo-Allen and Kuropat, 1994). The lower lethal oxygen level ranges from 0.2 mg O_2/L at 5 °C to 1.2 mg O_2/L at 25 °C (Aiken and Waddy, 1986; Mercaldo-Allen and Kuropat, 1994). At lower oxygen concentrations, *H. americanus* decrease oxygen consumption while increasing branchial water flow and increasing oxygen transport through an increase in the

oxygen affinity of the respiratory pigment haemocyanin (Mercaldo-Allen and Kuropat, 1994).

1.3.3 Nitrogen

The main excretory product in *H. americanus* is nitrogen waste ammonia. Lobsters are often housed in recirculating water systems, for experimental and commercial use, where concentrations of ammonia can accumulate and become toxic if uncontrolled (Young-Lai et al., 1991). Larvae and post-larvae are the most sensitive to ammonia with an LC_{50} value of 1.4 mg/L (Mercaldo-Allen and Kuropat, 1994). Adult *H. americanus* are more tolerant to ammonia as tolerance increases with development (Mercaldo-Allen and Kuropat, 1994). Concentrations less than 0.14 mg/L are considered optimal for culture facilities (Ennis, 1995). Ammonia toxicity is less of a concern in the marine environment as it is very rare that ammonia levels would reach a critical high that would cause mortality (Ennis, 1995).

1.3.4 pH

Historically, ocean pH was slightly basic at 8.2; however, over the past two decades it has experienced a drop of 0.1 pH units leaving the current ocean pH to be 8.1 (Meehl et al., 2007). As CO_2 emissions continue to enter our oceans, pH is predicted to decline to 7.7 by the year 2100 (Meehl et al., 2007). A decrease in ocean pH correlates to lower concentrations of carbonate ions available for the biosynthesis of calcium carbonate, suggesting that marine calcifiers, like *H. americanus*, may experience difficulty hardening their shells (Green et al., 2014; Keppel et al., 2012). Keppel et al. (2012) found that larval *H. americanus* reared in acidified seawater (pH 7.7) conditions have significantly shorter carapace lengths

and slowed larval development relative to controls (Keppel et al., 2012). A more recent study, conducted by Waller et al., (2016) examined the interactive effects of elevated temperature and pCO_2 in larval *H. americanus* and found that increased pCO_2 treatments caused no significant change in larval survival or development time but a significant increase in feeding rates, swimming speeds and carapace length relative to controls (Waller et al., 2016).

1.3.5 Temperature

H. americanus can be exposed to temperature extremes ranging from 0 ^{o}C to 30 ^{o}C (Aiken and Waddy, 1986; Lagerspetz and Vainio, 2006). As a result, different life stages of the animal demonstrate different thermal tolerances and preferences. Embryos require temperatures between 10 ^{o}C and 20 ^{o}C for development, whereas larvae require waters between 16 ^{o}C and 25 ^{o}C for optimal growth (Mercaldo-Allen and Kuropat, 1994; Waddy et al., 1995). Juveniles and adults can tolerate the broadest temperature range, with various studies reporting temperatures spanning from approximately 6 ^{o}C to 22 ^{o}C (Harding, 1992; Mercaldo-Allen and Kuropat, 1994; Waddy et al., 1995). Variable water temperatures directly impact *H. americanus*, as temperatures outside of the ideal thermal limit pose challenges for biological, physiological, molecular and immunological processes. It must also be noted that often suboptimal environments result in secondary stress impacts observed in *H. americanus*.

1.3.5.1 Larval Development, Growth and Reproduction

In *H. americanus* embryogenesis and larval development are heavily influenced by water temperature. Egg development is two months longer in colder waters compared to warmer waters, and at temperatures below 6 ^{o}C egg development is rare (Talbot and Helluy, 1995). In laboratory conditions, *H. americanus* larvae raised at 19 ^{o}C develop twice as fast as those raised at 16 ^{o}C (Waller et al., 2016). Additionally, larvae hatched in temperatures below 5 ^{o}C rarely survive to post-larval stage IV and moulting to juveniles does not occur below 10 ^{o}C (Ennis, 1995). In adults temperatures below 6 ^{o}C inhibit moulting all together (Waddy et al., 1995). The most rapid growth rate in *H. americanus* adults occurs when lobsters are held between 20 ^{o}C and 22 ^{o}C (Waddy et al., 1995). In *H. americanus* growth rate increases as a function of temperature throughout the animal's optimum temperature range and quickly begins to decrease when near the thermal limits (Green et al., 2014).

Temperature also stimulates early ovarian development in female *H. americanus*, causing reproductive maturity to occur earlier at higher temperatures (Green et al., 2014; Pugh et al., 2013). Egg extrusion and hatching are regulated by temperature in that temperatures below 5 ^{o}C cause females to delay egg extrusion in favour of warmer waters (Aiken and Waddy, 1986). Waters around 12 ^{o}C are required in order to ensure larval survival upon hatching and release (Aiken and Waddy, 1986; Green et al., 2014).

1.3.5.2 Physiology

Changes in environmental temperatures alter ion channels, neural circuits and contractile machinery in *H. americanus* (Qadri et al., 2007; Worden et al., 2006). For example, serotonin, a neurohormone known to regulate cardiac performance in *H. americanus*, is temperature dependent which contributes to the increased heartbeat frequency observed at warmer temperatures (Worden et al., 2006). Temperature is also inversely related to haemolymph pH, where abrupt increased temperatures can cause haemolymph acidosis, which in *H. americanus* can be compensated by an increase in ventilation rate (Qadri et al., 2007). Waller et al. (2016) also found increased oxygen consumption rates in larval *H. americanus* reared at warmer temperatures (19 ^{o}C) compared to colder temperatures (16 ^{o}C). Larvae at warmer temperatures also experienced increased growth rates suggesting that increased oxygen consumption rates may be the result of increased metabolic requirements at warmer temperatures (Waller et al., 2016).

1.3.5.3 Genes and Proteins

Temperature can also impact the rate of transcription of many genes (Hazel and Prosser, 1974). In *H. americanus* previous studies have examined the effect of thermal stress on heat shock protein (HSP) and polyubiquitin gene expression (Chang, 2005; Spees et al., 2002). HSPs are a highly conserved class of proteins that play an important role in protein stabilization (Usman et al., 2014). HSP 90 mRNA expression in muscle tissue has been found to increase during acute thermal stress in *H. americanus* (Chang, 2005). Polyubiquitin gene expression has been found to increase with thermal stress in hepatopancreas tissue, but not in muscle tissue

(Chang, 2005). Polyubiquitin is considered an indicator of protein degradation or permanent damage. As proteins become damaged, a larger number of polyubiquitin transcripts are required to support the degradation pathway (Spees et al., 2002). Results from Spees et al. (2002) suggest that different tissues may be more or less susceptible to protein degradation from thermal stress (Chang, 2005; Spees et al., 2002). Similarly, Edge et al. (2005), found 6 genes differentially expressed during thermal stress exposure in the Mountainous Star coral *Montastraea faveolata*. Carbonic anhydrase and three ribosomal genes showed down-regulation in response to increased temperature, indicating decreased ribosomal function at warmer temperatures in *M. faveolata* (Edge et al., 2005).

1.3.5.4 Immune Function

Increased temperatures, outside of the preferred thermal range, negatively influence the ability of *H. americanus* to deal with disease (Maynard et al., 2016; Steenbergen et al., 1978). Steenbergen et al., (1978) found that at temperatures above 22 ^{o}C *H. americanus* haemocytes show a significant decrease in their ability to phagocytize the pathogen *Aerococcus viridans* var. *homari*. More recently, Groner et al., (2016) found that susceptibility to epizootic shell disease (ESD) is also influenced by temperature, with disease being most prevalent in warmer temperatures around 20-22 ^{o}C.

In other marine invertebrates significant interaction occurs between temperature and immunocompetence (Cheng and Chen, 1998; Hernroth et al., 2012; Parry and Pipe, 2004; Vargas-Albores et al., 1998). Mussels *Mytilus edulis*, challenged with the bacterial pathogen *Vibrio tubiashii*, show a decrease in

haemocyte phagocytic function in warmer temperatures relative to controls (Parry and Pipe, 2004). In the giant freshwater prawn *Macrobrachium rosenbergii*, increased levels of mortality are observed in prawns challenged with an *Enterococcus*-like bacterium at high temperature and pH levels (Cheng and Chen, 1998). In the yellowleg shrimp *Penaeus californiensis*, increased water temperature correlates with a decrease in total haemocytic prophenoloxidase (proPO) (Vargas-Albores et al., 1998). Lastly, in the Norway lobster *Nephrops norvegicus*, negative impacts of ocean acidification on the immune system are exacerbated at increased temperatures, with a decrease in phagocytic capacity occurring at warmer temperatures (Hernroth et al., 2012).

The fruit fly *Drosophila melanogaster,* provides insights into the relationship between temperature and immunity on a molecular level (Cataln et al., 2012; Linder et al., 2008). *D. melanogaster* infected with a gram-positive bacteria, show an increase in expression of immune genes, such as Spätzle, Metchnikowin and HSP 83, at colder temperatures compared to warmer temperatures, indicating a more active and efficient immune system may be present at colder temperatures in the species (Catalán et al., 2012; Linder et al., 2008).

1.4 Immunity

Immunity is commonly classified into two parts, the innate (natural) response and the acquired (adaptive) response (Jiravanichpaisal et al., 2006). Adaptive contributions from lymphocytes however, are absent in invertebrates as they lack true lymphocytes (Rowley and Powell, 2007). As a result, the immune systems of

invertebrates rely solely on innate responses; which are comprised of complex interactions between cellular and humoral mechanisms (Hauton, 2012).

In arthropods, the exoskeleton is the first line of defence against potential pathogens (Hillyer, 2015). However, moulting, injuries (resulting in cracks and breaks in the cuticle), and the alimentary canal (ingestion) provide portals of entry for pathogens to gain access to the host (Hillyer, 2015; Söderhäll and Cerenius, 1992). Once a pathogen enters a host, non-self recognition results in the activation of immune signalling pathways, proteolytic immune cascades, and cellular and humoral defence mechanisms (Jiravanichpaisal et al., 2006; Sritunyalucksana and Söderhäll, 2000; Vazquez et al., 2009).

1.4.1 Pathogen Recognition

Microorganisms contain pathogen-associated molecular patterns (PAMPs), which are highly conserved molecular signatures that are absent from multicellular organisms (Goto and Kurata, 2012) and enable pathogens to be recognized by the host. PAMPs consist of cell wall components, such as bacterial lipopolysaccharides (LPSs) and peptidoglycans (PGNs), lipoteichoic acid (LTA), fungal glucans, unmethylated CpG DNA, and at times viral double-stranded RNA and envelope proteins (Cerenius et al., 2010a; Vazquez et al., 2009).

Crustaceans have a variety of haemocyte and plasma derived proteins, molecules and receptors whose main functions are to identify and signal the presence of these PAMPs (Cerenius et al., 2010a). These are termed pattern recognition proteins (PRPs) such as lipopolysaccharide and glucan binding protein (LGBP), gram-negative binding protein (GNBP), β-1,3-glucan binding protein

(BGBP), peptidoglycan recognition protein (PGRP), masquerade-like proteins such as serine proteinase homologues (SPHs), Down syndrome cell adhesion molecules (DSCAMs) and lectins (Cerenius et al., 2010a).

LGBP and GNBP bind fungi and gram-negative bacteria, resulting in initiation of the Toll pathway and melanization (Cerenius et al., 2010a). BGBP actively binds to β-1, 3-glucans and can also initiate the proPO system (Cerenius et al., 2010a; Wang and Wang, 2013). Within the *H. americanus* transcriptome 605 GNBP, 1 LGBP, 8 BGBP, and 31 PGRP putative immune transcripts have been identified (Clark and Greenwood, 2016).

Masquerade-like SPHs identified in crayfish are primarily involved in proteolytic cascades resulting in production of opsonins and immune signalling (Cerenius et al., 2010b; Wang and Wang, 2013). Interestingly, a masquerade-like SPH in *Penaeus monodon* appears to be a multifunctional immune molecule showing binding affinity for LPS and displaying opsonic activity (Jitvaropas et al., 2009; Wang and Wang, 2013). The *H. americanus* transcriptome contains 1760 serine proteinase transcripts and 24 masquerade-like protein transcripts (Clark, 2014; Clark and Greenwood, 2016).

DSCAMs are immunoglobulin-related proteins that contain highly variable extracellular regions speculated to function as pathogen binding sites (Cerenius and Söderhäll, 2013; Wang and Wang, 2013). Traditionally invertebrate immunity has been considered void of hypervariable antibodies but the presence of DSCAM isoforms suggests otherwise (Cerenius and Söderhäll, 2013). In *H. americanus*, 33 DSCAM isoforms have been identified (Cerenius and Söderhäll, 2013; Clark, 2014;

Clark and Greenwood, 2016). In crayfish, bacterial challenges result in the production of DSCAM protein isoforms, which are believed to act both as a phagocytic receptor and as an opsonin (Cerenius and Söderhäll, 2013; Wang and Wang, 2013).

Lastly, lectins are proteins that recognize and bind to specific sugar moieties, typically found in the cell wall of fungi and bacteria (Cerenius et al., 2010a). Binding of lectins to microbial surfaces mediates binding between haemocyte surface and pathogen, in turn enhancing the removal of pathogens (Cerenius et al., 2010a). Of particular interest are two C-type lectins, present in *Litopenaeus vannamei Lv*CTL1, and *Penaeus monodon Pm*AV, which have been found to function in virus defence by binding to the white spot syndrome virus (WSSV) envelope protein VP28 (Cerenius et al., 2010a). Within the *H. americanus* transcriptome 45 C-type lectin transcripts, 2 C-type lectin receptor transcripts, 2 agglutinin biogenesis protein transcripts and a single agglutinin receptor transcript have been identified (Clark and Greenwood, 2016).

1.4.2 Immune Signalling

There are three well-characterized immune pathways in invertebrate immunity: Toll (or Toll-like), immune deficiency (Imd) and Janus kinase-signal transducer and activator of transcription (JAK-STAT) (Murdock et al., 2012). The activation of these pathways produces signal transduction cascades or proteolytic cascades that result in the production or release of transcription factors that trigger release of immune effector molecules (Murdock et al., 2014). The Toll and Imd pathways are responsible for the regulation of various antimicrobial peptide (AMP)

encoding genes, whereas JAK-STAT is involved in antiviral responses (De Gregorio et al., 2002; Liu et al., 2009).

1.4.2.1 Toll

Several components of the Toll pathway have been identified in the *H. americanus* transcriptome (Clark, 2014; Clark and Greenwood, 2016). Most notably, 970 Toll transcripts, 57 Spätzle transcripts, 73 Myeloid differentiation primary response gene 88 (MyD88), 22 Dorsal, and 14 tube transcripts (Clark and Greenwood, 2016). The Toll pathway is well characterized in *Drosophila*, where it is activated by the presence of gram-positive bacteria and fungi (De Gregorio et al., 2002). The binding of PGRP-SA or GNBP1 to PGN, or the binding of GNBP3 to fungal β-1, 3-glucans triggers activation of a serine proteinase cascade. The serine proteinase cascade mediates the cleavage of pro-Spätzle (an inactive proenzyme), into Spätzle (Cerenius et al., 2010a). Spätzle is the ligand that binds to the Toll-like receptor (TLR) protein present on the membrane of the host's immune cells (Hoffmann and Reichhart, 2002). The binding of Spätzle to TLR, results in an intracellular signalling cascade involving adapter proteins, MyD88, tube and kinase Pelle (Hoffmann and Reichhart, 2002). The TLR adapter complex signals to an inactive transcription factor of the nuclear factor kappa-light-chain-enhancer of activated B cells (NF-κB) family which kinase Pelle then complexes the degradation of the inhibitor of kappa B-like (Iκ-B) protein cactus, resulting in the nuclear translocation of the NF-κB-like transcription factors Dorsal and Dorsal-related immunity factor (Dif) (De Gregorio et al., 2002; Hoffmann and Reichhart, 2002).

Dorsal and Dif activate transcription of genes encoding antimicrobial peptides (Hoffmann and Reichhart, 2002).

1.4.2.2 Imd

The immune deficiency pathway acts against gram-negative bacteria (Hoffmann and Reichhart, 2002). In *Drosophila*, the pathway is initiated by the binding of PGN to a variety of PGRPs (Myllymäki et al., 2014). PGRP-LC is believed to be a primary component of Imd pathway activation (Choe et al., 2005; Myllymäki and Rämet, 2014). PGRP-LE, a soluble receptor present in the haemolymph, also plays a role in Imd activation by binding to PGN and transporting it to PGRP-LC (Myllymäki et al., 2014). The end product of the Imd pathway is Relish, a NF-κB-like transactivator (Hoffmann and Reichhart, 2002). Imd activation results in the recruitment of signalling complex components (signalosome equivalent), including Imd, dFADD adapter protein and Dredd (Myllymäki et al., 2014). Dredd cleaves Imd leading to the recruitment of TAK1/TAB2 complex. The TAK1/TAB2 complex activates the Iκ-B complex which in turn phosphorylates Relish, cleaving it from the inhibitory ankyrin repeat domain, allowing it to regulate AMP transcription (Hoffmann and Reichhart, 2002; Myllymäki et al., 2014). Imd pathway components including Relish, Iκ-B related protein and several caspase isoforms have been identified in the *H. americanus* transcriptome (Clark, 2014; Clark and Greenwood, 2016).

1.4.2.3 JAK-STAT

The JAK-STAT pathway is involved in the production of antiviral cytokines and responds to invading viral infections (Myllymäki and Rämet, 2014). JAK-STAT

activation occurs when the Upd3 ligand binds to the Dome receptor (Myllymäki and Rämet, 2014). The Dome receptor contains an extracellular fibronectin type III domain, a cytokine-binding module, a janus kinase (JAK) tyrosine, a hopscotch (hop) and a signal transducer and activator of transcription (STAT) transcription factor coined STAT-92E (Myllymäki and Rämet, 2014). Activation of the pathway follows a canonical signalling model, where binding of the ligand to the receptor causes receptor dimerization and activation of the JAK (Myllymäki and Rämet, 2014). Activated JAK phosphorylates itself, a tyrosine residue, and the STAT molecule. The phosphorylation creates a docking site for the SH2 domains of the STAT molecule, which causes the STAT to translocate into the nucleus and bind to promoters of target genes responsible for cytokines, stress, and immune responses (Myllymäki and Rämet, 2014).

The mechanism by which virus is detected and the effectors of the JAK-STAT signalling pathway are not yet fully elucidated (Myllymäki and Rämet, 2014). However, Ren et al., (2015) recently presented microRNA (miRNA)-mediated regulation of the JAK-STAT signalling pathway, via thioester-containing proteins TEP1 and TEP2, following WSSV infection in *Penaeus japonicus*. Several of the JAK-STAT pathway components have identified homologues in the *H. americanus* transcriptome, including 220 Domeless transcripts, 2 cytokine receptor transcripts, 120 JAK-STAT signalling protein transcripts, 326 hopscotch transcripts and 4 JAK-STAT transcription factor transcripts (Clark and Greenwood, 2016). A striking feature of the JAK-STAT pathway is its benefit for white spot syndrome virus (Chen et al., 2008). In WSSV infected *Penaeus monodon*, the activated STAT has been

found to enter infected nuclei and activate the promoter region of the WSSV ie1 gene responsible for viral transcription (Chen et al., 2008; Liu et al., 2009).

1.4.3 RNAi

In addition to the JAK-STAT signaling pathway, the RNA interference (RNAi) pathway is also involved in antiviral defence. There are two main classes of RNAi, small interfering RNAs (siRNA) and micro-RNAs, which function to regulate transcriptional and post-transcriptional gene expression (Nowotny and Yang, 2009). Typically, RNAi bind to complementary sequences in the mRNA of target genes and regulate expression by either repressing or inducing translation (Verbruggen et al., 2015). Upon detection of a virus within a host, RNAi can limit viral replication or alter cellular processes that disadvantage the virus (Verbruggen et al., 2015). However, it has also been found that RNAi (or miRNAs) present within the genome of a virus can regulate either viral genes or host genes in an attempt to manipulate immune response and cellular functions to advantage the virus (Verbruggen et al., 2015).

The RNAi pathway has been well characterized in *Drosophila* and several shrimp species. Major RNAi pathway proteins such as Drosha, Dicer 1 and Dicer 2 proteins, Argonaute proteins, as well as several members of transactivation response RNA-binding protein have been characterized in a variety of shrimp species (Huang and Zhang, 2013). RNAi also play a critical role in WSSV infections, where a siRNA in *Marsupenaeus japonicus* has been found to target the VP28 gene of WSSV (an envelope protein required for WSSV infection) and exhibit antiviral activity (Xu et al., 2007).

1.4.4 Haemocytes

Haemocytes are the primary immune cells in crustaceans and are responsible for cell-mediated immune actions such as phagocytosis and encapsulation (Hillyer, 2015; Jiravanichpaisal et al., 2006; Johansson et al., 2000). They also contain several key proteins and enzymes critical for processes such as coagulation and melanization (Söderhäll, 2016). The regulation, storage and release of haemocytes occurs in the haematopoietic tissue (Johansson et al., 2000). Molecular regulation of haematopoiesis is only recently beginning to be elucidated in crustaceans, where P1Runt, a transcription factor, belonging to the Runx protein family, has been identified as a necessary component for haematopoiesis (Söderhäll, 2016).

Haemocytes are classified into three main cell types; hyaline haemocytes, granulocytes and semi-granulocytes (Martin and Hose, 1995). Hyaline haemocytes are morphologically characterized by their ovoid shape, high nucleocytoplasmic ratio and absence of granules (Hose et al., 1990; Söderhäll and Cerenius, 1992). Granulocytes are larger than hyaline cells and contain large cytoplasmic granules (>1 μm in diameter) (Battison et al., 2003). Granulocytes are responsible for the storage and release of components of the proPO system (Johansson et al., 2000). Semi-granulocytes are similar to granulocytes but contain smaller and fewer cytoplasmic granules (<1 μm in diameter) (Battison et al., 2003; Martin and Hose, 1995). Semi-granular cells contain lysosomal enzymes that aid in phagocytosis and encapsulation as well as storage and release of the proPO system (Johansson et al., 2000). In *H. americanus*, 11 different haemocyte types have been identified;

however several are considered precursors of the three main cell types mentioned above (Battison et al., 2003).

1.4.5 Effector Mechanisms

1.4.5.1 Clotting

Clotting acts as a means of sealing a wound and preventing loss of haemolymph during injury (Shields et al., 2006). Clotting also traps and isolates foreign particles within the body (known as nodule formation), preventing pathogen spread (Martin and Hose, 1995; Shields et al., 2006). The crustacean clotting process is initiated by rupture of hyaline haemocytes through cytolysis, releasing transglutaminase (TGase) which covalently bonds clotting proteins (Sritunyalucksana and Söderhäll, 2000). In crustaceans, coagulogen is a known plasma clotting protein (Martin and Hose, 1995). In the presence of Ca^{2+}, TGase cross-links with coagulogen resulting in the formation of a clot (Sritunyalucksana and Söderhäll, 2000). In freshwater crayfish *Pacifastacus leniusculus*, an α2-macroglobulin (α2-m), is responsible for exposing free lysine and glutamine residues, suggesting TGase likely utilizes α2-m to crosslink to the coagulogen (Theopold et al., 2004). In *H. americanus*, a variety of transglutaminases, clotting proteins, and coagulation transcription factors have been identified (Clark, 2014; Clark and Greenwood, 2016).

1.4.5.2 ProPO and Melanization

Melanization in crustaceans involves a series of enzymatic and proteolytic cascades that result in pathogen death through oxidative damage and the formation

of melanin, which encloses the pathogen (Hillyer, 2015). Formation of a PRR-PAMP complex initiates a serine protease cascade that activates the prophenoloxidase activating enzyme (PPAE), responsible for the cleavage of the zymogen prophenoloxidase into phenoloxidase (PO) (Hillyer, 2015). PO then hydroxylates tyrosine into DOPA and dopaquinone, which is further converted into dopachrome, followed by 5,6-dihydroxyindole, via the dopachrome conversion enzyme (Hillyer, 2015). PO further oxidizes 5,6-dihydroxyindole into indole-5,6-quinone which polymerizes to form melanin (Goto and Kurata, 2012; Hillyer, 2015). In the *H. americanus* transcriptome, 129 DOPA decarboxylase, 11 PPAE and 79 prophenoloxidase transcripts have been identified (Clark and Greenwood, 2016).

In crustaceans phenoloxidase is synthesized and released from the granular and semi-granular haemocytes (Jiravanichpaisal et al., 2006). The recognition of non-self triggers degranulation of granular haemocytes, in turn releasing the key proteins and enzymes (Jiravanichpaisal et al., 2006). The by-products of this pathway include quinones, which are extremely toxic metabolites and reactive oxygen species, therefore making pathway activation efficient at killing invading pathogens (Goto and Kurata, 2012). Gene knockdown studies conducted in shrimp have found that a reduction in total PO activity results in increased susceptibility to bacterial infections (Tassanakajon et al., 2013).

1.4.5.3 Phagocytosis and Encapsulation

In *H. americanus*, phagocytosis is accomplished primarily by the semi-granular haemocytes and aided by the hyaline and granular haemocytes (Martin and Hose, 1995). Phagocytosis occurs when PRRs, present on phagocytic cells, such as

PGRPs and DSCAM bind to PAMPs (Hillyer, 2015). Binding causes cytoskeleton modifications that lead to pathogen uptake (Hillyer, 2015; Jiravanichpaisal et al., 2006). Vesicular transport brings the pathogen to a membrane-delimited phagosome, which fuses with a lysosome that uses hydrolytic enzymes to digest the pathogen (Hillyer, 2015). Protozoans, bacteria, fungi and some viruses can be phagocytized via the PAMP mediated pathway (Rowley and Powell, 2007). Opsonization factors present in the plasma also circulate and mark particles or pathogens for phagocytosis (Jiravanichpaisal et al., 2006).

When a parasite is too large to be phagocytized, haemocytes will encapsulate the foreign particle sealing it off from circulation (Söderhäll and Cerenius, 1992). Encapsulation is carried out by granular and semi-granular haemocytes and results in a multilayered overlapping sheath of haemocytes (Jiravanichpaisal et al., 2006). The binding of haemocytes to the larger pathogen is dependent on binding of integrins to specific sites defined by Arg-Gly-Asp (RGD) sequences (Hillyer, 2015). Encapsulation can also be accompanied by melanization and production of toxic quinones that aid in pathogen death (Jiravanichpaisal et al., 2006).

1.4.5.4 Apoptosis

Currently, there exists some ambiguity regarding the benefit of apoptosis in viral immunity (Flegel and Sritunyalucksana, 2011). In early infections it is believed to help combat infection by limiting virus production, however, in late stages of infection many viruses have been found to induce apoptosis in an attempt to spread viral progeny to other neighbouring cells (Flegel and Sritunyalucksana, 2011; Liu et al., 2009). Caspases are the main effector proteases of apoptosis (Kornbluth and

White, 2005). The IAP family of anti-apoptotic proteins is responsible for regulation of apoptosis (Kornbluth and White, 2005). In *Penaeus monodon,* WSSV has been shown to inhibit caspase 3 resulting in a decrease in apoptosis and a decrease in host mortality in early infection (Liu et al., 2009). However, it is unknown if this correlated with an increase in late-stage host mortality (Liu et al., 2009). Over 600 caspase isoforms have been recently identified within the *H. americanus* transcriptome (Clark and Greenwood, 2016).

1.4.5.5 Antimicrobial Peptides

In *H. americanus,* Hoa-crustin, CAP-1 (Homarin), CAP-2 and anti-lipopolysaccharide factors (ALFs) are the most well characterized AMPs (Battison et al., 2008b; Beale et al., 2008; Christie et al., 2007; Clark, 2014). Hoa-crustin, CAP-1 and CAP-2 belong to a group of WAP domain containing proteins known as crustins which display activity against gram-positive bacteria and cultured scuticociliate parasites (Christie et al., 2007). Anti-lipopolysaccharide factors are small proteins that are involved in defending against bacterial and micro parasitic infections (Beale et al., 2008; Clark, 2014). *H. americanus* have 7 different ALF isoforms (Clark, 2014). Differential expression of the various ALF isoforms has been examined for bacterial, parasitic and viral infections (Clark et al., 2013a, 2013b, 2013c). Most notably, during WSSV infection in *H. americanus*, both Homame ALF-B1 and ALF*Ha*-4 were differentially expressed at 24 hours and 96 hours post infection, indicating a role for ALF in mediating viral immunity (Clark et al., 2013c). More recently, AMP pathway components including 9 ALF transcripts,

12 crustin transcripts and 3 AMP type 1-precursor transcripts have been annotated in the *H. americanus* transcriptome (Clark and Greenwood, 2016).

1.5 Pathogens

The marine environment presents numerous opportunities for interaction with pathogens (Hauton, 2012; Söderhäll and Cerenius, 1992). Disease resulting from these interactions is of concern for fisheries given the potential for lost productivity (Green et al., 2014). Surprisingly though, lobsters have few reported diseases compared to other decapod crustaceans (Martin and Hose, 1995). These few diseases, however, do pose threats to wild or impounded lobster populations (Behringer et al., 2012). Interestingly, there are currently no known naturally occurring viral pathogens of *H. americanus*, yet viral pathogens are of significant economic concern to other closely related crustacean species (Behringer et al., 2012; Cawthorn, 2011).

1.5.1 Bacterial Diseases

Gaffkaemia and shell disease are two of the most common bacterial diseases affecting *H. americanus* (Cawthorn, 2011). Gaffkaemia is the disease caused by the gram-positive bacterium *Aerococcus viridans* var. *homari* (Greenwood et al., 2005b). The bacterium, a free-living, tetrad-forming coccus, leads to systemic disease in *H. americanus* (Stewart, 1984). Gaffkaemia prevalence is low in wild populations but is a major disease of impounded lobster (Cawthorn, 2011). Increased temperatures, handling stress, overcrowding and strain of bacteria all contribute to how quickly infection progresses to disease and mortality (Cawthorn, 2011). In lobsters, there exist two forms of shell disease, classical shell disease and epizootic

shell disease. Classical shell disease presents as lesions that develop slowly on the setal pits of the dorsal carapace (Cawthorn, 2011). It has low prevalence and is traditionally associated with poor water quality in holding facilities (Martin and Hose, 1995; Shields, 2013). ESD however, appears grossly as melanization and necrosis of the lobster cuticle, develops rapidly and has been found at high prevalence in Southern New England (Cawthorn, 2011). ESD is associated with an initial disruption of cuticle coupled with environmental stress and chitinolytic bacteria *Aquimarina homari* (Castro et al., 2012; Cawthorn, 2011; Shields, 2013).

Vibriosis is also of concern for decapod crustaceans (Shields, 2011). Many *Vibrio* species such as *Vibrio harveyi, Vibrio alginolyticus, Vibrio parahaemolyticus* act as opportunistic secondary pathogens causing disease when lobsters are already significantly stressed (Cawthorn, 2011; Shields, 2011). In *H. americanus, Vibrio* are associated with diseases such as Limp lobster disease, classical shell disease and ulcerative enteritis (Battison et al., 2008a; Beale et al., 2008; Cawthorn, 2011).

1.5.2 Fungal Diseases

In crustaceans, fungal pathogens are of concern mostly for aquaculture and hatchery facilities (Cawthorn, 2011; Stewart, 1984). The fungal pathogen *Lagenidium callinectes* has been known to infect embryos and larval *H. americanus* resulting in fouling of eggs and larval death (Cawthorn, 2011). Water mould, caused by *Haliphthoros mildfordensis* is also of concern for eggs and larval lobsters where disease is associated with unhealthy rearing conditions (Cawthorn, 2011). *Fusarium solani* a deuteromycete fungus responsible for black gill disease has been reported in shrimp, spiny lobsters and clawed lobster from aquaculture facilities where subpar

environmental factors are thought to facilitate outbreaks (Alderman, 1981; Lightner and Fontaine, 1975; Shields, 2011). The fungus is an opportunistic pathogen that infects lobsters through previously dead or damaged tissues resulting in black lesions on the exoskeleton and gills of the animal (Trang and Hoa, 2009).

1.5.3 Protozoal Diseases

Anophryoides haemophila, the causative agent of bumper car disease, is a scuticociliate protozoan pathogen that impacts both wild and impounded *H. americanus* (Cawthorn, 1997; Greenwood et al., 2005a). Upon infection, ciliates initially (1-4 weeks post infection) replicate locally in the vesicular spaces and are undetectable in the haemolymph (Athanassopoulou et al., 2004). However, at late stage infections (4+ weeks post infection) the ciliates begin to spread throughout the body to tissues and organs resulting in haemocyte granulomas and a marked haemocytopenia (Athanassopoulou et al., 2004; Battison et al., 2004).

Other protozoal pathogens of *H. americanus* include *Neoparamoeba pemaquidensis* and *Porospora gigantea* (Cawthorn, 2011; Shields et al., 2006). *Neoparamoeba pemaquidensis*, is an amoebozoan pathogen, that has been previously identified as a primary contributor to the 1999 Long Island Sound mortality event (Cawthorn, 2011). The amoeba infects the ventral nerve cord, brain and neurosecretory organs of the eye (Shields et al., 2006). The disease is transmitted horizontally and spreads rapidly making it a significant problem for situations involving high stocking density (Shields et al., 2006). *Porospora gigantea* is an apicomplexan parasite that uses *H. americanus* as its definitive host (Shields et al., 2006). The parasite is found free within the lumen of the mid and hind gut of the

animal with epimeres attached to the gut wall (Brattey and Campbell, 1986; Shields et al., 2006). No gross pathological changes are associated with infection and lobsters tend to appear relatively healthy when infected (Boghen, 1978).

1.5.4 Viral Diseases in Other Crustaceans

Naturally occurring viral infections have yet to be conclusively documented in *H. americanus*, however, viral diseases continue to be a significant impediment to the growth and sustainability of other wild and cultured crustacean populations (Behringer et al., 2001; Cawthorn, 2011). Viral agents include, but are not limited to, *Panulirus argus* virus 1 (*Pa*V1), *Penaeus stylirostris Brevidensovirus* (PstDNV), and white spot syndrome virus (WSSV) (Shields, 2011; Sweet and Bateman, 2015).

*Pa*V1 is the first recorded naturally occurring viral infection of spiny lobsters *Panulirus argus* (Shields, 2011; Sweet and Bateman, 2015). It infects *P. argus* juveniles only and has been recorded at prevalence levels as high as 50% during outbreaks (Sweet and Bateman, 2015). The virus infects haemocytes, soft connective tissues and fixed phagocytes, with heavily infected lobsters becoming slow, lethargic and losing haemolymph clotting ability (Shields, 2011).

*Pst*DNV infects a wide variety of *Penaeus* shrimp species, with *Penaeus stylirostris* being the most susceptible (Chayaburakul et al., 2005). PstDNV is a small DNA virus that infects haematopoietic tissue, nervous tissue, gills, gonad, connective tissues and antennal gland (Chayaburakul et al., 2005; Sweet and Bateman, 2015). The virus is a major impediment to shrimp aquaculture as previous outbreaks in shrimp farms have resulted in mass mortalities of 90% (Chayaburakul et al., 2005).

Similarly, WSSV infects farmed shrimp and has caused serious pandemics to the *Penaeus* shrimp aquaculture industry worldwide (Shekhar and Ponniah, 2015). Strikingly though, the virus appears to be non-specific with over 93 crustacean species reported as susceptible either from natural or experimental infection (Sánchez-Paz, 2010). Included among those experimentally susceptible, are *H. americanus* and the European lobster *H. gammarus* (Bateman et al., 2012; Clark et al., 2013c).

1.6 White Spot Syndrome Virus

WSSV was first discovered in the early 1990's in shrimp aquaculture facilities in Southeast Asia (Soto et al., 2001). Since its emergence the virus has had serious economic impact on the cultured shrimp industry with infections in aquaculture ponds leading to 100% mortality within three to ten days (Shekhar and Ponniah, 2015; Zwart et al., 2010). The virus is highly virulent and spreads quickly. The original host of the virus, *Penaeus japonicus,* inhabited waters in Southeast Asia and was one of the original commercially reared shrimp species (Lo et al., 2005). It is believed that WSSV first became established in wild populations, amounting to little impact, and then spread from wild populations to farms resulting in significant economic losses (Lo et al., 2005). International transport of live shrimp and brood stock for both consumption and aquaculture has resulted in the distribution of the virus to shrimp facilities globally (Lo et al., 2005).

1.6.1 WSSV Genome and Morphology

WSSV is a double stranded DNA virus with a 300 kilobase pair genome, making it one of the largest animal virus genomes (Zwart et al., 2010). It is the sole

member of the *Nimaviridae* virus family (Zwart et al., 2010). Four WSSV isolates have been sequenced with each differing only slightly in genome size and sequence suggesting a high degree of genomic stability (Pradeep et al., 2012; Verbruggen et al., 2016). The Thai isolate in particular has the smallest genome and has been found to be the most virulent in *Penaeus* shrimp species (Marks et al., 2005).

WSSV virions (Fig. 1.1) are ovoid to elliptical in shape and range between 210 and 420 nm in length and 70 and 167 nm in diameter (Sánchez-Paz, 2010). The virions possess a striated nucleocapsid core and a long tail like projection at one extremity (Bateman et al., 2012). WSSV currently contains 58 known structural proteins (Sánchez-Paz, 2010). The most well characterized are envelope proteins VP28 and VP26 which constitute 60% of the viral envelope (Sánchez-Paz, 2010). VP28 has been found to be critical for virus entry and attachment to host cells, whereas VP26 plays a suspected role in movement of virus towards the nucleus following host cell entry (Sánchez-Paz, 2010).

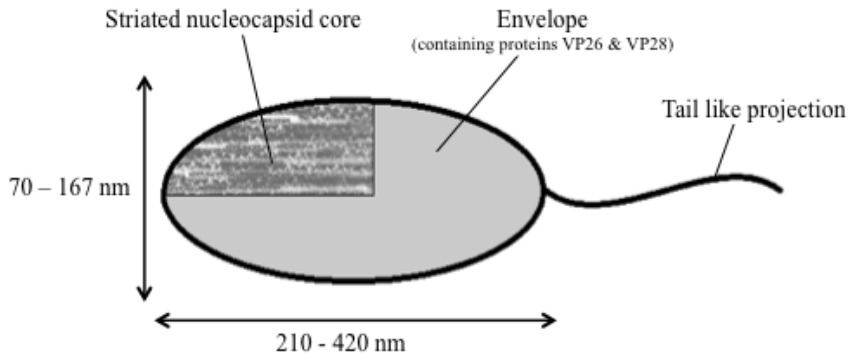

Figure 1.1: White spot syndrome virus morphology.

1.6.2 Virus Entry and Tissue Tropism

WSSV utilizes an endocytic-mediated pathway to enter shrimp cells (Huang et al., 2013). WSSV envelope proteins interact with a variety of host receptors including but not limited to C-type lectins, integrins and Rab7 (Verbruggen et al., 2016). The virus uses either clathrin-mediated endocytosis or caveolae-mediated endocytosis to penetrate the cell (Verbruggen et al., 2016). Once inside, the virus matures within the endosome, until it exits and travels to the nucleus (Verbruggen et al., 2016). The mechanism by which the virus travels to and enters the nucleus is currently unknown. However, once inside the nucleus, host transcription factors bind to the ie1 promoter gene, which in turn activates viral transcription factors allowing for viral replication (Verbruggen et al., 2016).

WSSV infection in penaeid shrimp is characterized by a rapid reduction in food consumption and a lethargic state (Pradeep et al., 2012). The virus gets its name from the presence of tiny abnormal calcium deposits that, although rare, appear on the cuticular epidermis (Lo et al., 2005). The virus targets tissues of ectodermal and mesodermal origin (Lo et al., 2005). Infection can be recognized histologically by the presence of enlarged nuclei with inclusion bodies (Bateman et al., 2012). At the early stages of infection nuclei show marginated chromatin. The stomach, gills, cuticular epithelium, lymphoid organ and haematopoietic tissue are amongst the most heavily infected tissues at late stages of infection (Pradeep et al., 2012).

1.6.3 Transmission

WSSV is a problem for the shrimp industry affecting both acquisition of healthy, virus-free brood stock and animal husbandry. In less developed countries, shrimp aquaculture facilities still use wild-caught brood stock and seed, instead of specific pathogen free (SPF) shrimp, to stock culture ponds (Treece, 2000). WSSV prevalence in wild populations of *Penaeus monodon* along the coast of East India have been recorded as high as 56.2% (de la Peña et al., 2007; Dutta et al., 2015; Octovianus and Yanuhar, 2015). Shrimp farms harvesting brood stock or seed from contaminated marine environments risk introducing WSSV infection into their hatcheries. WSSV eradication efforts (heat killing the virus for 1 min at 65 ^{o}C) result in lost production time meaning that it is more prudent to control stock, improve biosecurity and implement low stress hatchery conditions to mitigate impacts of WSSV infection (Karunasagar and Ababouch, 2012).

When WSSV gains entry into an aquaculture pond, the virus spreads quickly through horizontal transmission. Ingestion of infected tissue (cannibalism) or exposure to virus particles present in the water results in disease outbreak within several days (Lo et al., 2005; Sánchez-Paz, 2010). Infection in mature eggs has yet to be documented suggesting that vertical transmission likely results in death of eggs prior to maturation (Lo et al., 1997; Sánchez-Paz, 2010).

1.6.4 Host Range

Arguably the most interesting feature of WSSV is its broad host range. Both the World Organization for Animal Health (Office International des Epizooties, OIE) and the National Aquatic Animal Health Program (Canada; NAAHP) consider

WSSV a notifiable disease with the potential to infect all crustacean decapods. The virus is reported from a wide range of hosts such as shrimp, crabs, lobsters, and crayfish (Sánchez-Paz, 2010). Amongst these reports, are various degrees of susceptibility, disease, infection and resistance (Bateman et al., 2012). In total, 93 species of arthropods have been reported as hosts or carriers of WSSV from wild or experimental scenarios, including the aforementioned experimental infection of *H. americanus* (Clark et al., 2013c; Maeda et al., 2000; Sánchez-Paz, 2010).

1.6.5 Host Pathogen Environment Interactions

WSSV is not only able to survive within a variety of hosts but also within the broad range of environments occupied by those hosts. Marine crustaceans, estuarine species and freshwater crayfish are all reported as universally susceptible (Bateman et al., 2012).

Environmental temperature in particular, plays a critical role in WSSV infection dynamics. WSSV experimental infection has been reported at temperatures ranging from 15 ^{o}C in *H. gammarus* (Bateman et al., 2012) to 36 ^{o}C in *Penaeus monodon* (Raj et al., 2012) inclusively. It is believed that the ideal temperature for the virus is between 16 ^{o}C and 30 ^{o}C (Moser et al., 2012). In *Penaeus japonicus*, a significant increase in mortality is observed in animals infected at 27 ^{o}C compared to 31 ^{o}C (You et al., 2010). In *Penaeus monodon*, 100% mortality is observed in infected animals held at temperatures between 16 ^{o}C and 30 ^{o}C, with a reduction in mortality observed in animals held at 32 ^{o}C and 36 ^{o}C (Raj et al., 2012). In WSSV infected freshwater signal crayfish *Pacifastacus leniusculus* temperatures below 12 ^{o}C, result in no mortality over a period of 45 days (Jiravanichpaisal et al., 2004).

On a molecular level the interactions between host immunity and WSSV are only recently beginning to be understood. Wang et al. (2006) found an up-regulation of immune related genes such as HSP 70, HSP 90, trehalose-phosphate synthase (TPS) and ubiquitin C, 6 hours post infection in Chinese white shrimp *Fenneropenaeus chinensis.* Similarly, Rao et al., (2016) found a total of 74 immune related unigenes were up-regulated in response to WSSV infection in the giant freshwater prawn, *Macrobrachium rosenbergii.* Components of the pro-PO pathway, ALFs, lysozymes, components of the coagulation cascade and caspases were among those up-regulated (Rao et al., 2016). Lastly, Clark et al. (2013c) examined the molecular immune response in *H. americanus* experimentally infected with WSSV at 20 ^{o}C, a temperature near the upper thermal tolerance of the animal and found a total of 136 genes including trypsin isoforms, eTIF3-5e, cathepsin C2, and ecdysone-inducible protein E75 (EIPE75) were differentially expressed (Clark et al., 2013c).

1.7 Rationale

Recently, research effort has focused on characterizing the molecular immune response of lobsters in an attempt to better understand host pathogen interactions (Clark et al., 2013a, 2013b, 2013c). *H. americanus* inhabit ocean waters that fluctuate in temperature between 0 ^{o}C and 20 ^{o}C, yet the full impact of these temperature variations on the immune response of *H. americanus* is unknown. Previous research shows that adult *H. americanus* produce a targeted immune response to WSSV, following intramuscular injection of the virus at 20 ^{o}C (Clark et

al., 2013c). However, how *H. americanus* responds to WSSV at various temperatures is unknown.

The purpose of this study was to determine the effect of variable water temperature on the overall immune response of *H. americanus* experimentally infected with WSSV. The study will conduct a WSSV injection challenge model and use a lobster specific microarray, RT-qPCR, and light and electron microscopy to explore the clinical, tissue and molecular immune response of experimentally infected *H. americanus* at four different water temperatures (10 ^{o}C, 15 ^{o}C, 17.5 ^{o}C, 20 ^{o}C). It is hypothesized that *H. americanus* infected with WSSV will display measurable differences in overall immune response between individuals at different temperatures. It is also hypothesized that increased WSSV pathogenicity and highest infection levels will be observed at warmer temperatures (20 ^{o}C), moderate levels of infection and diminishing pathological changes will be observed at intermediate temperatures (15 ^{o}C, 17.5 ^{o}C), and WSSV infection will be absent at colder temperatures (10 ^{o}C).

The main objectives of this study are to:

- Conduct a white spot syndrome virus *in vivo* challenge in *H. americanus* at four different water temperatures: 10 ^{o}C, 15 ^{o}C, 17.5 ^{o}C, 20 ^{o}C.
- Monitor WSSV infection throughout the trial.
- Identify WSSV associated changes in target tissues using histology and transmission electron microscopy.
- Identify differently expressed immune related genes using a lobster specific microarray.

- Verify microarray gene expression findings using RT-qPCR.
- Begin to elucidate the immune pathways and processes that are impacted by WSSV infection at varying temperatures.

1.8 References

Ahearn, G.A., Mandal, P.K., Mandal, A., 2004. Calcium regulation in crustaceans during the molt cycle: a review and update. Comp. Biochem. Physiol. Part A Mol. Integr. Physiol. 137, 247–257.

Aiken, D.E., Waddy, S.L., 1986. Environmental influence on recruitment of the American lobster, *Homarus americanus*: a perspective. Can. J. Fish. Aquat. Sci. 43, 2258–2270.

Alderman, D.J., 1981. *Fusarium solani* causing an exoskeletal pathology in cultured lobsters, *Homarus vulgaris*. Trans. Br. Mycol. Soc. 76, 25–27.

Athanassopoulou, F., Speare, D., Cawthorn, R.J., MacMillan, R., Després, B.M., 2004. Pathology of *Anophryoides haemophila* (Scuticociliatida: Orchitophryidae), parasite of American lobster *Homarus americanus* kept under experimental conditions. Aquaculture 236, 103–117.

Barker, P.L., Gibson, R., 1977. Observations on the feeding mechanism, structure of the gut, and digestive physiology of the European lobster *Homarus gammarus* (Decapoda: Nephropidae). J. Exp. Mar. Bio. Ecol. 26, 297–324.

Bateman, K.S., Tew, I., French, C., Hicks, R.J., Martin, P., Munro, J., Stentiford, G.D., 2012. Susceptibility to infection and pathogenicity of white spot disease (WSD) in non-model crustacean host taxa from temperate regions. J. Invertebr. Pathol. 110, 340–351.

Battison, A.L., Cawthorn, R.J., Horney, B., 2004. Response of American lobsters *Homarus americanus* to infection with a field isolate of *Aerococcus viridans* var. *homari* (Gaffkemia): survival and haematology. Dis. Aquat. Organ. 61, 263–268.

Battison, A.L., Cawthorn, R.J., Horney, B., 2003. Classification of *Homarus americanus* hemocytes and the use of differential hemocyte counts in lobsters infected with *Aerococcus viridans* var. *homari* (Gaffkemia). J. Invertebr. Pathol. 84, 177–197.

Battison, A.L., Després, B.M., Greenwood, S.J., 2008a. Ulcerative enteritis in *Homarus americanus*: case report and molecular characterization of intestinal aerobic bacteria of apparently healthy lobsters in live storage. J. Invertebr. Pathol. 99, 129–135.

Battison, A.L., Summerfield, R.L., Patrzykat, A., 2008b. Isolation and characterisation of two antimicrobial peptides from haemocytes of the American lobster *Homarus americanus*. Fish Shellfish Immunol. 25, 181–187.

Beale, K.M., Towle, D.W., Jayasundara, N., Smith, C.M., Shields, J.D., Small, H.J., Greenwood, S.J., 2008. Anti-lipopolysaccharide factors in the American lobster *Homarus americanus*: Molecular characterization and transcriptional response to *Vibrio fluvialis* challenge. Comp. Biochem. Physiol. Part D Genomics Proteomics 3, 263–269.

Behringer, D.C., Butler, M.J., Shields, J.D., 2001. The first viral disease reported in lobsters. Lobster Newsl. Res. News 14, 1–3.

Behringer, D.C., Butler, M.J., Stentiford, G.D., 2012. Disease effects on lobster fisheries, ecology, and culture: overview of DAO Special 6. Dis. Aquat. Organ. 100, 89–93.

Boghen, A.D., 1978. A parasitological survey of the American lobster *Homarus americanus* from the Northumberland Strait, southern Gulf of St. Lawrence. Can. J. Zool. 56, 2460–2462.

Brattey, J., Campbell, A., 1986. A survey of parasites of the American lobster, *Homarus americanus* (Crustacea: Decapoda), from the Canadian maritimes. Can. J. Zool. 64, 1998–2003.

Castro, K.M., Cobb, J.S., Gomez-Chiarri, M., Tlusty, M., 2012. Epizootic shell disease in American lobsters *Homarus americanus* in southern New England: past, present and future. Dis. Aquat. Organ. 100, 149–158.

Cataln, T.P., Wozniak, A., Niemeyer, H.M., Kalergis, A.M., Bozinovic, F., 2012. Interplay between thermal and immune ecology: effect of environmental temperature on insect immune response and energetic costs after an immune challenge. J. Insect Physiol. 58, 310–317.

Cawthorn, R.J., 2011. Diseases of American lobsters (*Homarus americanus*): a review. J. Invertebr. Pathol. 106, 71–78.

Cawthorn, R.J., 1997. Overview of "bumper car" disease—Impact on the North American lobster fishery. Int. J. Parasitol. 27, 167–172.

Cerenius, L., Jiravanichpaisal, P., Liu, H., Söderhäll, I., 2010a. Crustacean Immunity, in: Söderhäll, K. (Ed.), Invertebrate Immunity, Advances in Experimental Medicine and Biology. Landes Bioscience and Springer Science, pp. 239–259.

Cerenius, L., Kawabata, S., Lee, B.L., Nonaka, M., Söderhäll, K., 2010b. Proteolytic cascades and their involvement in invertebrate immunity. Trends Biochem. Sci. 35, 575–583.

Cerenius, L., Söderhäll, K., 2013. Variable immune molecules in invertebrates. J. Exp. Biol. 216, 4313–4319.

Chang, E.S., 2005. Stressed-out lobsters: crustacean hyperglycemic hormone and stress proteins. Integr. Comp. Biol. 45, 43–50.

Chang, E.S., Mykles, D.L., 2011. Regulation of crustacean molting: a review and our perspectives. Gen. Comp. Endocrinol. 172, 323–330.

Chayaburakul, K., Lightner, D. V., Sriurairattana, S., Nelson, K.T., Withyachumnarnkul, B., 2005. Different responses to infectious hypodermal and hematopoietic necrosis virus (IHHNV) in *Penaeus monodon* and *P. vannamei*. Dis. Aquat. Organ. 67, 191–200.

Chen, W.Y., Ho, K.C., Leu, J.-H., Liu, K.-F., Wang, H.-C., Kou, G.-H., Lo, C.-F., 2008. WSSV infection activates STAT in shrimp. Dev. Comp. Immunol. 32, 1142–1150.

Cheng, W., Chen, J.-C., 1998. Enterococcus-like infections in *Macrobrachium rosenbergii* are exacerbated by high pH and temperature but reduced by low salinity. Dis. Aquat. Organ. 34, 103–108.

Choe, K.-M., Lee, H., Anderson, K. V., 2005. *Drosophila* peptidoglycan recognition protein LC (PGRP-LC) acts as a signal-transducing innate immune receptor. Proc. Natl. Acad. Sci. U. S. A. 102, 1122–1126.

Christie, A.E., Rus, S., Goiney, C.C., Smith, C.M., Towle, D.W., Dickinson, P.S., 2007. Identification and characterization of a cDNA encoding a crustin-like, putative antibacterial protein from the American lobster *Homarus americanus*.

Mol. Immunol. 44, 3333–3337.
Clark, K.F., 2014. Characterization and functional classification of American lobster (*Homarus americanus*) immune factor transcripts. Fish Shellfish Immunol. 41, 12–26.
Clark, K.F., Acorn, A.R., Greenwood, S.J., 2013a. Differential expression of American lobster (*Homarus americanus*) immune related genes during infection of *Aerococcus viridans* var. *homari*, the causative agent of Gaffkemia. J. Invertebr. Pathol. 112, 192–202.
Clark, K.F., Acorn, A.R., Greenwood, S.J., 2013b. A transcriptomic analysis of American lobster (*Homarus americanus*) immune response during infection with the bumper car parasite *Anophryoides haemophila*. Dev. Comp. Immunol. 40, 112–122.
Clark, K.F., Greenwood, S.J., 2016. Next-Generation sequencing and the crustacean immune system: The need for alternatives in immune gene annotation. Integr. Comp. Biol. 56, 1113–1130.
Clark, K.F., Greenwood, S.J., Acorn, A.R., Byrne, P.J., 2013c. Molecular immune response of the American lobster (*Homarus americanus*) to the white spot syndrome virus. J. Invertebr. Pathol. 114, 298–308.
Dall, W., 1970. Osmoregulation in the Lobster *Homarus americanus*. J. Fish. Res. Board Canada 27, 1123–1130.
Davis, J.C., 1975. Minimal dissolved oxygen requirements of aquatic life with emphasis on Canadian species: a review. J. Fish. Res. Board Canada 32, 2295–2332.
De Gregorio, E., Spellman, P.T., Tzou, P., Rubin, G.M., Lemaitre, B., 2002. The Toll and Imd pathways are the major regulators of the immune response in *Drosophila*. EMBO J. 21, 2568–2579.
de la Peña, L.D., Lavilla-Pitogo, C.R., Villar, C.B.R., Paner, M.G., Sombito, C.D., Capulos, G.C., 2007. Prevalence of white spot syndrome virus (WSSV) in wild shrimp *Penaeus monodon* in the Philippines. Dis. Aquat. Organ. 77, 175–179.
Devaraj, H., Natarajan, A., 2006. Molecular mechanisms regulating molting in a crustacean. FEBS J. 273, 839–846.
Dutta, S., Chakrabarty, U., Mallik, A., Mandal, N., 2015. White spot syndrome virus (WSSV) prevalence associated with disease resistance among wild populations of black tiger shrimp, *Penaeus monodon* (Fabricius). Aquac. Res. 46, 453–461.
Edge, S.E., Morgan, M.B., Gleason, D.F., Snell, T.W., 2005. Development of a coral cDNA array to examine gene expression profiles in *Montastraea faveolata* exposed to environmental stress. Mar. Pollut. Bull. 51, 507–523.
Ennis, G., 1995. Larval and postlarval ecology, in: Factor, J.R. (Ed.), Biology of the Lobster *Homarus americanus*. Academic Press, pp. 23–46.
Factor, J.R., 1995. Introduction, anatomy and life history, in: Factor, J.R. (Ed.), Biology of the Lobster *Homarus americanus*. Academic Press, pp. 1–11.
Fisheries and Oceans Canada, 2016. DFO-Canada's Fisheries Fast Facts 2015 [WWW Document]. URL http://www.dfo-mpo.gc.ca/stats/facts-Info-15-eng.htm
Fisheries and Oceans Canada, 2015. Lobster [WWW Document]. URL http://www.dfo-mpo.gc.ca/fm-gp/sustainable-durable/fisheries-peches/lobster-

homard-eng.htm
Fisheries and Oceans Canada, 2013. American Lobster, *Homarus americanus*, Stock Status in the Southern Gulf of St. Lawrence LFA 23, 24, 25, 26A and 26B. DFO Can. Sci. Advis. Secr. Sci. Advis. Rep. 9, 1–21.
Flegel, T.W., Sritunyalucksana, K., 2011. Shrimp molecular responses to viral pathogens. Mar. Biotechnol. 13, 587–607.
Goto, A., Kurata, S., 2012. Immune response of insects and crustaceans, in: Tufail, M., Takeda, M. (Eds.), Hemolymph Proteins and Functional Peptides: Recent Advances in Insects and Other Arthropods. Bentham eBooks, pp. 62–77.
Green, B.S., Gardner, C., Hochmuth, J.D., Linnane, A., 2014. Environmental effects on fished lobsters and crabs. Rev. Fish Biol. Fish. 24, 613–638.
Greenwood, S.J., Després, B.M., Cawthorn, R.J., Lavallée, J., Groman, D.B., Desbarats, A., 2005a. Case report: outbreak of bumper car disease caused by *Anophryoides haemophila* in a lobster holding facility in Nova Scotia, Canada. J. Aquat. Anim. Health 17, 345–352.
Greenwood, S.J., Keith, I.R., Després, B.M., Cawthorn, R.J., 2005b. Genetic characterization of the lobster pathogen *Aerococcus viridans* var. *homari* by 16S rRNA gene sequence and RAPD. Dis. Aquat. Organ. 63, 237–246.
Groner, M.L., Maynard, J., Breyta, R., Carnegie, R.B., Dobson, A., Friedman, C.S., Froelich, B., Garren, M., Gulland, F.M.D., Heron, S.F., Noble, R.T., Revie, C.W., Shields, J.D., Vanderstichel, R., Weil, E., Wyllie-Echeverria, S., Harvell, C.D., 2016. Managing marine disease emergencies in an era of rapid change. Philos. Trans. R. Soc. B Biol. Sci. 371, 20150364.
Harding, G.C., 1992. American lobster (*Homarus americanus* Milne Edwards): A discussion paper on their environmental requirements and the known anthropogenic effects on their populations. Can. Tech. Rep. Fish. Aquat. Sci. 1887, vi + 16p.
Hauton, C., 2012. The scope of the crustacean immune system for disease control. J. Invertebr. Pathol. 110, 251–260.
Hazel, J.R., Prosser, C.L., 1974. Molecular mechanisms of temperature compensation in poikilotherms. Physiol. Rev. 54, 620–677.
Helluy, S.M., Beltz, B.S., 1991. Embryonic development of the American Lobster (*Homarus americanus*): quantitative staging and characterization of an embryonic molt cycle. Biol. Bull. 180, 355–371.
Hernroth, B., Sköld, H.N., Wiklander, K., Jutfelt, F., Baden, S., 2012. Simulated climate change causes immune suppression and protein damage in the crustacean *Nephrops norvegicus*. Fish Shellfish Immunol. 33, 1095–1101.
Hillyer, J.F., 2015. Insect immunology and hematopoiesis. Dev. Comp. Immunol. 58, 102–118.
Hoffmann, J.A., Reichhart, J.-M., 2002. *Drosophila* innate immunity: an evolutionary perspective. Nat. Immunol. 3, 121–126.
Hose, J.E., Martin, G.G., Gerard, A.S., 1990. A Decapod hemocyte classification scheme integrating morphology, cytochemistry, and function. Biol. Bull. 178, 33–45.
Huang, T., Zhang, X., 2013. Host defense against DNA virus infection in shrimp is mediated by the siRNA pathway. Eur. J. Immunol. 43, 137–146.

Huang, Z.-J., Kang, S.-T., Leu, J.-H., Chen, L.-L., 2013. Endocytic pathway is indicated for white spot syndrome virus (WSSV) entry in shrimp. Fish Shellfish Immunol. 35, 707–715.

Jiravanichpaisal, P., Lee, B.L., Söderhäll, K., 2006. Cell-mediated immunity in arthropods: hematopoiesis, coagulation, melanization and opsonization. Immunobiology 211, 213–236.

Jiravanichpaisal, P., Söderhäll, K., Söderhäll, I., 2004. Effect of water temperature on the immune response and infectivity pattern of white spot syndrome virus (WSSV) in freshwater crayfish. Fish Shellfish Immunol. 17, 265–275.

Jitvaropas, R., Amparyup, P., Gross, P.S., Tassanakajon, A., 2009. Functional characterization of a masquerade-like serine proteinase homologue from the black tiger shrimp *Penaeus monodon*. Comp. Biochem. Physiol. Part B Biochem. Mol. Biol. 153, 236–243.

Johansson, M.W., Keyser, P., Sritunyalucksana, K., Söderhäll, K., 2000. Crustacean haemocytes and haematopoiesis. Aquaculture 191, 45–52.

Jury, S.H., 1994. The behavior of lobster in response to reduced salinity. J. Exp. Mar. Bio. Ecol. 23–37.

Karunasagar, I., Ababouch, L., 2012. Shrimp viral diseases, import risk assessment and international trade. Indian J. Virol. 23, 141–148.

Keppel, E.A., Scrosati, R.A., Courtenay, S.C., 2012. Ocean acidification decreases growth and development in American lobster (*Homarus americanus*) larvae. J. Northwest Atl. Fish. Sci. 44, 61–66.

Kim, S., Lee, S.-H., Park, M.-H., Choi, H.-G., Park, J.-K., Min, G.-S., 2011. The complete mitochondrial genome of the American lobster, *Homarus americanus* (Crustacea, Decapoda). Mitochondrial DNA 22, 47–49.

Kornbluth, S., White, K., 2005. Apoptosis in *Drosophila*: neither fish nor fowl (nor man, nor worm). J. Cell Sci. 118, 1779–1787.

Lagerspetz, K.Y.H., Vainio, L.A., 2006. Thermal behaviour of crustaceans. Biol. Rev. Cambridge Philos. Soc. 81, 237–258.

Lawton, P., Lavalli, K.L., 1995. Postlarval, juvenile, adolescent and adult ecology, in: Factor, J.R. (Ed.), Biology of the Lobster *Homarus americanus*. Academic Press, pp. 47–88.

Lightner, D. V., Fontaine, C.T., 1975. A mycosis of the American lobster, *Homarus americanus*, caused by *Fusarium* sp. J. Invertebr. Pathol. 25, 239–245.

Linder, J.E., Owers, K.A., Promislow, D.E.L., 2008. The effects of temperature on host–pathogen interactions in *D. melanogaster*: who benefits? J. Insect Physiol. 54, 297–308.

Liu, H., Söderhäll, K., Jiravanichpaisal, P., 2009. Antiviral immunity in crustaceans. Fish Shellfish Immunol. 27, 79–88.

Lo, C.-F., Ho, C.-H., Chen, C.-H., Liu, K.-F., Chiu, Y.-L., Yeh, P.-Y., Peng, S.-E., Hsu, H.-C., Liu, H.-C., Chang, C.-F., Su, M.-S., Wang, C.-H., Kou, G.-H., 1997. Detection and tissue tropism of white spot syndrome baculovirus (WSBV) in captured brooders of *Penaeus monodon* with a special emphasis on reproductive organs. Dis. Aquat. Organ. 30, 53–72.

Lo, C.-F., Peng, S.-E., Chang, Y.-S., Kou, G.-H., 2005. White spot syndrome—what we have learned about the virus and the disease. Dis. Asian Aquac. 5, 421–433.

Maeda, M., Itami, T., Mizuki, E., Tanaka, R., Yoshizu, Y., Doi, K., Yasunaga-Aoki, C., Takahashi, Y., Kawarabata, T., 2000. Red swamp crawfish (*Procambarus clarkii*): an alternative experimental host in the study of white spot syndrome virus. Acta Virol. 44, 371–374.

Marks, H., van Duijse, J.J.A., Zuidema, D., van Hulten, M.C.W., Vlak, J.M., 2005. Fitness and virulence of an ancestral white spot syndrome virus isolate from shrimp. Virus Res. 110, 9–20.

Martin, G.G., Hose, J.E., 1995. Circulation, the blood, and disease, in: Factor, J.R. (Ed.), Biology of the Lobster *Homarus americanus*. Academic Press, pp. 464–495.

Maynard, J., van Hooidonk, R., Harvell, C.D., Eakin, C.M., Liu, G., Willis, B.L., Williams, G.J., Groner, M.L., Dobson, A., Heron, S.F., Glenn, R., Reardon, K., Shields, J.D., 2016. Improving marine disease surveillance through sea temperature monitoring, outlooks and projections. Philos. Trans. R. Soc. B Biol. Sci. 371, 20150208.

McGrath, L.L., Vollmer, S. V, Kaluziak, S.T., Ayers, J., 2016. De novo transcriptome assembly for the lobster Homarus americanus and characterization of differential gene expression across nervous system tissues. BMC Genomics 17, 63.

McLeese, D.W., 1956. Effects of temperature, salinity and oxygen on the survival of the American lobster. J. Fish. Res. Board Canada 13, 247–272.

McMahon, B.R., 1995. The physiology of gas exchange, circulation, ion regulation and nitrogen excretion: an integrative approach, in: Factor, J.R. (Ed.), Biology of the Lobster *Homarus americanus*. Academic Press, pp. 497–517.

Meehl, G.A., Stocker, T.F., Collins, W.D., Friedlingstein, P., Gaye, A.T., Gregory, J.M., Kitoh, A., Knutti, R., Murphy, J.M., Akira, N., Raper, S.C.B., Watterson, I.G., Weaver, A.J., Zhao, Z.-C., 2007. Global climate projections, in: Solomon, S., Qin, D., Manning, M., Chen, Z., Miller, H.L., Tignor, M., Averyt, K.B., Marquis, M. (Eds.), Climate Change 2007: The Physical Science Basis. Cambridge University Press, pp. 749–844.

Mercaldo-Allen, R., Kuropat, C.A., 1994. Review of American lobster (*Homarus americanus*) habitat requirements and responses to contaminant exposure. NOAA Tech. Memo. NMFS-NE-105.

Moser, J.R., Álvarez, D.A.G., Cano, F.M., Garcia, T.E., Molina, D.E.C., Clark, G.P., Marques, M.R.F., Barajas, F.J.M., López, J.H., 2012. Water temperature influences viral load and detection of white spot syndrome virus (WSSV) in *Litopenaeus vannamei* and wild crustaceans. Aquaculture 326–329, 9–14.

Murdock, C.C., Cox-Foster, D., Read, A.F., Thomas, M.B., 2014. Rethinking vector immunology: the role of environmental temperature in shaping resistance. Nat. Rev. Microbiol. 10, 869–876.

Murdock, C.C., Paaijmans, K.P., Bell, A.S., King, J.G., Hillyer, J.F., Read, A.F., Thomas, M.B., 2012. Complex effects of temperature on mosquito immune function. Proc. R. Soc. B Biol. Sci. 279, 3357–3366.

Mykles, D.L., 2011. Ecdysteroid metabolism in crustaceans. J. Steroid Biochem. Mol. Biol. 127, 196–203.

Myllymäki, H., Rämet, M., 2014. JAK/STAT pathway in *Drosophila* immunity. J.

Immunol. 79, 377–385.
Myllymäki, H., Valanne, S., Rämet, M., 2014. The *Drosophila* imd signaling pathway. J. Immunol. 192, 3455–3462.
Nowotny, M., Yang, W., 2009. Structural and functional modules in RNA interference. Curr. Opin. Struct. Biol. 19, 286–293.
Octovianus, S., Yanuhar, U., 2015. The prevalence of white spot syndrome virus on Tiger Shrimp (*Penaeus monodon*) traditional farming in Tarakan, Indonesia. J. Life Sci. Biomed. 5, 137–140.
Parry, H.E., Pipe, R.K., 2004. Interactive effects of temperature and copper on immunocompetence and disease susceptibility in mussels (*Mytilus edulis*). Aquat. Toxicol. 69, 311–325.
Pradeep, B., Rai, P., Mohan, S.A., Shekhar, M.S., Karunasagar, I., 2012. Biology, host range, pathogenesis and diagnosis of white spot syndrome virus. Indian J. Virol. 23, 161–174.
Pugh, T.L., Goldstein, J.S., Lavalli, K.L., Clancy, M., Watson, W.H., 2013. At-sea determination of female American lobster (*Homarus americanus*) mating activity: patterns vs. expectations. Fish. Res. 147, 327–337.
Qadri, S.A., Camacho, J., Wang, H., Taylor, J.R., Grosell, M., Worden, M.K., 2007. Temperature and acid-base balance in the American lobster *Homarus americanus*. J. Exp. Biol. 210, 1245–1254.
Raj, S., Vijayan, K.K., Alavandi, S. V., Balasubramanian, C.P., Santiago, T.C., 2012. Effect of temperature and salinity on the infectivity pattern of white spot syndrome virus (WSSV) in giant tiger shrimp. Indian J. Fish. 59, 109–115.
Rao, R., Bhassu, S., Bing, R.Z.Y., Alinejad, T., Hassan, S.S., Wang, J., 2016. A transcriptome study on *Macrobrachium rosenbergii* hepatopancreas experimentally challenged with white spot syndrome virus (WSSV). J. Invertebr. Pathol. 136, 10–22.
Ren, Q., Huang, Y., He, Y., Wang, W., Zhang, X., 2015. A white spot syndrome virus microRNA promotes the virus infection by targeting the host STAT. Sci. Rep. 16, 18384.
Richards, S., 2015. It's more than stamp collecting: how genome sequencing can unify biological research. Trends Genet. 31, 411–21.
Rowley, A.F., Powell, A., 2007. Invertebrate immune systems specific, quasi-specific, or nonspecific? J. Immunol. 179, 7209–7214.
Sánchez-Paz, A., 2010. White spot syndrome virus: an overview on an emergent concern. Vet. Res. 41, 43.
Shekhar, M.S., Ponniah, A.G., 2015. Recent insights into host-pathogen interaction in white spot syndrome virus infected *Penaeid* shrimp. J. Fish Dis. 38, 599–612.
Shields, J.D., 2013. Complex etiologies of emerging diseases in lobsters (*Homarus americanus*) from Long Island Sound. Can. J. Fish. Aquat. Sci. 70, 1576–1587.
Shields, J.D., 2011. Diseases of spiny lobsters: a review. J. Invertebr. Pathol. 106, 79–91.
Shields, J.D., Stephens, F.J., Jones, B., 2006. Pathogens, parasites and other symbionts, in: Phillips, B. (Ed.), Lobsters: Biology, Management, Aquaculture and Fisheries. Blackwell Publishing, pp. 146–204.

Söderhäll, I., 2016. Crustacean hematopoiesis. Dev. Comp. Immunol. 58, 129–141.
Söderhäll, K., Cerenius, L., 1992. Crustacean immunity. Annu. Rev. Fish Dis. 2, 3–23.
Soto, A.M., Shervette, V.R., Lotz, J.M., 2001. Transmission of white spot syndrome virus (WSSV) to *Litopenaeus vannamei* from infected cephalothorax, abdomen, or whole shrimp cadaver. Dis. Aquat. Organ. 45, 81–87.
Spees, J.L., Chang, S.A., Snyder, M.J., Chang, E.S., 2002. Thermal acclimation and stress in the American lobster, *Homarus americanus*: equivalent temperature shifts elicit unique gene expression patterns for molecular chaperones and polyubiquitin. Cell Stress Chaperones 7, 97–106.
Sritunyalucksana, K., Söderhäll, K., 2000. The proPO and clotting system in crustaceans. Aquaculture 191, 53–69.
Steenbergen, J.F., Steenbergen, S.M., Schapiro, H.C., 1978. Effects of temperature on phagocytosis in *Homarus americanus*. Aquaculture 14, 23–30.
Stewart, J.E., 1984. Lobster diseases. Helgolander Meeresunters 37, 243–254.
Sweet, M.J., Bateman, K.S., 2015. Diseases in marine invertebrates associated with mariculture and commercial fisheries. J. Sea Res. 104, 16–32.
Talbot, P., Helluy, S.M., 1995. Reproduction and embryonic development, in: Factor, J.R. (Ed.), Biology of the Lobster *Homarus americanus*. Academic Press, pp. 177–216.
Tassanakajon, A., Somboonwiwat, K., Supungul, P., Tang, S., 2013. Discovery of immune molecules and their crucial functions in shrimp immunity. Fish Shellfish Immunol. 34, 954–967.
Templeman, W., 1940. Embryonic developmental rates and egg-laying of Canadian lobsters. J. Fish. Res. Board Canada 5, 71–83.
Theopold, U., Schmidt, O., Söderhäll, K., Dushay, M.S., 2004. Coagulation in arthropods: defence, wound closure and healing. Trends Immunol. 25, 289–294.
Trang, N., Hoa, K., 2009. Black gill disease of cage-cultured ornate rock lobster *Panulirus ornatus* in central Vietnam caused by *Fusarium* species. Aquac. Asia XIV, 35–37.
Treece, G.D., 2000. Shrimp maturation and spawning. UJNR Tech Rep 28, 121–134.
Usman, M.G., Rafii, M.Y., Ismail, M.R., Malek, M.A., Latif, M.A., Oladosu, Y., 2014. Heat shock proteins: functions and response against heat stress in plants. Int. J. Sci. Technol. Res. 3, 204–218.
Vargas-Albores, Hinojosa-Baltazar, Portillo-Clark, Magallon-Barajas, 1998. Influence of temperature and salinity on the yellowleg shrimp, *Penaeus californiensis*, prophenoloxidase system. Aquac. Res. 29, 549–553.
Vazquez, L., Alpuche, J., Maldonado, G., Agundis, C., Pereyra-Morales, A., Zenteno, E., 2009. Review: Immunity mechanisms in crustaceans. Innate Immun. 15, 179–88.
Verbruggen, B., Bickley, L.K., Santos, E.M., Tyler, C.R., Stentiford, G.D., Bateman, K.S., van Aerle, R., 2015. *De novo* assembly of the *Carcinus maenas* transcriptome and characterization of innate immune system pathways. BMC Genomics 16, 458.

Verbruggen, B., Bickley, L.K., van Aerle, R., Bateman, K.S., Stentiford, G.D., Santos, E.M., Tyler, C.R., 2016. Molecular mechanisms of white spot syndrome virus infection and perspectives on treatments. Viruses 8, 1–29.

Waddy, S.L., Aiken, D.E., Kleijn, D., 1995. Control of growth and reproduction, in: Factor, J.R. (Ed.), Biology of the Lobster *Homarus americanus*. Academic Press, pp. 217–266.

Wahle, R.A., Fogarty, M.J., 2006. Growth and development: understanding and modelling growth variability in lobsters, in: Phillips, B. (Ed.), Lobsters: Biology, Management, Aquaculture and Fisheries. Blackwell Publishing, pp. 1–44.

Wahle, R.A., Incze, L.S., Fogarty, M.J., 2004. First projections of American lobster fishery recruitment using a settlement index and variable growth. Bull. Mar. Sci. 74, 101–114.

Waller, J.D., Wahle, R.A., McVeigh, H., Fields, D.M., 2016. Linking rising pCO2 and temperature to the larval development and physiology of the American lobster (*Homarus americanus*). ICES J. Mar. Sci. fsw154.

Wang, B., Li, F., Dong, B., Zhang, X., Zhang, C., Xiang, J., 2006. Discovery of the genes in response to white spot syndrome virus (WSSV) infection in *Fenneropenaeus chinensis* through cDNA microarray. Mar. Biotechnol. 8, 491–500.

Wang, X.-W., Wang, J.-X., 2013. Pattern recognition receptors acting in innate immune system of shrimp against pathogen infections. Fish Shellfish Immunol. 34, 981–989.

Worden, M.K., Clark, C.M., Conaway, M., Qadri, S.A., 2006. Temperature dependence of cardiac performance in the lobster *Homarus americanus*. J. Exp. Biol. 209, 1024–1034.

Xu, J., Han, F., Zhang, X., 2007. Silencing shrimp white spot syndrome virus (WSSV) genes by siRNA. Antiviral Res. 73, 126–131.

You, X.X., Su, Y.Q., Mao, Y., Liu, M., Wang, J., Zhang, M., Wu, C., 2010. Effect of high water temperature on mortality, immune response and viral replication of WSSV-infected *Marsupenaeus japonicus* juveniles and adults. Aquaculture 305, 133–137.

Young-Lai, W.W., Charmantier-Daures, M., Charmantier, G., 1991. Effect of ammonia on survival and osmoregulation in different life stages of the lobster *Homarus americanus*. Mar. Biol. 110, 293–300.

Zwart, M.P., Dieu, B.T.M., Hemerik, L., Vlak, J.M., 2010. Evolutionary trajectory of white spot syndrome virus (WSSV) genome shrinkage during spread in Asia. PLoS One 5, e13400.

2.0 IMPACT OF WATER TEMPERATURE ON IMMUNE-RELATED GENE EXPRESSION OF *Homarus americanus* EXPERIMENTALLY INFECTED WITH WHITE SPOT SYNDROME VIRUS

2.1 Abstract

The American lobster, *Homarus americanus*, inhabits ocean waters that fluctuate between 0 ^{o}C and 20 ^{o}C. Water temperature can influence processes such as larval development, growth, and reproduction. The full impact of these temperature variations on the immune response of *H. americanus* is unknown. White spot syndrome virus (WSSV) is currently one of the most virulent pathogens affecting the farmed shrimp aquaculture industry; however, a considerable number of other crustacean hosts also exhibit varying degrees of susceptibility. The present study used an injection challenge model to explore the molecular immune response to WSSV infection in American lobster, *H. americanus*, held at four different temperatures (10 ^{o}C, 15 ^{o}C, 17.5 ^{o}C and 20 ^{o}C). A decline in clinical condition (measured via total haemocyte concentration) and an increase in WSSV viral amplification (measured via WSSV-qPCR) was observed in WSSV infected *H. americanus* held at warmer temperatures (17.5 ^{o}C and 20 ^{o}C) compared to colder temperatures (10 ^{o}C and 15 ^{o}C). A lobster specific microarray was used to monitor transcriptomic changes for 14,592 genes during viral challenge. Hepatopancreas mRNA revealed 771 significantly differentiated genes between control and infected *H. americanus* one and two-weeks post infection (PI) across all temperatures. Microarray results were verified via RT-qPCR. At 15 ^{o}C, C-type lectin was downregulated 0.54 and 0.93 fold one and two-weeks PI respectively. At 17.5 ^{o}C prolyl-4-hydroxylase-alpha was down regulated in infected animals relative to controls and at 20 ^{o}C a Pol-like protein was down-regulated one and two-weeks PI.

Other differentially expressed genes included, several ribosomal proteins (L27a, L13, L11, L39), mitogen-activated protein kinase organizer 1, prolyl-4-hydroxylase-alpha, laminin subunit gamma-3, short-chain dehydrogenase and acute phase serum amyloid A. Overall results from this study are helping to characterize temperature dependent changes in *H. americanus* viral immunity.

2.2 Introduction

In recent years, global climate change, and its resulting impact on marine environments has become increasingly important. In 2001, the Intergovernmental Panel on Climate Change (IPCC) predicted a 1-7 ^{o}C increase in mean global temperature over the next 100 years (IPCC, 2001). Data already suggests that climate change is impacting our marine environments through increased water temperature, altered oceanic circulation, increased ocean stratification, increased CO_2 levels and decreased sea ice (Burge et al., 2014). Waller et al., (2016) recently examined the joint effects of the IPCC predicted temperature and pCO_2 levels in *Homarus americanus* larvae and found that temperature had the greatest adverse effects on larval survival. Increased temperature has also been identified as the prominent driver of mass scale coral reef bleaching events along the coast of Australia and Dermo disease *Perkinsus marinus* outbreaks in U.S. oyster populations (Burge et al., 2014). Mean annual bottom temperatures in the Gulf of Maine above 8–10 ^{o}C have been found to increase the prevalence of epizootic shell disease among *H. americanus* (Maynard et al., 2016). Changes in temperature impact marine organisms, and the commercial fisheries they support, by influencing

basic biological functions such as survival, growth, reproduction, immune function and even frequency of disease (Burge et al., 2014; Doney et al., 2012).

White spot syndrome virus, a double-stranded DNA virus belonging to the Nimaviridae virus family, is currently one of the largest impediments to the growth of the shrimp aquaculture industry (Sánchez-Paz, 2010). In shrimp, WSSV is highly virulent, with infections often resulting in 100% mortality within 3-10 days (Pradeep et al., 2012). Furthermore, the virus appears to be non-specific, with over 93 other crustacean species reported as susceptible via natural or experimental infection (Sánchez-Paz, 2010; Sweet and Bateman, 2015). The World Organization for Animal Health (Office International de Epizootic; OIE) and the National Aquatic Animal Health Program (Canada; NAAHP) consider WSSV a notifiable disease based on its potential to infect all crustacean decapods. *H. americanus* and the European lobster *Homarus gammarus*, two commercially valuable species, are known to be experimentally susceptible to WSSV (Bateman et al., 2012a; Clark et al., 2013c). Previous research shows that at 20 ^{o}C, *H. americanus* produces a targeted molecular immune response to WSSV injection (Clark et al., 2013c). *Per os* feeding trials at 10 ^{o}C suggest that *H. americanus* can only become infected with WSSV following an unnatural route of exposure such as injection (Byrne, unpublished). In *H. gammarus* viral replication and disease have been demonstrated following both experimental injection and feeding trials conducted at 15 ^{o}C (Bateman et al., 2012a, 2012b).

The thermal preference for WSSV is believed to be between 15 ^{o}C and 30 ^{o}C (Moser et al., 2012; Sun et al., 2014). In *Penaeus* shrimp species, a group known to

be highly susceptible to WSSV, temperatures above 30 ^{o}C and below 15 ^{o}C result in reduced mortality rates (Lua and Hirono, 2015; Raj et al., 2012; You et al., 2010). On a molecular level, the ridgetail white prawn, *Exopalaemon carincauda*, infected with WSSV at 25 ^{o}C showed an increase in expression of anti-apoptosis genes and a decrease in expression of genes involved in regulation of cell death compared to animals infected at 18 ^{o}C (Sun et al., 2014). This suggests that during early infection at warmer temperatures (up to 30 ^{o}C) the virus may inhibit host cell death to benefit its propagation (Sun et al., 2014). Increased temperatures are also speculated to increase WSSV susceptibility by reducing host immune defence mechanisms (Jiravanichpaisal et al., 2004). The efficacy of an animal's immune response is in part influenced by general temperature-dependent physiological changes occurring in the host (Linder et al., 2008). For example, yellow leg shrimp *Penaeus californiensis*, acclimated to 18 ^{o}C have been found to have a higher concentration of prophenoloxidase (proPO), a major component of invertebrate immunity, compared to animals acclimated to 32 ^{o}C, regardless of the presence of a pathogen (Vargas-Albores et al., 1998). In *H. americanus*, phagocytosis occurs more rapidly at 10 ^{o}C and 15 ^{o}C (temperatures within the thermal preference of the animal) compared to 4 ^{o}C, suggesting that temperatures outside of an animal's thermal preference may impact the ability to overcome pathogens (Le Moullac and Haffner, 2000). The underlying molecular mechanisms by which temperature is shaping immunity, specifically in *H. americanus*, are poorly understood.

A previously established viral model of disease in *H. americanus* (Clark et al., 2013c) presents an opportunity to study the interaction between temperature,

WSSV and host immunity on a molecular level. The purpose of this study was to explore the influence that a range of temperatures (10 ^{o}C, 15 ^{o}C, 17.5 ^{o}C, and 20 ^{o}C) might have on the molecular immune response of *H. americanus* experimentally infected with WSSV. Additionally, a variety of clinical and molecular tools will be used to characterize WSSV infection in the host at varying temperatures and elucidate temperature specific transcriptomic differences between WSSV-infected *H. americanus* at different temperatures. This study is the first to provide insights as to how temperature may be impacting host-WSSV dynamics in *H. americanus*.

2.3 Materials and Methods

2.3.1 Animal Holding

Adult, male, market sized American lobster (*Homarus americanus*) (n = 48, wt: 568 g ± 18.63 g) were purchased from a local commercial seafood supplier (Clearwater Seafoods®, Bedford, NS, Canada) and housed at the Gulf Biocontainment Unit-Aquatic Animal Health Laboratory (GBU-AAHL; Fisheries and Oceans Canada, Charlottetown, PEI, Canada). Upon arrival, *H. americanus* were assigned unique identification, labeled (Adhesive Systems Incorporated, Frankfort IL, USA) and randomly assigned (using a computer generated random number list) to individual compartments in a perforated plastic tote (BioNovations, Antigonish, NS, Canada). Each tote housed six lobsters. The totes were randomly assigned to one of four 400 L tanks maintained at 8 ^{o}C (Waterline®, Santa Ana, CA, USA). Each tank held two totes yielding a total of 12 lobsters per tank. *H. americanus* received a one-week acclimation period at 8 ^{o}C. Water temperature was then increased in 1 ^{o}C per day increments, from 8 ^{o}C to 10 ^{o}C for the first tank, to 15

^{o}C for the second, to 17.5 ^{o}C for the third and to 20 ^{o}C for the fourth. *H. americanus* received a second one-week acclimation period at their final temperatures (10 ^{o}C, 15 ^{o}C, 17.5 ^{o}C and 20 ^{o}C) before beginning the infection trial.

All *H. americanus* tanks were supported by an independent recirculating artificial seawater (ASW) system maintained at a salinity of 31 ± 1 ppt (Instant Ocean®, Spectrum Brands, Blacksburg, VA, USA). Each tank system was equipped with a 25 µm filter (Ocean Clear, Red Sea®, Houston, TX, USA), UV filter (Emperor® Smart UV Sterilizer, Langley, BC, Canada), protein skimmer, (Berlin, Red Sea®, Houston, TX, USA) and biofiltration using floating matrix (1" Bio-balls®, Pentair, Langley, BC, Canada). The recirculating ASW system was provided with 10-15% water replacement per day. Temperature (programmed temp. ± 0.1 ^{o}C), pH (8.1 – 8.4) and salinity (31 ± 1 ppt) were recorded daily. Oxygen concentration (8.0 – 8.7 mg/L), nitrite (<1.0 mg/L), nitrate (<4 mg/L) and total ammonia nitrogen (<1.0 mg/L) were recorded weekly. Nitrite, nitrate and total ammonia nitrogen were checked using HACH® kits (London, ON, Canada) and read on a spectrophotometer (HACH® model DR 5000, London, ON, Canada). *H. americanus* were fed three times per week for the duration of the trial. They received thawed pieces of haddock and mussel. *H. americanus* feed was acquired from commercial suppliers (Charlottetown, PE, Canada).

Specific pathogen free (SPF) Pacific white shrimp *Litopenaeus vannamei,* used to generate WSSV inoculum (Section 2.3.3), were obtained from the Oceanic Institute (Waimanalo, HI, USA) and housed at GBU-AAHL facility. *L. vannamei* were maintained in a semi-open multi-tank recirculating ASW system (Aquabiotech,

Coaticook, QC, Canada). The aquaria (9 L) were maintained at 27 ^{o}C (± 1 ^{o}C) and a salinity of 31 ppt (Instant Ocean®, Spectrum Brands, Blacksburg, VA, USA). *L. vannamei* were fed a maintenance diet of approximately 2 - 4% body weight (Ziegler® shrimp feed, Gardners, PA, USA).

Waste material generated from the study was decontaminated before disposal. Effluent wastewater was autoclaved, and animal carcasses were incinerated. Laboratory gloves, clothing, and disposable materials were autoclaved. Work areas were bleached (500 ppm, Javex), rinsed with water, and sprayed with 70% isopropanol following work. Work involving WSSV was conducted within biocontainment facilities certified aquatic containment level 3 (AQC3) *in vivo* by the Canadian Food Inspection Agency as per the Canadian aquatic animal pathogen standards (CFIA Biohazard Containment and Safety, 2010). Live animal based projects at GBU-AAHL were monitored and audited by the Fisheries and Oceans Regional Animal Care Committee.

2.3.2 Health Assessments

H. americanus health assessments (Appendix A Fig. A1) were conducted three days post arrival. Briefly, defensive posture, tail tone, eyestalk withdrawal and shell hardness of *H. americanus* was examined. *H. americanus* were weighed, and haemolymph (~2 mL) was collected. *H. americanus* were screened for bacterial and ciliated protist infection by culturing haemolymph in trypticase soy broth (TSB), phenylethyl alcohol media (PEA) and modified marine axenic medium (MMAM) (Acorn et al., 2011). Haemolymph refractive index was recorded using a handheld refractometer (R2 Mini, Reichert Technologies®, Depew, NY, USA). Pleopod and

haemolymph samples were collected and tested for WSSV using qPCR (Section 2.3.4). Haemolymph was also used to calculate total haemocyte concentration (THC). To calculate THC, 500 µL of haemolymph was placed in 4.5 mL of filtered ASW and formalin solution (37% formaldehyde) and inverted gently ten times for fixation. Fixed haemocytes were placed onto a Bright-Line™ Haemocytometer (Hausser Scientific, Horsh PA, USA) and counted under a light microscope (Nikon Eclipse 80I, Nikon Canada Inc., Mississauga, ON). Only healthy and confirmed WSSV-negative *H. americanus* were used for the infection trial; no WSSV positive individuals were identified during pre-trial assessments.

2.3.3 Preparation of WSSV Inoculum

WSSV inoculum was prepared at the GBU-AAHL facility. WSSV infected shrimp tissue generated from previous infection challenges conducted at the GBU-AAHL facility was used (Clark et al., 2013c). Previous infection challenges used WSSV infected shrimp tissue (isolate AF332093) obtained from Dr. Donald Lightner at the OIE reference laboratory for WSSV at the University of Arizona (Tucson, USA) (Clark et al., 2013c). WSSV was first passed through *L. vannamei* as a bioassay to assess the viability of WSSV before infection trial with *H. americanus*.

WSSV infected shrimp tissue (250 mg) was thawed on ice, minced using a scalpel, and placed into a 1.5 mL microfuge tube. Tissue was homogenized with phosphate buffered saline (PBS; 0.1 M, pH 7.4), using a disposable pestle for two mins and then centrifuged (Eppendorf centrifuge 5430R, Hamburg, Germany) at 5000 x *g* for 20 mins at 4 ^{o}C. The supernatant was collected and pipetted into a new 1.5 mL microfuge tube. The original sample was centrifuged a second time at 5000 x

g for 20 mins at 4 ^{o}C. The supernatant was collected and pipetted into the previous 1.5 mL tube. The supernatant was diluted 1:4 (supernatant: PBS), vortexed, filtered (0.45 µM, Acrodisc® syringe filters, Pall Corporation, Mississauga, ON, Canada) and placed into a 50 mL tube. Inoculum, comprising of the filtered supernatant and PBS, was collected into a 1 mL syringe with 25 G needle and placed on ice for *L. vannamei* inoculation.

L. vannamei (n=4) were removed from their aquarium, held under a net and 70% alcohol was applied to back segments, 2 through 5, via a Q-tip® applicator. *L. vannamei* received a single 75 µL injection of WSSV inoculum between tail segments 3 and 4. Inoculated *L. vannamei* were placed in a 40 L aquarium with static ASW at 27± 1 ^{o}C. The aquarium contained an air stone and a water filter comprised of wool and granular activated charcoal (GAC; Univar, Dartmouth, NS, Canada). Approximately 20 – 30 % of the water volume was manually exchanged every 1 - 2 days. Following inoculation, *L. vannamei* were monitored every four hours or more frequently until death. Dead and moribund *L. vannamei* were immediately removed from the aquarium, weighed and stored at -80 ^{o}C. WSSV-qPCR viral quantification was conducted from DNA extracted from a distal portion of the abdomen collected from each shrimp (Section 2.3.4). The remainder of tissue not used for WSSV-qPCR was used to generate fresh inoculum (in the same manner described above). Fresh inoculum was stored at -80 ^{o}C for subsequent *H. americanus* infection challenge (Section 2.3.5) and negative staining bioassay (Chapter 3).

2.3.4 WSSV-qPCR

Detection of WSSV via qPCR was conducted using DNA extracted from haemolymph and various tissues (*H. americanus* and *L. vannamei*). DNA was extracted using a DNeasy® Blood & Tissue Kit (Qiagen®, Toronto, ON, Canada) as per the manufacturer's instructions (Appendix B). Briefly, 30 mg of tissue or 100 µL of haemolymph tissue was lysed overnight at 56 ^{o}C using 20 µL of proteinase K. Buffering conditions were adjusted using 180 µL of ATL buffer (if using tissue), 200 µL of AL buffer and 200 µL of 100% EtOH to ensure optimal DNA binding conditions. Lysate was then pipetted onto a DNeasy® mini spin column and centrifuged (Eppendorf centrifuge 5430R, Hamburg, Germany) at 6000 x *g* for 1 min, for DNA to bind to the DNeasy® membrane. DNA contaminants and enzyme inhibitors were removed in two wash steps using AW1 buffer (500 µL) centrifuged at 6000 x *g* for 1 min followed by AW2 buffer (500 µL) centrifuged at 20,000 x *g* for 3 min. The DNA was then eluted in 100 µL of AE buffer, aliquoted (2 x 50 µL) and stored at -20 ^{o}C until required for qPCR.

Previously designed primers (Clark et al., 2013c) targeting the VP28 gene region of WSSV were used to amplify WSSV DNA. A single qPCR reaction consisted of 12.5 µL of TaqMan® Universal PCR master mix (Applied Biosystems ™, CA, USA), 2 µL of DNA extract, 0.75 µL of 10 µM forward primer F1-WSDvp28 (5'GTGACCAACACCATCGAAAC3'), 0.75 µL of 10 µM reverse primer R1-WSDvp28 (5'TGAAGTAGCCTGATCCAACC3'), 0.375 µL of 10 µM TaqMan® probe P1-WSDvp28 (5'CCTCCGCATTCCTGTGACTGC3'-FAM/TAMRA), and 8.6 µL of nuclease-free water (UltraPure™ DNase/RNase-Free

Distilled water, Applied Biosystems ™, CA, USA) to yield a final reaction volume of 25 µL. Reactions were carried out on a Chromo4™ Real-Time PCR system (Bio-Rad Laboratories, CA, USA) as follows: 50 °C for 2 min, 95 °C for 10 min, 40 cycles of 95 °C for 15 sec, 60 °C for 1 min, plate read, and a final incubation at 20 °C for 5 min. A plasmid standard (10^7 viral copies) was diluted with nuclease-free water and used to quantify WSSV viral titre in samples. Viral copy number and cycle threshold (C_T) value were recorded using Opticon Monitor™ software (Bio-Rad Laboratories, CA, USA).

2.3.5 WSSV Lobster Infection Challenge

A total of 48.8 µL of WSSV-qPCR confirmed and quantified infected shrimp tissue homogenate (fresh inoculum) was thawed on ice and diluted with PBS (1951 µL) to yield an equivalent of 10^4 plasmid copies/µL. Diluted WSSV shrimp tissue homogenate was filtered (0.45 µM, Acrodisc® syringe filters, Pall Corporation, Mississauga, ON, Canada) and 200 µL of filtrate was loaded into a 1 mL syringe with 25 G needle for inoculation. A total of 12 syringes were prepared in advance (8 WSSV and 4 non-infected shrimp tissue extract). Loaded syringes were kept on ice. *H. americanus* were randomly assigned to receive either a 200 µL injection of 10^4 WSSV plasmid copies/µL or 200 µL of non-infected shrimp tissue homogenate (control). *H. americanus* were injected through the ventral cuticle in the second tail segment, off centre (on the right side) to avoid damaging the ventral nerve. The needle was angled and inserted approximately 1.5 cm into the tail. The anterior ventral abdomen area was sprayed with 70% alcohol prior to inoculation.

2.3.6 Infection Trial Sampling

H. americanus haemolymph samples (800 µL) were repeatedly collected from all individuals 12, 24, 48, 96, 144, 168, 192, 240, 288 and 336 hours post inoculation (PI). Haemolymph was collected from the third or fourth tail segment on the ventral abdomen slightly off medial relative to the ventral nerve cord. Haemolymph was collected to monitor clinical condition via THC (Section 2.3.2) and WSSV-qPCR (Section 2.3.4). THC and WSSV-qPCR results were analyzed for statistical significance using repeated measures two-way ANOVA. Behaviour such as responsiveness to food, defensive posture, and eyestalk withdrawal was also assessed during sampling and feeding events to corroborate THC and WSSV-qPCR data. One-week PI (168 h), four infected lobsters were randomly selected to be necropsied from each tank. The remaining 8 lobsters in each tank (4 controls & 4 infected) were necropsied two-weeks PI (336 h).

Immediately prior to euthanasia, *H. americanus* were weighed and final haemolymph samples were collected for THC and WSSV-qPCR. *H. americanus* were euthanized as per Clark et al. (2013a) by severing the ventral nerve cord anterior to the chelicerae coxae as well as near the first tail segment. Hepatopancreas (~100 mg each) was collected, homogenized (OMNI International, Kennesaw, GA, USA) in 1 mL of Tri-reagent® solution (Sigma-Aldrich, Oakville, ON, Canada), flash frozen in liquid nitrogen and stored at -80 ^{o}C for RNA extraction (Section 2.3.7). A portion of antennal gland was also collected and stored for RNA extraction. A portion (~1 mm^3) of antennal gland, hepatopancreas and cuticular epithelium were carefully excised and placed into 4 mL of 2.5% glutaraldehyde

(SPI® Supplies, Toronto, ON, Canada) in 0.1 M phosphate buffer for transmission electron microscopy (Chapter 3). A total of 12 tissues, cuticular epithelium, antennal gland, pleopod, heart, gill, hepatopancreas, intestine, stomach, gonad, brain, nerve cord and tail muscle were collected and preserved in 10% neutral buffered formalin (NBF; Sigma-Aldrich, Oakville, ON, Canada) for subsequent histological analysis (Chapter 3). Antennal gland, cuticular epithelium, heart, gonad, hepatopancreas, gill, intestine and pleopod tissue (~1 cm^3 each) were also collected and placed in 95% EtOH for WSSV-qPCR testing (Chapter 3). Lastly, tail muscle (~25 g) was excised, placed in a 2 oz. sterile Whirl-Pak® bag (Cole-Parmer, Montreal, QC, Canada), flash frozen using liquid nitrogen and stored at -20 ^{o}C.

2.3.7 RNA Extraction

RNA was extracted from hepatopancreas tissue using a combined chloroform and RNeasy® Mini Kit (Qiagen®, Toronto, ON, Canada) protocol. Briefly, samples were thawed and chloroform (200 µL per 1 mL of Tri-reagent® solution) was added. Samples were inverted 15 times, incubated at room temperature for three mins, and then centrifuged at 12 000 x *g* (Beckmann Allegra 25R Centrifuge, Beckmann Coulter, Brea, CA, USA) for 15 min at 4 ^{o}C. Supernatant (600 µL) was collected and placed in a new 1.5 mL microfuge tube containing 70% EtOH (600 µL). The remainder of RNA extraction was completed according to RNeasy® Mini Kit (Qiagen®, Toronto, ON, Canada) manufacturer's instructions. Samples were mixed via pipetting, added to an RNeasy® spin column and centrifuged (Eppendorf 5415R Centrifuge, Eppendorf, Hamburg, Germany) at 8000 x *g* for 30 sec in order for total RNA to bind to the RNeasy® spin column membrane. RNA contaminants were

removed in two wash steps using RW1 buffer (350 µL) and RPE buffer (500 µL) centrifuged 8000 x *g* for 30 sec. A DNase® I reaction buffer treatment (80 µL; Qiagen®, Toronto, ON, Canada) was added to the column and centrifuged at 8000 x *g* for 30 sec in between the buffered washes to degrade any contaminated DNA. Total RNA was eluted using 60 µL of nuclease-free water (UltraPure™ DNase/RNase-Free Distilled water, Applied Biosystems™, CA, USA). 2 µL of total RNA was diluted 1/5 with nuclease-free water for total RNA spectrophotometric quantification using the NanoDrop ND-1000 (Thermo Fisher Scientific, Waltham, MA, USA). RNA quantification was conducted in triplicate for each sample. An absorbance ratio of 260/280 ≥ 1.9 was considered pure RNA. RNA quality was also assessed using a Bioanalyzer® capillary electrophoretic chip system (Agilent®, Santa Clara, CA, USA) examining 18S and 28S ribosomal RNA peaks. Remaining RNA was aliquoted and stored at -80 ^{o}C to be used for microarray and RT-qPCR analysis.

2.3.8 cDNA/aRNA Synthesis for Microarray

Complementary DNA (cDNA) was synthesized using 20 µg of extracted hepatopancreas RNA using an Invitrogen SuperScript™ Plus Indirect cDNA Labeling Kit (Life Technologies, Burlington, ON, Canada) according to manufacturer instructions. For each sample the volume for 20 µg of total RNA was adjusted using a miVac DNA concentrator™ (Genevac Ltd., Ipswich, England). Samples were centrifuged at 250 x *g* at 50 ^{o}C until total RNA volume was ≤ 16 µL. For samples adjusted to < 16 µL, nuclease-free water (UltraPure™ DNase/RNase-Free Distilled water, Applied Biosystems™, CA, USA) was added to make the final

volume 16 µL. A total of 2 µL of anchored oligo(dT)20 primer (2.5 µg/µL) was added to the total RNA, then incubated at 70 ^{o}C for 5 min in a DNA Engine thermal cycler with heated lid (Bio-Rad Laboratories Inc., CA, USA). Samples were then placed on ice and a master mix comprised of 6 µL 5X First-Strand buffer, 1.5 µL 0.1M DTT, 1.5 µL dNTP mix, 1.0 µL RNaseOUT™ and 2.0 µL SuperScript™ III Reverse Transcriptase was added yielding a total reaction volume of 30 µL. Reverse transcription reactions were incubated at 46 ^{o}C for 3 hours. Once cDNA was synthesized, RNA was degraded with 15 µL of 1 M NaOH and incubated at 70 ^{o}C for 10 mins. Samples were neutralized with 15 µL of HCL. The cDNA was then purified using Invitrogen SuperScript™ Plus Indirect cDNA Labeling Systems manufacturers spin column protocol. Briefly, neutralized cDNA was added to 700 µL of binding buffer, mixed via inversion, transferred to a Low-Elution volume spin column and centrifuged at 3300 x *g* for 1 min (Eppendorf 5415R Centrifuge, Eppendorf, Hamburg, Germany). Wash buffer (600 µL) was added and sample was centrifuged twice at 10 000 x *g* for 30 sec and then placed in a new collection tube. cDNA was eluted with 30 µL of DEPC treated H_2O. 1 µL of cDNA was diluted 1/5 with nuclease-free water for spectrophotometric quantification using the NanoDrop ND-1000. The remainder of cDNA was stored at -80 ^{o}C until cDNA labeling and microarray hybridization.

Reference antisense RNA (aRNA) was generated by Clark et al. (2013b) from 5 µg of pooled *H. americanus* hepatopancreas total RNA. aRNA was synthesized via reverse transcription and purified using an Amino Allyl Message

AMP™ II aRNA Amplification Kit (Ambion®, Austin TX, USA) according to manufacturer instructions.

2.3.9 cDNA/aRNA labeling for Microarray

Purified first strand cDNA was labeled using an Invitrogen SuperScript™ Plus Indirect cDNA labeling System and Alexa Fluor® 555 dye (Life Technologies, Burlington, ON, Canada). cDNA was thawed and adjusted to 3 µL using the miVac DNA concentrator™ (Genevac Ltd., Ipswich, England) set to 50 ^{o}C and 250 g. 5 µL of 2X Coupling buffer was added to concentrated cDNA. Room temperature dimethyl sulfoxide (DMSO; 10 µL) was added to a vial of Alexa Fluor® 555 dye to reconstitute the dye. DMSO/dye mixture (2.5 µL) was then added to each sample and incubated in darkness at room temperature for 2 hours. Labeled cDNA was then re-purified according to Invitrogen SuperScript™ Plus Indirect cDNA labeling Systems manufacturers spin column protocol (Section 2.3.8). cDNA was eluted with 30 µL of DEPC treated H_2O. 1 µL of cDNA was diluted 1/5 with nuclease-free water for spectrophotometric quantification using the NanoDrop ND-1000 and the remainder was stored at 4 ^{o}C until hybridization.

aRNA was labeled using Alexa Fluor® 647 dye (Life Technologies, Burlington, ON, Canada), MEGAclear™ Kit (Ambion®, Austin TX, USA) and cDNA filter cartridges (Ambion®, Austin TX, USA). aRNA (12 µg) volume was adjusted to 0.5 µL using the miVac DNA concentrator™ (Genevac Ltd., Ipswich, England) set to 50 ^{o}C and 250 g. Coupling buffer (9 µL) was added to the concentrated aRNA. Room temperature DMSO (11 µL) was added to a vial of Alexa Fluor® 647 dye to reconstitute the dye. Entire DMSO/dye mixture was then added

to the aRNA and incubated in darkness at room temperature for 2 hours. aRNA was re-purified by adding 105 µL of aRNA binding solution and 75 µL of 100% EtOH. Reaction was added to a cDNA low elution column and centrifuged at 10 000 x *g* for 1 min (Eppendorf 5415R Centrifuge, Eppendorf, Hamburg, Germany). Flow-through was discarded, 500 µL of wash solution was added, and centrifuged twice at 10 000 x *g* for 1 min. The flow-through was discarded and column was placed in a new collection tube. For elution, 10 µL of 55 ^{o}C nuclease-free water was added and sample was incubated at 55 ^{o}C for 2 mins and then centrifuged at 10 000 x *g* for 1.5 min. Elution was repeated a second time resulting in a two-step elution. 1 µL of aRNA was diluted 1/5 with nuclease-free water for spectrophotometric quantification using the NanoDrop ND-1000 and remainder was stored at 4 ^{o}C for until hybridization.

aRNA was fragmented prior to hybridization using a 10X Fragmentation Kit (Ambion®, Austin TX, USA). 10X fragmentation solution (1 µL) was added to aRNA and incubated for 10 mins at 70 ^{o}C. Fragmentation was terminated with 1 µL of stop solution.

2.3.10 Microarray

A previously designed microarray platform was used (Clark et al., 2013b). Arrays were designed using a combination of publicly available gene sequences and expressed sequence tags (EST) determined from a *H. americanus* cDNA library comprised of multiple male and female *H. americanus* tissues from various physiological conditions (Towle and Greenwood, unpublished). A total of 15 864 unique sequences were identified; of which 14 592 (50 mer) probes with high

binding specificity, GC content and annealing temperature were designed. Probes were designed using Array Designed 4 software (Premier Biosoft International, CA, USA), and used to construct the array (Towle and Greenwood, unpublished). Probes were synthesized by Integrated DNA Technologies (Coralville, IA, USA), submitted to the Vancouver Prostate Centre DNA Microarray Facility (Vancouver, BC, CA) for printing onto Erie C28 aminosilane coated glass slides (2 arrays per slide) using a Qarraymax arrayer. Oligonucleotide printing quality was monitored using a 9 mer Hybridization GenePix 4200 AL Scanner (Molecular Devices, Sunnyvale, CA, USA) and visualized with ImaGene version 8.0.1 (BioDiscovery Inc., CA, USA). In total, microarrays contained 14,592 *H. americanus* sequences, 210 Sigma Alien DNA controls, 78 Green Florescent Protein (GFP) controls, 80 GFP landmarks, and 416 buffer controls; yielding a total of 15,376 spots on the array.

2.3.11 Microarray Preparation and Hybridization

Hepatopancreas mRNA was extracted (Section 2.3.7) from each lobster in the study and hybridized independently, yielding a total of 48 hybridization reactions. Hybridization reactions were performed on a Tecan 400 HS Pro hybridization system (Tecan, NC, USA). A pre-hybridization priming protocol, comprised of a series of washes using hybridization buffer solutions (Buffer 1: 5X SCC/0.01% SDS/0.2% BSA, Buffer 2: 2X SCC/0.2%SDS, Buffer 3: 0.2X SSC, Buffer 4: 5X SCC, Buffer 5: diH_2O) was completed before each hybridization reaction. Hybridization buffers and conditions were identical for all arrays and reactions were conducted according to manufacturer instructions (Appendix C).

Microarray hybridization mix was prepared using 140 ng of Alexa Fluor® 555 fluorescently labeled cDNA, 100 pmol of Alexa Fluor® 657 fluorescently labeled and fragmented aRNA, 50 µL of Ambion® SlideHyb™ Glass Array Hybridization Buffer #3, 1 µL of LNA dt blocker (Genisphere®, Hatfield, PA, USA) and nuclease-free water (to adjust cDNA and aRNA to a combined volume of 25 µL). Hybridization mix was incubated at 80 ^{o}C for 10 mins and then held at 65 ^{o}C until prompted by the Tecan 400 HS Pro hybridization system (Tecan, NC, USA) to inject sample. Hybridization protocol (Appendix C) ran for a total of 16 hours. Briefly, arrays were incubated at 65 ^{o}C for 10 mins, washed twice with hybridization buffer 1 for 20 sec at room temperature, incubated at 50 ^{o}C for 13 mins and washed with buffer 1 for 20 sec. Arrays were then incubated at 48 ^{o}C for 13 mins, washed with buffer 1 for 1 min followed by buffer 4 for 1 min. The sample (~62.5 µL) was then injected into the microarray chamber, using a positive displacement pipette, and hybridized using sample agitation at 48 ^{o}C for 16 hours. Arrays were then washed with buffer 2 at 40 ^{o}C for 1 min, incubated at 40 ^{o}C for 2 mins, washed again with buffer 2 at 30 ^{o}C for 1 min and then with buffer 5 at 30 ^{o}C for 1 min. Arrays were incubated at 30 ^{o}C for 2 mins, washed with buffer 5 at 23 ^{o}C for 1 min, washed with buffer 3 at 23 ^{o}C for 1 min, incubated at 23 ^{o}C for 2 mins, washed with buffer 3 for 1 min and lastly, dried with nitrogen gas for 3 mins. Upon completion, microarray slides were removed and placed in a microarray slide box to air dry in the dark before scanning. A post-hybridization cleaning protocol was completed after each reaction using blank microarray slides.

2.3.12 Microarray scanning and analysis

Microarray slides were scanned using a Molecular Devices GenePix 4000B Microarray Scanner (Molecular Devices, Sunnyvale, CA, USA). Microarray slides were placed upside down into the scanner and GenePix software (Molecular Devices, Sunnyvale, CA, USA) was used to generate a preview scan of the microarray. The area including the microarray was selected and scanned. Fluorescence was detected using a photo multiplier tube (PMT) with values set to 100% for both red and green channels.

Generated images were saved as tagged information file format (.tiff) images and imported into Spot Reader (Niles Scientific, Portola Valley, CA) where features were extracted, assessed (for uneven colour, bright specs, low foreground, high background, offset centres and small diameter), flagged and processed into result files. Result files were then locally weighted linear regression (LOWESS) normalized and $\log_2$ expression ratios of sample to reference gene intensity were generated using MIDAS (Microarray Data analysis software V2.2.2). Data was imported into TM4 Multiexperiment Viewer (MeV v4.8.1) and individual samples were grouped based on temperature (Fig. 2.1 green boxes) and sampling time (Fig. 2.1 orange boxes). Groupings were as follows: 10 ^{o}C comparing individuals one-week PI, two-weeks PI and controls; 15 ^{o}C comparing individuals one-week PI, two-weeks PI, and controls; 17.5 ^{o}C comparing individuals one-week PI, two-weeks PI and controls; 20 ^{o}C comparing individuals one-week PI, two-week PI and controls; 10 ^{o}C, 15 ^{o}C, 17.5 ^{o}C and 20 ^{o}C comparing individuals one-week PI and lastly, 10 ^{o}C, 15 ^{o}C, 17.5 ^{o}C and 20 ^{o}C comparing individuals two-weeks PI (Fig. 2.1). Each

grouping was analyzed independently using one-way ANOVA with 1000 permutations and $\alpha=0.05$ with a false discovery rate not exceeding 0.05 and a cutoff for statistical significance of $\alpha=0.001$. Heat maps with hierarchical clustering and K-means clustering were used to identify similar expression profiles among the significantly differentially expressed genes within each of the different groupings. Blast2GO (BioBam©, Valencia, Spain) was used to retrieve annotations for significantly differentially expressed genes.

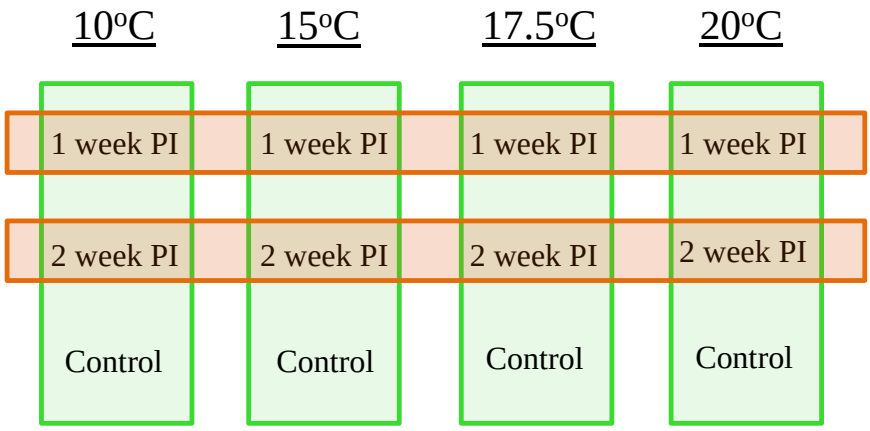

Figure 2.1: Schematic of temperature and sampling schedule for *Homarus americanus* groupings used in microarray analysis.

Temperature groupings (green boxes) consisted of all *H. americanus* necropsied one-week post inoculation (PI), two-weeks PI and the control animals (yielding n=12 for each temperature except for 20 °C that was n=11). One-week PI group (n=16) and two-week PI (n=15) consisted of all infected *H. americanus* necropsied one-week PI and two-week PI, respectively, at all four temperatures (orange boxes). Each grouping was separately analyzed using a one-way ANOVA with a cut-off of for statistical significance of α=0.001 or α=0.05 with the proportion of false significant genes not exceeding 0.05.

2.3.13 Primer Design

Microarray findings were verified using RT-qPCR on a select number of genes (Table 2.1). Primers were designed from EST sequences using PrimerQuest® (Integrated DNA Technologies, Coralville, CA). Primers were assessed for GC content (>45%), product size, and annealing temperature. Primer specificity was verified using Blastn (http://blast.ncbi.nlm.nih.gov/) to assure little to no non-specific binding. Primers were synthesized with an oligonucleotide concentration of 100 nmol and shipped dry from Integrated DNA Technologies (Integrated DNA Technologies, Coralville, CA). Lyophilized primers were re-suspended, using nuclease-free water, to a stock concentration of 100 µM and stored at – 20 ^{o}C.

2.3.14 cDNA Synthesis for RT-qPCR

cDNA was synthesized from total RNA (1 µg) extracted from *H. americanus* hepatopancreas (Section 2.3.7) using an Invitrogen SuperScript™ III First-Strand Synthesis SuperMix kit (Life Technologies, Burlington, ON, Canada) according to manufacturer instructions. Briefly, total RNA (1 µg), 1 µL of oligo(dT) Primer (50 µM), 1 µL of annealing buffer and DEPC-treated water to yield a reaction volume of 8 µL, were combined and incubated at 65 ^{o}C for 5 mins in a DNA Engine thermal cycler with heated lid (Bio-Rad Laboratories Inc., CA, USA). Reverse transcription reactions were placed on ice for 1 min to cool before adding 10 µL of 2X First strand reaction mix and 2 µL SuperScriptIII/RNaseOUT™ Enzyme Mix. The reactions were then incubated at 50 ^{o}C for 50 mins and terminated at 85 ^{o}C for 5 mins. A no template control (NTC; sample containing no RNA) and a no reverse transcriptase control (NRTC; pooled cDNA sample without

SuperScriptIII/RNaseOUT™ Enzyme Mix) were also generated. The samples were then placed on ice and 40 µL nuclease-free water was added. cDNA was aliquoted (2 µL x 30) and stored at -80 ^{o}C until RT-qPCR.

2.3.15 Primer Optimization

Each primer pair was optimized for annealing temperature, efficiency and specificity (Table 2.1). Optimization reactions were completed using pooled cDNA synthesized for RT-qPCR (Section 2.3.14). cDNA (2 µL) from each sample was mixed together, re-aliquoted (2 µL x 48) and labelled as pooled cDNA. Reactions were conducted in 0.2 mL semi-skirted 96-well plates covered with Microseal 'B' seals (Bio-Rad Laboratories Inc., CA, USA). Optimizations were performed in 10 µL reactions assembled using the Qiagility liquid handling robot (Qiagen®, Valencia CA, USA). Reactions consisted of 5 µL 2X Express SYBR GreenER™ qPCRSupermix (Life Technologies, Burlington, ON, Canada), 0.2 µL forward primer (10 µM), 0.2 µL reverse primer (10 µM), 2 µL pooled cDNA, and 2.6 µL nuclease-free water.

T_m optimization cycling parameters were as follows: 95 ^{o}C for 2 mins, 40 cycles of 95 ^{o}C for 5 sec, gradient from 55 ^{o}C to 70 ^{o}C for 20 sec, and lastly a melt curve analysis from 65 ^{o}C to 90 ^{o}C in 1 ^{o}C increments with 3 sec at each temperature. Reactions were conducted in triplicate and run on a Chromo4™ Real-Time PCR system (Bio-Rad Laboratories Inc., CA, USA). Optimal temperature was selected based on the temperature that provided the lowest C_T value at the highest temperature with a single peak in the melt curve at a high temperature (>80 ^{o}C) indicating high specificity.

Reaction volumes were identical for efficiency optimizations; however cycling parameters were modified to incorporate the optimized annealing temperatures, resulting in either two-step or three-step reactions. For two-step reactions, cycling parameters were: 95 ^{o}C for 5 mins, 40 cycles of 95 ^{o}C for 5 sec, annealing temperature for 20 sec, and a melt curve analysis from 65 ^{o}C to 90 ^{o}C in 1 ^{o}C increments with 3 sec at each temperature. For three-step reactions, cycling parameters were: 95 ^{o}C for 5 mins, 40 cycles of 95 ^{o}C for 5 sec, annealing temperature for 20 sec, 72 ^{o}C for 20 sec and a melt curve analysis from 65 ^{o}C to 90 ^{o}C in 1 ^{o}C increments with 3 sec at each temperature. A total of three, 5-fold dilutions (1/5, 1/25, 1/125) were conducted to generate a standard curve and dilutions were run in quadruplicate technical reactions to assure three different master mixes within a single assay had efficiencies within 5-8% of each other. The slope of log copy number (dilution) versus C_T were generated and used to calculate efficiency. Only primers with average amplification efficiencies >85% and a linear trend line fit of $R > 0.98$ were used for microarray verification.

Primers were assessed for specificity by running qPCR product on a 2% agarose gel. SYBR® Safe DNA gel stain 10 000X in DMSO (Life Technologies, Burlington, ON, Canada) was used to stain the gel, and a 100 bp DNA ladder (BioShop Canada Inc., Burlington, ON, CA) was used to size the amplicon. Amplicons were run at 90 V for 1 hour using a Bio-Rad PowerPac™ (Bio-Rad Laboratories Inc., CA, USA). The gel was imaged using Bio-Rad VersaDoc™ (Bio-Rad Laboratories Inc., CA, USA).

Table 2.1: Forward and reverse primer sequences for genes of interest and normalization genes used to verify microarray findings via RT-qPCR.

Guanylate kinase, Calponin, Prolyl-4-hydroxylase-alpha and Short-chain dehydrogenase were selected as genes of interest from the microarray data. Previously designed, R301, HYP, PRP, CHP and R044 were used as normalization genes.

Gene Name (Abbreviation)	Accession Number	Forward Primer Sequence / Reverse Primer Sequence	Annealing Temp. (°C)	Reaction Efficiency (%)	# Step Reaction
Guanylate kinase (GUA)	EX471111	GTCTTCATCAGACCACCATCAA / CCCTTTACAGCTCCATACTCTAAC	61.4	100	3
Calponin (CAL)	FD699000	GGGTGTGTGGCTTATGGTATC / CAGACAGTCCACAACCATGTATAA	57.5	92	3
Prolyl-4-hydroxylase-alpha (PRO)	EW997795	TAATGCCTACCTGTTGGTGAAG / CCTCAGGAAATCAGCCATACTC	61.4	112	2
Short-chain dehydrogenase (DEH)	FD585222	GCGGAGTGTGCTAGACATTTA / CAACTGGCCTCACCAGATATT	61.4	90	2
WD repeat protein 26 (R044)	FF277218	GTGTTCATTTGTGGGACCTACGCA / TGTCTTCATTCCAGATGCCACGA	65	99.7	2
Pre-mRNA processing factor 38 domain containing B (PRP)	DV774783	CAGGAGGTGGGCAAACAACAACAA / AGTCCTTCTGGATTGGCACAGGAA	66	91	2
Conserved hypothetical protein (CHP)	FE659358	TCAAGCCTGAAGCTGGGATATGCT / AAACACATGGGTTGGATGGCACAG	66.5	92	2
Hypothetical protein (HYP)	FE535262	ACATGGCAGTGGAAGACTCAAGGA / AAAGGAAACTGCGAACACTGCTGG	62.5	89	2
Microtubule associated protein (R301)	EX827404	CAAGATCTTGCAGTATGCCTT / TGAACCAGTGAAGGAATTCA	57	101.4	3

2.3.16 RT-qPCR Reactions and Analysis

All *H. americanus* samples used for microarray validation were run in duplicate and on a Chromo4™ Real-Time PCR system (Bio-Rad Laboratories Inc., CA, USA). Reactions were conducted as either two-step or three-step reactions with cycling parameters, reaction volumes, and preparation using liquid handling robot identical to efficiency optimization parameters (Section 2.3.15). RT-qPCR reactions were run using a sample maximum approach with all samples for each gene of interest assayed on a single plate. The expression of each gene of interest was measured in the lobster samples corresponding to the temperature grouping it was identified as statistically significant in. For example, guanylate kinase was differentially expressed between one-week PI, two-weeks PI and control animals at 10 ^{o}C resulting in expression of guanylate kinase (Table 2.1) being measured in 10 ^{o}C animals only. All reactions included a no template control and a no reverse transcriptase control. RT-qPCR C_T values were imported into qBase+ qPCR data analysis software version 3.1 (Biogazelle, Zwijnaarde, Belgium) for analysis. Previously determined gene specific amplification efficiencies were used for quantification. qBase+ v. 3.1 default quality control settings were used; C_T range for technical replicates < 0.5 C_T and a negative control threshold of 5 (Bustin et al., 2009; Hellemans et al., 2007).

The expression stability of 9 previously designed reference genes (Bauer et al., 2013; Clark et al., 2013b, 2013c) was analyzed for all samples using the GeNorm module integrated in qBase+ qPCR data analysis software version 3.1 (Biogazelle, Zwijnaarde, Belgium). GeNorm V < 0.15 and M < 1.0 determined 5

genes (R301, HYP, PRP, CHP and R044) to be the optimal number of reference gene targets required. The optimal normalization factor was calculated as the geometric mean of the determined reference genes. Normalization factors were used to compute normalized relative quantities (NRQ) for each gene of interest. RT-qPCR results were mean $\log_2$ transformed for comparison with microarray data.

2.4 Results

2.4.1 WSSV Infection trial

Overall health and clinical condition of *H. americanus* was monitored closely during the infection trial. Haemolymph cultures, collected at the start and end of the trial, revealed the absence of bacterial or ciliate protist infections in all *H. americanus*. Haemolymph refractive index was not statistically significant between infected and control animals across all four temperatures. All *H. americanus* infected at 10 ^{o}C, 15 ^{o}C and 17.5 ^{o}C survived the infection period. At 20 ^{o}C, a single mortality was observed 144 hours PI (lobster #41). Necropsy revealed the cause of death to be a rubber claw band present within the stomach contents of the lobster and as a result this lobster was omitted from future statistical analysis. This resulted in the two-weeks PI group to be n=3 instead of 4. Additionally, at 288 hours PI the total haemocyte concentration of WSSV infected animals at 20 ^{o}C fell below $3.0x10^{9}$/L. All challenged *H. americanus* in this treatment appeared moribund so the remaining infected and control animals at 20 ^{o}C were sampled one day early at 312 hours post inoculation. For analysis 312 hours PI at 20 ^{o}C is still referred to as the 20 ^{o}C two-weeks PI group.

2.4.2 Total Haemocyte Concentration

Average THC was calculated for infected and control *H. americanus* at each of the four temperatures for the duration of the two-week trial (Fig 2.2). THC decreased slightly during the sampling period for all *H. americanus*, regardless of temperature (Fig. 2.2). However, at 10 ^{o}C and 15 ^{o}C, there was no significant difference in the average THC between the infected and control animals during the two-week trial (Fig. 2.2 A & B; repeated measures two-way ANOVA, p=0.41 and p=0.98 respectively). At 17.5 ^{o}C and 20 ^{o}C, THC was significantly lower in infected *H. americanus* relative to controls across the sampling time points (Fig. 2.2 C & D; repeated measures two-way ANOVA, p=0.03 and p=0.04 respectively).

2.4.3 WSSV-qPCR

Haemolymph samples for all control group *H. americanus* were negative for WSSV. Among infected *H. americanus* WSSV viral replication was temperature dependent (Fig. 2.3). WSSV viral copy number was significantly different between the temperatures (repeated measures two-way ANOVA, p=0.04), with a higher WSSV viral titre present at the warmer temperatures (17.5 ^{o}C and 20 ^{o}C) compared to the colder temperatures (10 ^{o}C and 15 ^{o}C). Infected *H. americanus* at 17.5 ^{o}C and 20 ^{o}C exhibited a linear increase in relative WSSV viral copy number during the infection trial (Fig. 2.3). At 15 ^{o}C relative viral copy number increased linearly until 96 hours PI, after which relative viral copy number reached a plateau (Fig. 2.3). At 15 ^{o}C WSSV viral copy number did not exceed 10^{6} viral copies per 100 µL. At 10 ^{o}C, one lobster remained negative throughout the entire two week trial. The remaining three lobsters at 10 ^{o}C showed variable low levels of WSSV titre. For all

infected *H. americanus* at 10 ^{o}C, relative viral copy number remained below 10 viral copies per 100 µL (Fig. 2.3). All C_T values for *H. americanus* infected at 15 ^{o}C, 17.5 ^{o}C and 20 ^{o}C were below 35. All C_T values for *H. americanus* infected at 10 ^{o}C were below 40.

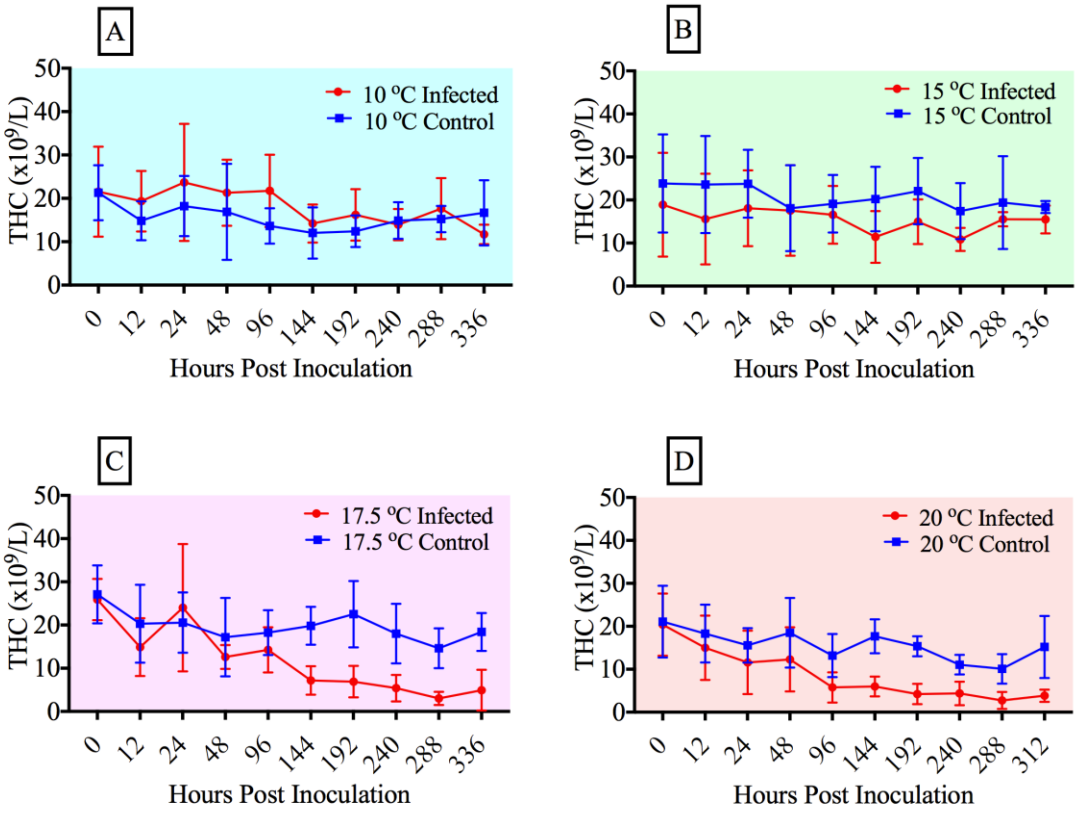

Figure 2.2: **Average total haemocyte concentrations (THC) in *Homarus americanus* at the four experimental temperatures during WSSV infection challenge.**

(A) THC for infected and control *H. americanus* at 10 °C. (B) THC for infected and control *H. americanus* at 15 °C. (C) THC for infected and control *H. americanus* at 17.5 °C. (D) THC for infected and control *H. americanus* at 20 °C. At 20 °C final sampling event occurred at 312 hours post inoculation instead of 336 hours. Data is represented as means ± SD and n=4 for each temperature, with the exception of 20 °C infected that is n=3.

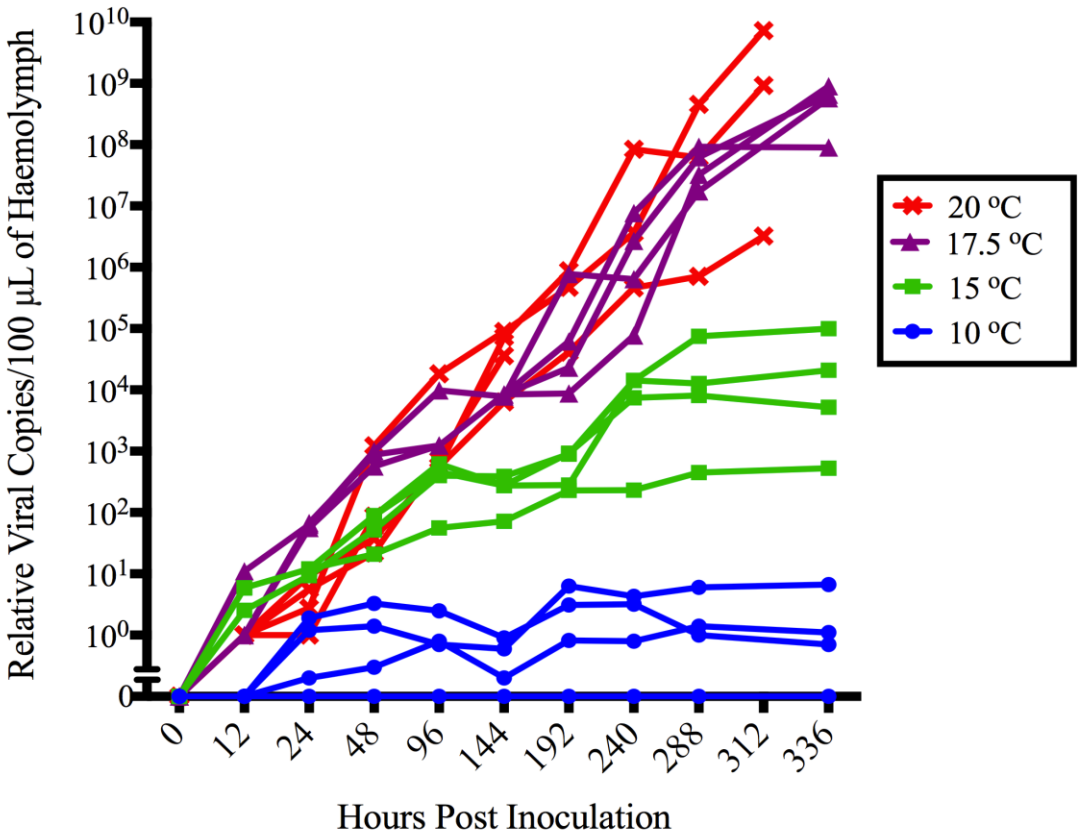

Figure 2.3: WSSV viral titre in *Homarus americanus* haemolymph during WSSV infection challenge at the four experimental temperatures.

WSSV viral titre was measured via WSSV-qPCR testing. All control *H. americanus*, at all temperatures, were negative. Data was log transformed. Break in the Y-axis highlights the transition from numerical scale to log scale; required in order to plot true zero values as true zeros.

2.4.4 Microarray

Two levels of significance (for one-way ANOVA) were compared to determine which provided the most accurate and relevant number of significantly differentially expressed genes for each grouping. One-way ANOVA analysis with α=0.001 as the meaningful statistical cutoff determined that in total 771 genes were significantly differentially expressed (Table 2.2). At this level of significance, 24 genes were differentially expressed between one-week PI, two-weeks PI and controls at 10 ^{o}C, 54 genes at 15 ^{o}C, 11 genes at 17.5 ^{o}C and 56 genes at 20 ^{o}C, respectively (Table 2.2). Blast2Go was used to search for functional annotations for the significantly differentially expressed genes. Of the significantly differentially expressed genes a, total of 38% were functionally annotated (Table 2.2). Of these, a surprisingly low number appeared to be involved in immune processes. Additionally, none of the annotated identified genes were shared between temperature groupings.

At 10 ^{o}C significantly differentially expressed genes (between one-week PI, two-weeks PI, and controls) included several ribosomal proteins (L27a, L13, L11, L39), guanylate kinase and protein O-mannosyl-transferase, which increased in expression one-week PI but decreased in expression two-weeks PI relative to controls (Appendix D Table D.1). At 15 ^{o}C, annotated genes included endonuclease/reverse transcriptase, calponin, DEAD-box ATP-dependent RNA helicase, which was up-regulated two-weeks PI and C-type lectin which was down-regulated 0.374 fold one-week PI and 0.887 fold two-weeks PI (Appendix D Table D.2). At 17.5 ^{o}C, only three genes were annotated, mitogen-activated protein kinase

organizer 1, prolyl-4-hydroxylase-alpha and Dpol isoform A (Appendix D Table D.3). At 20 ^{o}C *Drosophila melanogaster* pol-like was up-regulated 1.326 fold one-week PI but down-regulated 0.878 fold two-weeks PI. Laminin subunit gamma-3 was also down-regulated 0.495 fold in infected animal's two-weeks PI relative to controls at 20 ^{o}C (Appendix D Table D.4).

Heat maps with hierarchical clusters were generated for the significant genes identified in each temperature grouping (Fig. 2.4). At 10 ^{o}C hierarchical clustering was not able to differentiate between control, one-week PI and two-weeks PI samples (Fig. 2.4 A; Appendix D Table D1). However, at 15 ^{o}C (Fig. 2.4 B; Appendix D Table D2), 17.5 ^{o}C (Fig 2.4 C; Appendix D Table D3) and 20 ^{o}C (Fig. 2.4 D; Appendix D Table D4), hierarchical clustering revealed that control individuals had expression profiles more similar to themselves than to one-week and two-week PI individuals. At 15 ^{o}C and 20 ^{o}C hierarchical clustering of significant genes could clearly differentiate between controls, one-week PI and two-weeks PI (Fig 2.4 B & D). Hierarchical clusters for the significantly differentially expressed genes one-week PI and two-weeks PI were also differentiated between infected individuals at the different temperatures. Infected *H. americanus* within a given temperature demonstrated more similar expression profiles to themselves than to individuals infected at another temperature (Fig 2.5; Appendix D Table D5 for one-week PI and Table D6 for two-weeks PI).

One-way ANOVA analysis with α=0.001 of one-week PI *H. americanus* across all temperatures resulted in the largest number of significantly differentially expressed genes (Table 2.2; Appendix D Table D5). As a result, a second more

rigorous one-way ANOVA analysis was conducted with a false discovery rate > 0.05 and α=0.05. Under this analysis, a total of 5 genes (2 annotated, 3 un-annotated) were significantly differentially expressed between the infected animals one-week PI across all temperatures. This analysis for all other grouping resulted in zero significantly differentially expressed genes. Average Log_2 expression ratios of the 5 identified genes were plotted (Fig. 2.6). The annotated genes included acute phase serum amyloid A (Fig 2.6 A) which increased in expression as temperature increased from 10 ^{o}C to 20 ^{o}C, and prostaglandin E synthase 2 (Fig. 2.6. B), which decreased from 10 ^{o}C to 17.5 ^{o}C but then increased from 17.5 ^{o}C to 20 ^{o}C. The remaining genes (named by accession number) DV774720 and DV773674 showed an increase in expression with temperature (Fig. 2.6 C & E) whereas FF277877 (Fig 2.6 D) showed a decrease in expression with temperature.

One-way ANOVA analysis with α=0.001 among infected *H. americanus* two-weeks PI across all temperatures yielded a total of 75 significantly differentially expressed genes. Of these genes, 31 were functionally annotated (Table 2.2; Appendix D Table D6). Figure of merit (FOM) algorithm and K-means clustering was used to cluster these significant genes based on similar expression profiles. Each gene was represented only once within a given cluster, providing insight into the function of non-annotated genes. FOM identified 6 clusters to be the minimum number of K-means clusters needed for strong predictive power. Cluster 1 contained 20 genes, cluster 2, 16 genes, cluster 3, 14 genes, cluster 4, 13 genes, cluster 5, 7 genes and cluster 6, 5 genes (Appendix E Tables E1-E6). Average expression profiles for each cluster were generated (Fig 2.7). Clusters 1, 2 and 6 showed

variable patterns of expression, with differences in expression typically occurring between 17.5 ^{o}C and 20 ^{o}C (Fig. 2.7; Appendix E Table E1, E2, E6 respectively). Genes within clusters 4 and 5 differed in fold change but both showed decreased expression as temperature increased (Fig 2.7; Appendix E Table E4, E5). Interestingly, cluster 4 contained crustin-like protein *fc*-1, NADH dehydrogenase subunit 5, membrane associated ring finger, sterile alpha motif domain containing isoform 1 and a suite of genes with no functional annotation. Lastly, Cluster 3 genes, including pontin, glutamate dehydrogenase and sec1 family domain containing 2, showed very little upregulation from 10 ^{o}C to 17.5 ^{o}C but then increased significantly at 20 ^{o}C (Fig 2.7; Appendix E Table E3).

Table 2.2: Number of significantly differentially expressed genes identified using microarray analysis and percentage annotated in *Homarus americanus* under WSSV infection challenge.

Number of significantly differentially expressed genes in each temperature and sampling time group identified using one-way ANOVA analysis with 1000 permutations and α=0.001. Percentage of significantly differentially expressed genes with functional annotations available. Post inoculation (PI).

Groupings	Number of significant genes	Number of annotated genes	Percent annotated (%)
10 ^{o}C	24	13	54
15 ^{o}C	54	25	46
17.5 ^{o}C	11	3	27
20 ^{o}C	56	17	30
One-week PI	551	204	37
Two-weeks PI	75	31	41
Total	771	293	38

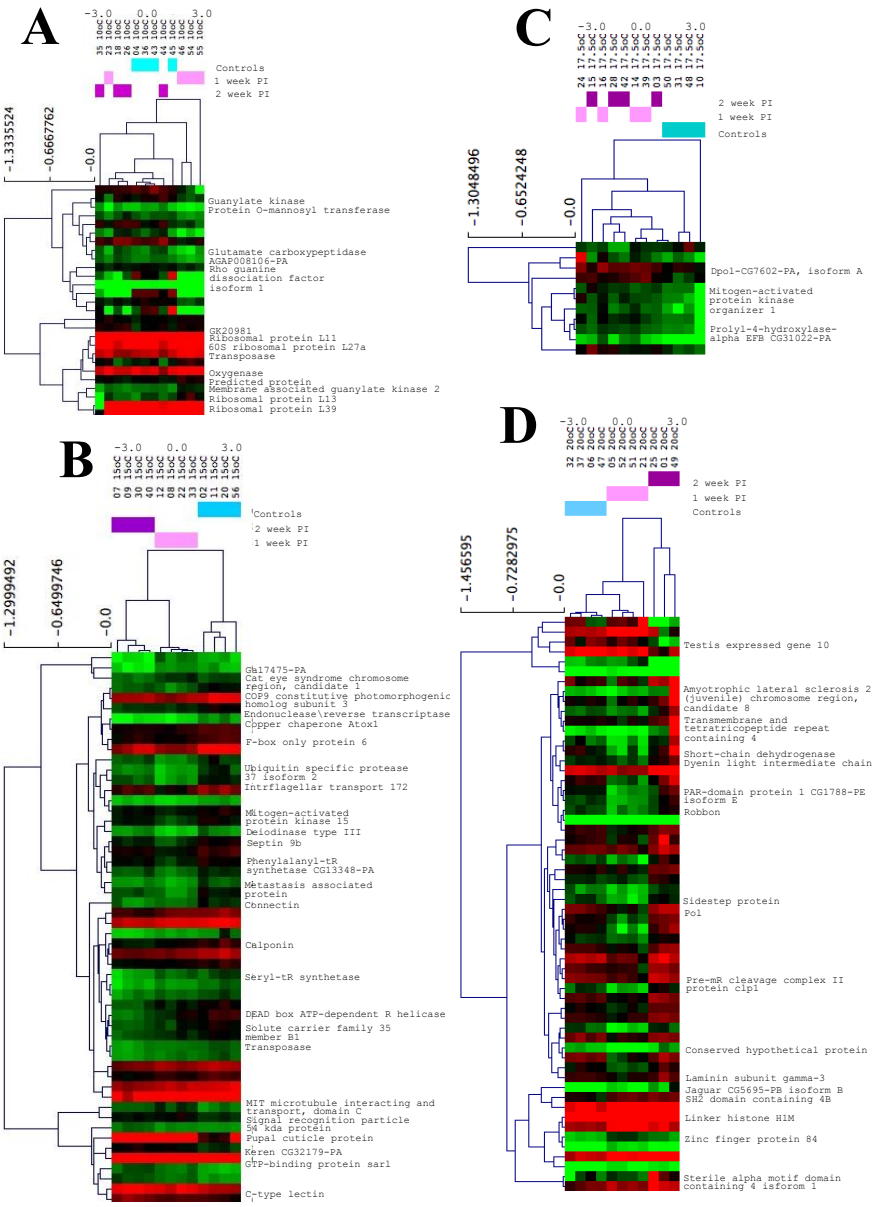

Figure 2.4: Heat maps with hierarchical clustering of significantly differentially expressed genes identified between *Homarus americanus* infected one-week PI, two-weeks PI and control *H. americanus* at each of the four experimental temperatures.

Heat maps illustrate $\log_2$ expression ratio of experimental sample (Alexa flour 555) to reference sample (Alexa flour 647), with significant genes identified using one-way ANOVA at α=0.001, along the x-axis and experimental samples along the y-axis. Red represents a threefold or greater decrease in gene expression whereas green represents a threefold or greater increase in gene expression. Colours separating treatments are as follows blue corresponding to controls, pink to one-week PI and purple to two-weeks PI. (A) 10 ^{o}C, (B) 15 ^{o}C, (C) 17.5 ^{o}C, (D) 20 ^{o}C.

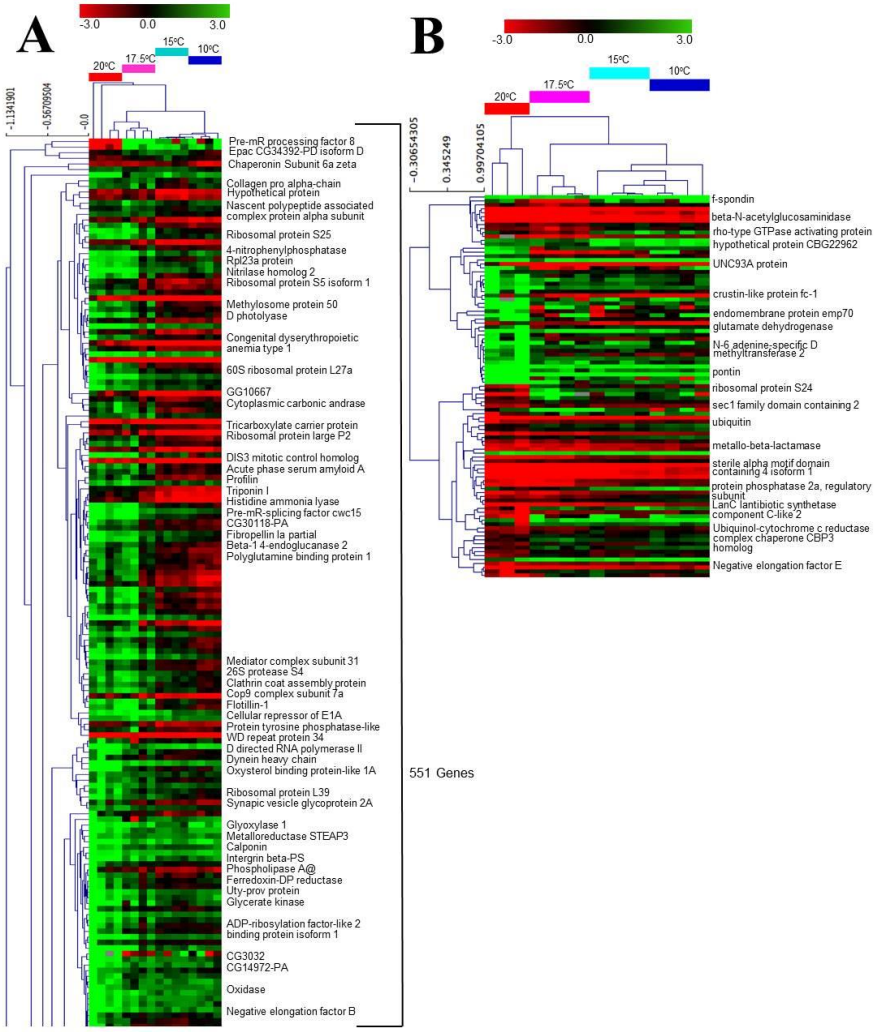

Figure 2.5: Heat maps with hierarchical clustering of significantly differentially expressed genes identified between infected *Homarus americanus* one-week and two-weeks PI across the four experimental temperatures.

Heat maps illustrate $\log_2$ expression ratio of experimental sample to reference sample, with significant genes, identified using one-way ANOVA at α=0.001, listed along the x-axis and experimental samples along the y-axis. Red represents a threefold or greater decrease in gene expression whereas green represents a threefold or greater increase in gene expression. Colours separating treatments are as follows, red corresponding to 20 ^{o}C, pink corresponding to 17.5 ^{o}C, light blue to 15 ^{o}C and navy blue to 10 ^{o}C. (A) one-week PI across all temperatures (B) two-weeks PI across all temperatures.

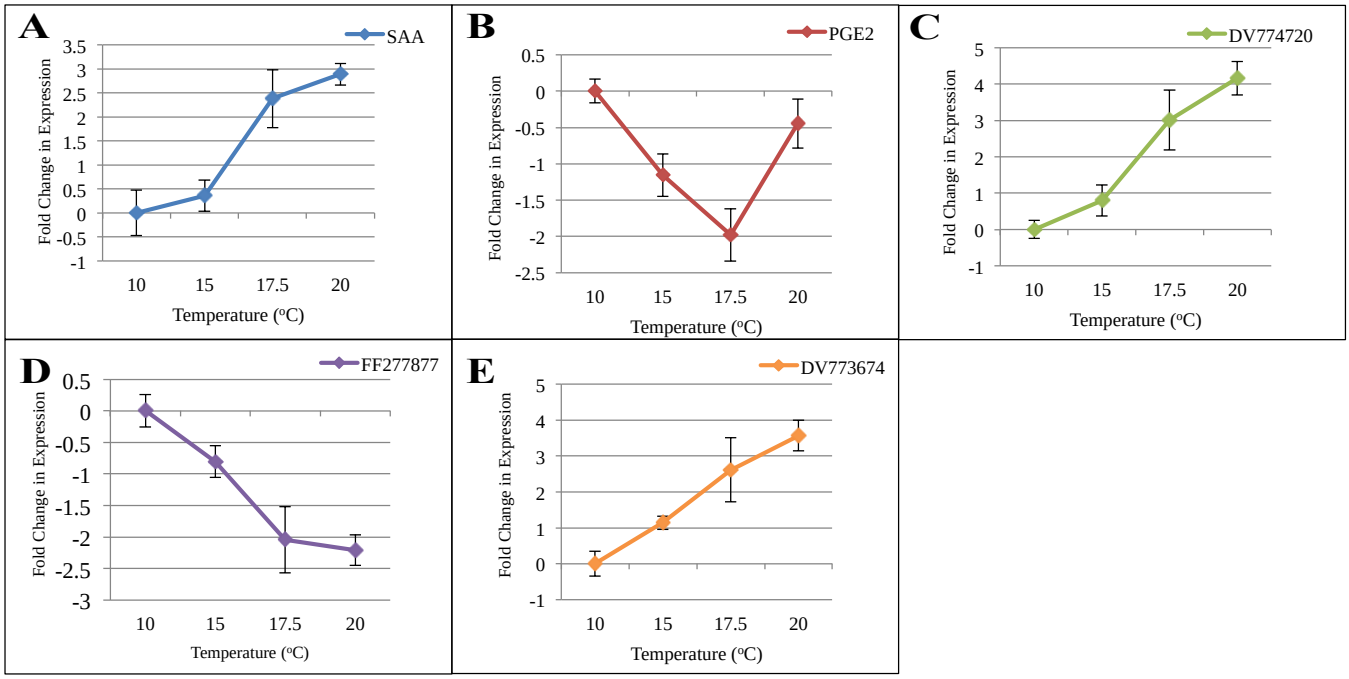

Figure 2.6: Average log_2 expression ratios for significantly differentially expressed genes identified in WSSV infected *Homarus americanus* one-week PI across all four experimental temperatures.

Significantly differentially expressed genes identified by one-way ANOVA α=0.05 and false discovery rate > 0.05. Fold change in expression represents average log_2 expression ratios of sample/ref. Data are normalized to 10 ^{o}C. (A) Acute phase serum amyloid A (SAA), (B) Prostaglandin E 2 Synthase (PGE2), (C) Accession #DV774720, (D) Accession # FF277877, (E) Accession # DV77367.

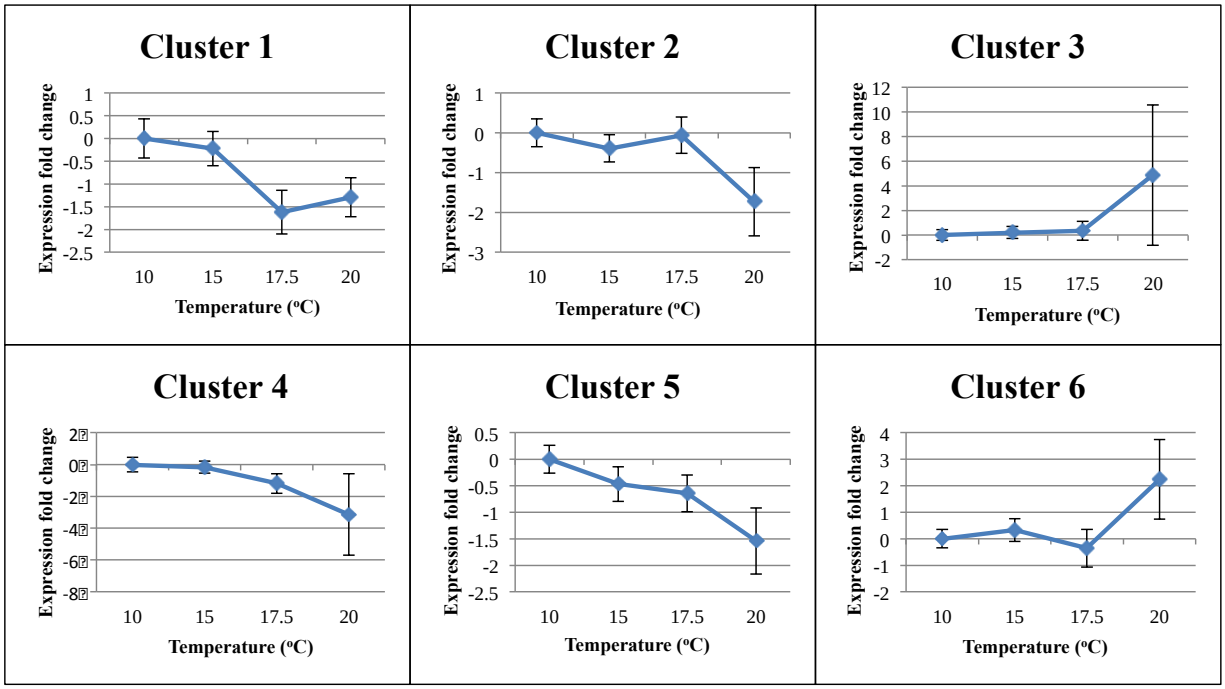

Figure 2.7: K-means clusters of significantly differentially expressed genes identified for WSSV infected *Homarus americanus* two-weeks PI across all four experimental temperatures (10 °C, 15 °C, 17.5 °C, 20 °C).

Significantly differentially expressed genes identified via one-way ANOVA with α=0.001. Fold change in expression represents average $\log_2$ expression ratios of sample/ref. Data are normalized to 10 °C. Cluster 1 contains 20 genes, cluster 2, 16 genes, cluster 3, 14 genes, cluster 4, 13 genes, cluster 5, 7 genes and cluster 6, 5 genes.

2.4.5 RT-qPCR

Microarray findings were verified using a select number of genes (Table 2.1). Microarray and RT-qPCR results agreed well and were similar in identifying up and down-regulated genes (Table 2.3). The fold change in expression, however, differed slightly between the two techniques. At 10 ^{o}C RT-qPCR found the expression intensity for guanylate kinase to be slightly less than identified via microarray (Table 2.3). At 15 ^{o}C RT-qPCR results found that calponin was down-regulated 1.51 fold in the control group *H. americanus* compared to the microarray findings that identified a 0.675 fold down-regulation. Small differences in fold change in expression were also observed at 17.5 ^{o}C and 20 ^{o}C (Table 2.3), however overall RT-qPCR and microarray findings were in agreement.

Table 2.3: Mean log_2 expression ratios of genes selected for RT-qPCR verification of microarray data for WSSV infected *Homarus americanus* one-week and two-weeks PI and control *H. americanus* at the four experimental temperatures.

Temperature	Gene Name (Abbreviation)	Accession #	Technique	Controls	One-week PI	Two-weeks PI	p-value
10 °C	Guanylate Kinase (GUA)	EX471111	Microarray	-0.096	1.031	-0.286	0.001
			RT-qPCR	-0.07	0.92	-0.24	
15 °C	Calponin (CAL)	FD699000	Microarray	-0.675	-0.095	0.315	0.001
			RT-qPCR	-1.51	-0.94	0.76	
17.5 °C	Prolyl-4-hydroxylase-alpha (PRO)	EW997795	Microarray	1.932	0.237	0.791	0.001
			RT-qPCR	1.43	0.55	0.13	
20 °C	Short-chain dehydrogenase (DEH)	FD585222	Microarray	-0.139	1.922	-2.096	0.001
			RT-qPCR	-0.01	0.90	-0.67	

2.5 Discussion

White spot syndrome virus is highly virulent, with over 93 crustacean species reported as susceptible to date (Sánchez-Paz, 2010; Sweet and Bateman, 2015). Clark et al., (2013c) previously demonstrated that at 20 ^{o}C, following intramuscular injection of the virus, *Homarus americanus* is susceptible to WSSV infection. Temperatures permissive to WSSV infection range between 15 ^{o}C to 30 ^{o}C depending on the host (Moser et al., 2012; Sun et al., 2014). Given that *H. americanus* inhabit ocean waters that fluctuate between (approximately) 0 ^{o}C and 20 ^{o}C, understanding the interaction between temperature, immunity and WSSV infection in the atypical host is important. This study is the first to explore the impact of these temperature variations on the immune response of WSSV infected *H. americanus*. The goal of the study was to characterize the molecular immune response, revealed through transcriptomic differences between WSSV infected *H. americanus* across a range of temperatures.

An infection period of two-weeks was selected for this study because previous studies found that WSSV-challenged *H. americanus* at 20 ^{o}C became moribund approximately one to two-weeks PI (Clark et al., 2013c; Byrne, unpublished). All *H. americanus* received a one-week acclimation period upon arrival to the GBU-AAHL facility and then a second one-week acclimation period once at their respective temperatures in order to minimize thermal stress prior to the study. Clinical condition of the animals was closely monitored, as it was imperative that *H. americanus* were sampled before they died in order to collect good quality RNA required for microarray analysis.

Total haemocyte concentration is considered a useful indicator of health in *H. americanus* (Battison et al., 2004). Average THC was statistically significant between infected and control animals during the trial at 17.5 ^{o}C and 20 ^{o}C, but not at 10 ^{o}C and 15 ^{o}C. This suggests an overall decline in the clinical condition of infected animals at the warmer temperatures. Haemocytes are responsible for a variety of immune functions within crustaceans, including phagocytosis. In the presence of pathogens, haemocytes are mobilized, until demand exceeds supply, in which case THC then decreases and less effective pathogen clearance is observed (Battison et al., 2004). In *Penaeus japonicus*, inhibition of phagocytosis results in a pronounced increase in WSSV viral copies and mortality (Wang and Zhang, 2008). THC data correlates with viral amplification data (measured by WSSV-qPCR) which showed that replication rates were higher at the warmer temperatures compared to the colder temperatures (Fig. 2.3). At 17.5 ^{o}C and 20 ^{o}C the most rapid rates of viral replication were observed in addition to the significant decrease in THC. At 15 ^{o}C viral amplification increased initially but then appeared to slow down during the trial whereas at 10 ^{o}C, relative WSSV-viral copy number remained very low. The 10 ^{o}C data suggests that at colder temperatures *H. americanus* can be infected, but no clinical signs manifest. The present study cannot conclude that viral replication was occurring at 10 ^{o}C as WSSV-qPCR data may be detecting residual WSSV from inoculation.

Moser et al. (2012) demonstrated that in *Litopenaeus vannamei*, viral amplification and onset of WSSV disease occurred more rapidly at warmer temperatures (29 ^{o}C) compared to colder temperatures (18 ^{o}C). Previous work

conducted by Jiravanichpaisal et al., (2004) noted that moving WSSV infected Freshwater crayfish *Pacifastacus leniusculus* from 12 ^{o}C (where no mortality was observed) to 22 ^{o}C resulted in 100% mortality. Jiravanichpaisal et al., (2004) speculated that individuals infected at colder temperatures may be subclinical carriers of the virus; however, whether the virus is in a latent state versus simply experiencing a very low replication rate at the colder temperatures was also not determined. It would be of interest to explore the duration of WSSV viability in *H. americanus* held at 10 ^{o}C and whether *H. americanus* infected and held at 10 ^{o}C, then moved to 20 ^{o}C would be permissive and enable WSSV-viral amplification at the warmer temperature.

Hepatopancreas tissue gene expression was measured using a previously designed microarray chip (Clark et al., 2013c). The hepatopancreas serves as a major site of humoral immune factor production in *H. americanus* (Martin and Hose, 1995). Rao et al., (2016) completed a transcriptome study on the hepatopancreas of the giant freshwater prawn *Macrobrachium rosenbergii* and found that pattern recognition protein (PRP) expression was affected by WSSV challenge, with the majority being up-regulated in response. In *M. rosenbergii,* and *L. vannamei* the hepatopancreas is the primary site for PRP production (Rao et al., 2016). In addition, Clark et al., (2013a, 2013b, 2013c) used hepatopancreas tissue gene expression to compare bacterial, parasitic and viral (WSSV at 20 ^{o}C) infections in *H. americanus* and identified several humoral immune factor transcripts. Unfortunately, very few findings were conserved between the present study and Clark et al., (2013c). This is likely due to the differences in the sampling design of the two studies, as Clark et al.,

(2013c) examined the immune response of WSSV infected *H. americanus* at several time points prior to one-week PI, where as the present study examined the immune response only beginning one-week and two-weeks PI.

Microarray data was analyzed using two statistical cutoffs. A rigorous false discovery correction (proportion of false significant genes does not exceed 0.05) resulted only in significantly differentially expressed genes identified in the infected animals one-week PI across all temperatures group. However, the incorporation of the limited false discovery rate allows for increased confidence in the differential expression of identified gene (i.e. truly are differentially expressed, not false positive). The one-way ANOVA with α=0.001 allows us to assure we are not missing any possible genes while still being a more robust analysis, than α=0.05 which is frequently used and can result in false positives. One-way ANOVA with α=0.001 and coupled with microarray verification using RT-qPCR allowed for confidence in the identified differentially expressed genes.

Of the significantly differentially expressed genes a surprising low percentage (Table 2.1) were functionally annotated and even fewer were involved in immune function. At 10 ^{o}C there was no clear link to primary immune function or immune activation based on available annotated sequences. Similarly, at 10 ^{o}C hierarchical clustering was not able to differentiate between infected and control animals, suggesting that the host is not eliciting a targeted immune response to WSSV infection. Rahman et al. (2007) previously reported that extreme high water temperatures (above 33 ^{o}C) are capable of inhibiting the expression of the VP28 envelope protein in WSSV resulting in delayed or reduced viral replication. The

effects of extreme hypothermia on WSSV are currently unknown, however the present data may suggest that 10 ^{o}C might be outside of the permissive thermal range for WSSV replication.

Interestingly, at 15 ^{o}C hierarchical clustering clearly differentiated between infected and control animals. Genes including calponin, C-type lectin and DEAD-box ATP-dependent R helicase were significantly differentially expressed. C-type lectins are primarily involved in pathogen recognition and immune processes such as phagocytosis, melanization and the activation of prophenoloxidase (Zhao et al., 2009). Most notably, a C-type lectin identified in *L. vannamei* (*Lv*CTL1) has been found to interact with several WSSV envelope proteins in WSSV infected shrimp (Zhao et al., 2009); with increased expression of LvCTL1 exhibited by WSSV-resistant shrimp (Zhao et al., 2009). More recently, Feng et al., (2016) identified a C-type lectin in *M. rosenbergii* (*Mr*Lec) that was up-regulated in the gills and the intestine 24 hours following WSSV challenge. The C-type lectin identified in our study demonstrated a 0.374 fold decrease in expression one-week PI and a 0.887 fold decrease two-weeks PI relative to controls at 15 ^{o}C. Interestingly, at 15 ^{o}C, WSSV viral replication occurred, yet a significant decline in clinical condition of *H. americanus* was not observed. Given that C-type lectins are involved in the immune responses of several shrimp species to WSSV it may be speculated that at 15 ^{o}C *H. americanus* is not mounting a typical WSSV immune response (based on shrimp C-type lectin results).

Interestingly, at 15 ^{o}C, DEAD-box ATP-dependent R helicase was up-regulated one and two-weeks PI among infected animals. DEAD-box ATP-

dependent R helicase is known to be involved in *H. americanus* development of primordial germ cells necessary for reproductive success (Sellars et al., 2007). Interestingly, Bauer et al., (2013) identified DEAD-box ATP-dependent R helicase to be up-regulated following endosulfan exposure in larval *H. americanus*.

At 17.5 ^{o}C and 20 ^{o}C, rapid viral amplification and a significant decrease THC were observed. Dpol isoform A was down regulated at two-weeks PI relative to controls at 17.5 ^{o}C; and *Drosophila melanogaster* Pol-like was down-regulated two-weeks PI at 20 ^{o}C. In *Drosophila* Pol II is involved in regulation of signal transduction cascades including immune pathways (Gilchrist et al., 2012). Previous research shows that knockdown of Pol II constituents results in an attenuated immune gene activation (Gilchrist et al., 2012); suggesting that *H. americanus* immune function may be inhibited by warmer temperatures allowing for increased WSSV amplification.

When all temperatures are compared at one-week and two-weeks PI, additional patterns can be elucidated. One-week PI acute phase serum amyloid A showed a 2.888 fold increased expression as temperature increased from 10 ^{o}C to 20 ^{o}C. SAA is an acute phase protein that has previously been found to be an indicator of immune activation against bacterial and parasitic infections in *H. americanus* (Clark et al., 2013a, 2013b). The present data further suggests that SAA may be an indicator of compromised health in the species and may be a useful health biomarker moving forward. SAA is an acute phase protein used as a health indicator in a variety of other animals. SAA expression increased significantly between 10 ^{o}C and

20 ^{o}C, which correlates with the statistically significant decrease in THC observed at the warmer temperatures.

Lastly, limited immune genes were expressed across all temperatures two-weeks PI. However, of interest is the 2.106 fold down-regulation of crustin-like protein *fc*-1 as temperature increases. Crustins are antibacterial proteins expressed by circulating haemocytes of crustaceans (Fredrick and Ravichandran, 2012). Most of the focus on crustins has been on their involvement against bacterial pathogens, however, down-regulation of crustin in WSSV infected *Penaeus monodon* has been previously described (Christie et al., 2007). Christie et al. (2007) noted that 48 hours post infection a down-regulation of crustin correlated with the animals succumbing to disease. A down-regulation of lectins (another group of AMP's) has also been reported post WSSV infection in *Penaeus chinensis* (Christie et al., 2007). It is possible that because, crustin expression decreased with higher temperature among the infected animals, it may act as an indicator of late stage WSSV disease in *H. americanus*. Alternatively, the reduced expression of crustin might be due to the loss of haemocytes also observed at the warmer temperatures. Regardless both hypotheses are supported by the fact that crustin was not differentially expressed in infected *H. americanus* one-week PI but was two-weeks PI.

In summary, this study demonstrated that temperature has a profound effect on WSSV-host interactions in *H. americanus*. At warmer temperatures, WSSV viral amplification was increased and overall clinical condition of the animal was decreased. At colder temperatures, WSSV viral amplification appeared attenuated. The transcriptomic profiles of individuals infected at the different temperatures

differed significantly. At colder temperatures *H. americanus* did not show a targeted immune response to WSSV. At the warmer temperatures a few of the annotated genes provides the initial insights into how temperature is impacting the immune response of WSSV infected *H. americanus*.

2.7 References

Acorn, A.R., Clark, K.F., Jones, S., Després, B.M., Munro, S., Cawthorn, R.J., Greenwood, S.J., 2011. Analysis of expressed sequence tags (ESTs) and gene expression changes under different growth conditions for the ciliate *Anophryoides haemophila*, the causative agent of bumper car disease in the American lobster (*Homarus americanus*). J. Invertebr. Pathol. 107, 146–154.

Bateman, K.S., Munro, J., Uglow, B., Small, H.J., Stentiford, G.D., 2012a. Susceptibility of juvenile European lobster *Homarus gammarus* to shrimp products infected with high and low doses of white spot syndrome virus. Dis. Aquat. Organ. 100, 169–184.

Bateman, K.S., Tew, I., French, C., Hicks, R.J., Martin, P., Munro, J., Stentiford, G.D., 2012b. Susceptibility to infection and pathogenicity of white spot disease (WSD) in non-model crustacean host taxa from temperate regions. J. Invertebr. Pathol. 110, 340–351.

Battison, A.L., Cawthorn, R.J., Horney, B., 2004. Response of American lobsters *Homarus americanus* to infection with a field isolate of *Aerococcus viridans* var. *homari* (Gaffkemia): survival and haematology. Dis. Aquat. Organ. 61, 263–268.

Bauer, M., Greenwood, S.J., Clark, K.F., Jackman, P., Fairchild, W., 2013. Analysis of gene expression in *Homarus americanus* larvae exposed to sublethal concentrations of endosulfan during metamorphosis. Comp. Biochem. Physiol. Part D Genomics Proteomics 8, 300–308.

Burge, C.A., Mark Eakin, C., Friedman, C.S., Froelich, B., Hershberger, P.K., Hofmann, E.E., Petes, L.E., Prager, K.C., Weil, E., Willis, B.L., Ford, S.E., Harvell, C.D., 2014. Climate change influences on marine infectious diseases: implications for management and society. Ann. Rev. Mar. Sci. 6, 249–277.

Bustin, S.A., Benes, V., Garson, J.A., Hellemans, J., Huggett, J., Kubista, M., Mueller, R., Nolan, T., Pfaffl, M.W., Shipley, G.L., Vandesompele, J., Wittwer, C.T., 2009. The MIQE Guidelines: minimum information for publication of quantitative real-time PCR experiments. Clin. Chem. 55, 611–622.

CFIA Biohazard Containment and Safety, 2010. Containment standards for facilities handling aquatic animal pathogens., 1st ed. Canadian Food Inspection Agency.

Christie, A.E., Rus, S., Goiney, C.C., Smith, C.M., Towle, D.W., Dickinson, P.S., 2007. Identification and characterization of a cDNA encoding a crustin-like, putative antibacterial protein from the American lobster *Homarus americanus*. Mol. Immunol. 44, 3333–3337.

Clark, K.F., Acorn, A.R., Greenwood, S.J., 2013b. A transcriptomic analysis of American lobster (*Homarus americanus*) immune response during infection with the bumper car parasite *Anophryoides haemophila*. Dev. Comp. Immunol. 40, 112–122.

Clark, K.F., Acorn, A.R., Greenwood, S.J., 2013a. Differential expression of American lobster (*Homarus americanus*) immune related genes during infection of *Aerococcus viridans* var. *homari*, the causative agent of Gaffkemia. J. Invertebr. Pathol. 112, 192–202.

Clark, K.F., Greenwood, S.J., Acorn, A.R., Byrne, P.J., 2013c. Molecular immune

response of the American lobster (*Homarus americanus*) to the white spot syndrome virus. J. Invertebr. Pathol. 114, 298–308.
Doney, S.C., Ruckelshaus, M., Emmett Duffy, J., Barry, J.P., Chan, F., English, C.A., Galindo, H.M., Grebmeier, J.M., Hollowed, A.B., Knowlton, N., Polovina, J., Rabalais, N.N., Sydeman, W.J., Talley, L.D., 2012. Climate change impacts on marine ecosystems. Ann. Rev. Mar. Sci. 4, 11–37.
Feng, J., Huang, X., Jin, M., Zhang, Y., Li, T., Hui, K., Ren, Q., 2016. A C-type lectin (MrLec) with high expression in intestine is involved in innate immune response of *Macrobrachium rosenbergii*. Fish Shellfish Immunol. 59, 345–350.
Fredrick, W.S., Ravichandran, S., 2012. Hemolymph proteins in marine crustaceans. Asian Pac. J. Trop. Biomed. 2, 496–502.
Gilchrist, D.A., Fromm, G., dos Santos, G., Pham, L.N., McDaniel, I.E., Burkholder, A., Fargo, D.C., Adelman, K., 2012. Regulating the regulators: the pervasive effects of Pol II pausing on stimulus-responsive gene networks. Genes Dev. 26, 933–944.
Hellemans, J., Mortier, G., De Paepe, A., Speleman, F., Vandesompele, J., 2007. qBase relative quantification framework and software for management and automated analysis of real-time quantitative PCR data. Genome Biol. 8, R19.
IPCC, 2001. Climate change 2001: the scientific basis contribution of working group I to the third assessment report of the Intergovernmental Panel on Climate Change. Cambridge University Press.
Jiravanichpaisal, P., Söderhäll, K., Söderhäll, I., 2004. Effect of water temperature on the immune response and infectivity pattern of white spot syndrome virus (WSSV) in freshwater crayfish. Fish Shellfish Immunol. 17, 265–275.
Le Moullac, G., Haffner, P., 2000. Environmental factors affecting immune responses in Crustacea. Aquaculture 191, 121–131.
Linder, J.E., Owers, K.A., Promislow, D.E.L., 2008. The effects of temperature on host–pathogen interactions in *D. melanogaster*: who benefits? J. Insect Physiol. 54, 297–308.
Lua, D.T., Hirono, I., 2015. Effect of low water temperature on the pathogenicity of white Spot Syndrome Virus (WSSV) in Kuruma shrimp (*Marsupenaeus japonicus*). J. Sci. Dev. 13, 1405–1414.
Martin, G.G., Hose, J.E., 1995. Circulation, the blood, and disease, in: Factor, J.R. (Ed.), Biology of the Lobster *Homarus americanus*. Academic Press, pp. 464–495.
Maynard, J., van Hooidonk, R., Harvell, C.D., Eakin, C.M., Liu, G., Willis, B.L., Williams, G.J., Groner, M.L., Dobson, A., Heron, S.F., Glenn, R., Reardon, K., Shields, J.D., 2016. Improving marine disease surveillance through sea temperature monitoring, outlooks and projections. Philos. Trans. R. Soc. B Biol. Sci. 371, 20150208.
Moser, J.R., Álvarez, D.A.G., Cano, F.M., Garcia, T.E., Molina, D.E.C., Clark, G.P., Marques, M.R.F., Barajas, F.J.M., López, J.H., 2012. Water temperature influences viral load and detection of white spot syndrome virus (WSSV) in *Litopenaeus vannamei* and wild crustaceans. Aquaculture 326–329, 9–14.
Pradeep, B., Rai, P., Mohan, S.A., Shekhar, M.S., Karunasagar, I., 2012. Biology, host range, pathogenesis and diagnosis of white spot syndrome virus. Indian J.

Virol. 23, 161–174.
Rahman, M.M., Corteel, M., Wille, M., Alday-Sanz, V., Pensaert, M.B., Sorgeloos, P., Nauwynck, H.J., 2007. The effect of raising water temperature to 33 °C in *Penaeus vannamei* juveniles at different stages of infection with white spot syndrome virus (WSSV). Aquaculture 272, 240–245.
Raj, S., Vijayan, K.K., Alavandi, S. V., Balasubramanian, C.P., Santiago, T.C., 2012. Effect of temperature and salinity on the infectivity pattern of white spot syndrome virus (WSSV) in giant tiger shrimp. Indian J. Fish. 59, 109–115.
Rao, R., Bhassu, S., Bing, R.Z.Y., Alinejad, T., Hassan, S.S., Wang, J., 2016. A transcriptome study on *Macrobrachium rosenbergii* hepatopancreas experimentally challenged with white spot syndrome virus (WSSV). J. Invertebr. Pathol. 136, 10–22.
Sánchez-Paz, A., 2010. White spot syndrome virus: an overview on an emergent concern. Vet. Res. 41, 43.
Sellars, M.J., Lyons, R.E., Grewe, P.M., Vuocolo, T., Leeton, L., Coman, G.J., Degnan, B.M., Preston, N.P., 2007. A PL10 vasa-like gene in the Kuruma shrimp, *Marsupenaeus japonicus* expressed during development and in adult gonad. Mar. Biotechnol. 9, 377–387.
Sun, Y., Li, F., Sun, Z., Zhang, X., Li, S., Zhang, C., Xiang, J., 2014. Transcriptome analysis of the initial stage of acute WSSV infection caused by temperature change. PLoS One 9, 1–16.
Sweet, M.J., Bateman, K.S., 2015. Diseases in marine invertebrates associated with mariculture and commercial fisheries. J. Sea Res. 104, 16–32.
Vargas-Albores, Hinojosa-Baltazar, Portillo-Clark, Magallon-Barajas, 1998. Influence of temperature and salinity on the yellowleg shrimp, *Penaeus californiensis*, prophenoloxidase system. Aquac. Res. 29, 549–553.
Waller, J.D., Wahle, R.A., McVeigh, H., Fields, D.M., 2016. Linking rising pCO2 and temperature to the larval development and physiology of the American lobster (*Homarus americanus*). ICES J. Mar. Sci. fsw154.
Wang, W., Zhang, X., 2008. Comparison of antiviral efficiency of immune responses in shrimp. Fish Shellfish Immunol. 25, 522–527.
You, X.X., Su, Y.Q., Mao, Y., Liu, M., Wang, J., Zhang, M., Wu, C., 2010. Effect of high water temperature on mortality, immune response and viral replication of WSSV-infected *Marsupenaeus japonicus* juveniles and adults. Aquaculture 305, 133–137.
Zhao, Z.-Y., Yin, Z.-X., Xu, X.-P., Weng, S.-P., Rao, X.-Y., Dai, Z.-X., Luo, Y.-W., Yang, G., Li, Z.-S., Guan, H.-J., Li, S.-D., Chan, S.-M., Yu, X.-Q., He, J.-G., 2009. A novel C-type lectin from the shrimp *Litopenaeus vannamei* possesses anti-white spot syndrome virus activity. J. Virol. 83, 347–56.

3.0 HISTOLOGICAL AND ULTRASTRUCTURAL ASSESSMENT OF AMERICAN LOBSTER (*Homarus americanus*) EXPERIMENTALLY INFECTED WITH WHITE SPOT SYNDROME VIRUS

3.1 Abstract

White spot syndrome virus (WSSV) is one of the most virulent pathogens affecting shrimp aquaculture worldwide. The World Organization for Animal Health considers all decapod crustaceans susceptible to WSSV. In shrimp, WSSV targets ectodermal and mesodermal tissue with cuticular epithelium being the most prominent site of infection. However, tissue tropism of WSSV in the American lobster *Homarus americanus* is mostly unknown. Previous research found that *H. americanus* produces a targeted immune response to experimentally created WSSV infection at 20 ^{o}C. WSSV virions were most easily identifiable in the antennal gland using light and electron microscopy. *H. americanus* inhabit waters that vary in temperature between 0 ^{o}C and 20 ^{o}C and temperature is known to influence WSSV infection in many species. The present study used a range of temperatures (10 ^{o}C, 15 ^{o}C, 17.5 ^{o}C and 20 ^{o}C) to explore the interactions between temperature, WSSV and the antennal gland in *H. americanus*. At 10 ^{o}C no WSSV associated pathology was observed in the examined tissues. At 15 ^{o}C a few suspected candidate nuclei were observed in the antennal gland, intestine and tail muscle tissue. At the warmer temperatures (17. 5 ^{o}C and 20 ^{o}C) the intestine and antennal gland revealed prominent WSSV-associated histopathology. Transmission electron microscopy was used to elucidate the general ultrastructure of the antennal gland and characterize changes associated with WSSV infection in the antennal gland of *H. americanus*. The antennal gland is comprised of two main regions the coelomosac and labyrinth.

The coelomosac contains cells with extensive apical blebbing. The labyrinth is composed of tall columnar cells with microvilli. WSSV virions were present in both the labyrinth and coelomosac cells of WSSV infected *H. americanus* at 17.5 ^{o}C and 20 ^{o}C. This study provides insight into the role that the antennal gland may play as a preferred site of viral replication and excretion in decapods.

3.2 Introduction

White spot syndrome virus (WSSV), a large DNA virus belonging to the *Nimaviridae* virus family, is currently one of the most prevalent and widespread viruses impacting shrimp aquaculture (Sánchez-Paz, 2010). WSSV targets tissues of ectodermal and mesodermal origin, such as gills, lymphoid organs and cuticular epithelium (Pradeep et al., 2012; Sánchez-Paz, 2010). WSSV-virions have also been reported to replicate within the circulating haemocytes (Sánchez-Paz, 2010). In crustaceans, haemolymph, and haemocytes, are responsible for supplying all organs and tissues with essential nutrients (Martin and Hose, 1995; Söderhäll, 2016). As a result, WSSV infections have been reported in all vital organs in shrimp, despite tissues of mesodermal origin being refractory to infection (Sánchez-Paz, 2010). Histologically WSSV is recognized by hypertrophied nuclei with inclusion bodies (Bateman et al., 2012). Under transmission electron microscopy, virions have been found to range in size from 210-420 nm in length and 70-167 nm in diameter (Sánchez-Paz, 2010).

The most notable feature of the virus is that it appears to be host non-specific with over 93 crustacean species reported as susceptible either from natural or experimental infection; including American and European lobsters, *Homarus*

americanus and *H. gammarus* respectively (Bateman et al., 2012; Clark et al., 2013b; Sánchez-Paz, 2010). Bateman et al., (2012) examined WSSV susceptibility in seven economically important crustacean species (*Cancer pagurus*, *H. gammarus*, *Nephrops norvegicus*, *Austropotamobius pallipes*, *Pacifastacus leniusculus*, *Eriocheir sinensis*, *Carcinus maenas)* and found that in all species WSSV associated pathology was most prominent in the cuticular epithelium of the gills. Interestingly, in *C. maenas*, WSSV associated pathology was observed at a much lower severity than all other species (Bateman et al., 2012). Water temperature during infection trial represented maximum summer temperatures for each species and ranged between 15 ^{o}C- 20 ^{o}C (Bateman et al., 2012). Similarly, Clark et al., (2013) found that upon experimental injection at 20 ^{o}C, WSSV replicates within *H. americanus*. Histological analysis of infected *H. americanus* revealed that WSSV pathology was most readily observed in the antennal gland as opposed to the frequently cited cuticular epithelium (Clark et al., 2013; Byrne, unpublished).

In decapod crustaceans, the gut, gill and antennal gland are the main excretory and ion-regulating organs (Khodabandeh et al., 2005b). The antennal gland differs fundamentally from the gills and gut as fluid input and exchange is entirely internal, between haemolymph and its filtrate (Khodabandeh et al., 2005b; McMahon, 1995). In *Homarus* species the antennal gland is triangular in shape and located in the anterior cephalothorax, near the base of the antennae (Khodabandeh et al., 2005b; McMahon, 1995). There are two main cell types in the antennal gland, the labyrinth and the coelomosac (Khodabandeh et al., 2005b). The coelomosac cells are responsible for ultrafiltration, whereas labyrinth cells function as a site of active

regulation of urinary ions (Khodabandeh et al., 2005b; McMahon, 1995). The ultrafiltration process is similar to that of vertebrates where large molecules are retained and small molecules continue to pass through the tubular labyrinth (Khodabandeh et al., 2005b; McMahon, 1995). The tubular region terminates in a large bladder where urine is collected prior to excretion through the excretory pore (McMahon, 1995). The function, organization and ultrastructure of the antennal gland is well characterized for many crustacean species including *Ocypode stimpsoni*, *Pacifastacus leniusculus*, *Astacus leptodactylus*, *Callinectes sapidus*, and *H. gammarus* (Cameron and Batterton, 1978; Fuller et al., 1989; Khodabandeh et al., 2005a, 2005b; Tsai and Lin, 2014) but only one review of the general structure of antennal gland in *H. americanus* exists (Waite 1899).

The American lobster, *H. americanus*, inhabits waters that span the Canadian and American North Atlantic coast. This broad geographical range means that the animal is exposed to temperatures that range between 0 ^{o}C and 20 ^{o}C (Lawton and Lavalli, 1995). Water temperature has been found to influence many biological processes of *H. americanus* such as larval development, growth, and reproduction (Aiken and Waddy, 1986). In *Marsupenaeus japonicus* and *Litopenaeus vannamei* water temperature has been found to influence WSSV infection and disease, with extreme low and high temperatures negating disease (Lua and Hirono, 2015; Moser et al., 2012; You et al., 2010).

Clark et al. (2013) examined WSSV infection in *H. americanus* at 20 ^{o}C, a temperature near the animal's upper thermal limit. Little is therefore known about WSSV infection over the broad range of temperatures the lobsters inhabit. This

study will use the research foundation previously established by (Clark et al., 2013b) to examine the relationship between temperature, WSSV and the antennal gland in *H. americanus*. The goals of the present study are to explore the constraints imposed by a range of water temperatures on WSSV infection in *H. americanus*, confirm the antennal gland as a key target tissue for WSSV replication, and provide an updated ultrastructural review of the antennal gland in adult *H. americanus*.

3.3 Methods

3.3.1 Experimental animals

Adult male market sized *Homarus americanus* (n = 48, 568 g ± 18.63 g) were purchased from a local commercial seafood supplier (Clearwater Seafood®, Bedford, NS, Canada) and housed at the Gulf Biocontainment Unit-Aquatic Animal Health Laboratory (GBU-AAHL; Fisheries and Oceans Canada, Charlottetown, PEI, Canada). As previously described (Section 2.3.1), upon arrival, lobsters were given unique identity labels and randomly assigned to individual compartments in a perforated plastic tote. Each tote housed six lobsters. Totes were randomly assigned to one of four 400 L tanks maintained at 8 ^{o}C. A single tank housed a total of 12 lobsters. Initial health assessments; comprised of physical surveys, haemolymph screening for bacterial and ciliated protist infections (Acorn et al., 2011), assessment of total haemocyte concentration and haemolymph refractive index, and WSSV-qPCR testing of haemolymph and pleopod tissue, were conducted three days post arrival (Section 2.3.2; Appendix A Fig. A1).

Each 400 L tank was supported by an independent recirculating artificial seawater (ASW) system maintained at 31 ppt (Instant Ocean® Aquarium Sea Salt

Mixture). Tanks were equipped with a 25 μm chemical filter, UV filter, protein skimmer with submersible pump and biological filtration. The recirculating ASW system received 10-15% replacement (new) water per day (Section 2.3.1). Temperature (programmed temp. ± 1 ^{o}C), pH (8.1 – 8.4) and oxygen concentration (8.0 – 8.7 mg/L) were recorded daily. Nitrite (<1.0 mg/L), nitrate (<4 mg/L) and total ammonia nitrogen (<1.0 mg/L) were recorded weekly. *H. americanus* were fed three times per week for the duration of the trial. Feed was acquired from commercial suppliers (Charlottetown, PE, Canada).

Specific pathogen free (SPF) Pacific white shrimp *Litopenaeus vannamei*, obtained from the Oceanic Institute (Waimanalo, HI, USA), were used to generate WSSV inoculum used for *H. americanus* infection challenge (Section 3.3.2). SPF *L. vannamei* were housed at the GBU-AAHL facility in a semi-open multi-tank (9 L) recirculating ASW system maintained at 27 ^{o}C (± 1 ^{o}C) and a salinity of 31 ppt (Section 2.3.1). Shrimp were fed a maintenance diet of Ziegler® Shrimp feed (Gardners, PA, USA).

All waste material was decontaminated prior to disposal. Effluent wastewater was autoclaved and animal carcasses were incinerated. Work areas were bleached (500 ppm, Javex®), rinsed with water, and sprayed with 70% isopropanol. Work involving WSSV was conducted within AQC3 *in vivo* biocontainment facilities as per the Canadian aquatic animal pathogen standards (CFIA Biohazard Containment and Safety, 2010). Live animal based projects at GBU-AAHL were monitored and audited by the Fisheries and Oceans Regional Animal Care Committee.

3.3.2 WSSV Inoculum, Infection Challenge and Sampling

WSSV inoculum was prepared under biocontainment at the GBU-AAHL facility (Section 2.3.3). Previously generated frozen WSSV infected *L. vannamei* muscle tissue (from previous GBU-AAHL studies) was thawed and homogenized with phosphate-buffered saline (PBS; 0.1 M, pH 7.4). The homogenate was centrifuged twice at 5000 x *g* for 20 mins at 4 ^{o}C. Supernatant was collected, diluted 1:4 with PBS, filtered (0.45 µM Acrodisc® syringe filter) and used to inoculate 4 SPF *L. vannamei* (Section 2.3.3).

Following inoculation, *L. vannamei* were monitored every four hours or more; dead or moribund *L. vannamei* were removed from the aquarium, weighed and frozen at -80 ^{o}C until all shrimp died. WSSV infected *L. vannamei* were then thawed on ice and tail muscle tissue was collected for viral load quantification (Section 3.3.4) and to generate fresh inoculum. Fresh inoculum, was prepared from the recently WSSV infected *L. vannamei* tail muscle tissue in the same manner described above and stored at -80 ^{o}C until infection challenge. Viral load in *L. vannamei* tissue was determined using qPCR (Section 3.3.4) prior to infection challenge with *H. americanus*.

Once viral load was quantified, fresh inoculum (viral filtrate) was thawed, diluted a second time using PBS (0.1 M, pH 7.4) to yield an equivalent of 10^4 WSSV plasmid copies/µL and loaded into eight 1 mL syringes with 25 G needles for *H. americanus* inoculation. Eight lobsters from each tank were randomly assigned to receive 200 µL injections of 10^4 WSSV plasmid copies/µL. The remaining four lobsters in each tank received 200 µL of non-infected *L. vannamei* tissue

homogenate (control). The anterior ventral abdomen area was sprayed with 70% alcohol prior to inoculation. *H. americanus* were injected in the second tail segment of the abdomen.

Haemolymph samples were collected from each lobster 12, 24, 48, 96, 144, 168, 192, 240, 288 and 336 hours post-inoculation (PI). One-week PI (168 hrs), four infected lobsters were randomly selected and necropsied from each tank. The remaining 8 lobsters in each tank (4 infected and 4 controls) were necropsied two-weeks PI (336 hrs). Lobsters were weighed, a final haemolymph sample was collected, and then euthanized as per Clark et al., (2013a) by severing the ventral nerve cord. A total of 12 tissues (cuticular epithelium, antennal gland, pleopod, heart, gill, hepatopancreas, intestine, stomach, gonad, brain, nerve cord and tail muscle) were collected for histological analysis (Section 3.3.5); 8 tissues (antennal gland, cuticular epithelium, heart, gonad, hepatopancreas, gill, intestine, and pleopod) were placed in 95% EtOH for WSSV-qPCR testing (Section 3.3.4); 3 tissues (antennal gland, hepatopancreas, and cuticular epithelium) were collected for transmission electron microscopy (Section 3.3.6) and 2 tissues (hepatopancreas and antennal gland) were collected for microarray analysis (Chapter 2).

3.3.3 Negative staining of WSSV

Fresh inoculum (Section 3.3.2) was also used to inject 3 SPF *L. vannamei* in a separate WSSV infection challenge designed to collect fresh WSSV infected tail muscle tissue for purification of intact WSSV viral particles following a modified protocol previously described for penaeid shrimp haemolymph (Durand et al., 1996). Infected tail muscle (~250 mg) was homogenized with 1000 µL of PBS (0.1 M, pH

7.4) and centrifuged (Eppendorf centrifuge 5430R, Hamburg, Germany) at 5000 x *g* for 10 mins. The supernatant was collected and 25% glutaraldehyde (960 µL) in 0.1 M phosphate buffer was added to make a final concentration of 3%. Viral suspension was fixed overnight at 4 ^{o}C and then centrifuged at 5000 x *g* for 10 mins. Supernatant was collected, and ultracentrifuged at 71900 x *g* (Model L8M, Beckman Coulter, Mississauga, ON, Canada) for 1 hour. The supernatant was discarded and pellet was re-suspended in 0.1 M phosphate buffer (5 mL). The viral suspension (10 µL) was placed on three collodion coated 400 mesh copper grids (Canemco Inc., Lakefield, QC, Canada) and negatively stained with phosphotungstic acid (PTA 2%, pH 6.2) for 1 min. Grids were triple washed in diH_2O for 30 sec in-between stains and set to dry at room temperature. Grids were examined using a transmission electron microscope (Hitachi H-7500, Nissei Sangyo, Rexdale, ON, Canada) operated at 80 kV and digital images were captured by AMT HR40 side mount digital camera (Advance Microscopy Techniques, Danvers, Ma, USA).

3.3.4 WSSV-qPCR

WSSV-qPCR was conducted using DNA extracted from haemolymph and various tissues (lobster and shrimp). DNA was extracted using a DNeasy® Blood & Tissue Kit (Qiagen®, Toronto, ON, Canada) following manufacturer's instructions (Appendix B). As previously described (Section 2.3.4), 30 mg of tissue or 100 µL of haemolymph tissue was lysed overnight at 56 ^{o}C using 20 µL of proteinase K. Buffering conditions were adjusted using 180 µL of ATL buffer (if beginning with tissue), 200 µL of AL buffer and 200 µL of 100% EtOH. Lysate was pipetted onto a DNeasy® mini spin column and centrifuged (Eppendorf centrifuge 5430R,

Hamburg, Germany) at 6000 x *g* for 1 min. DNA contaminants and enzyme inhibitors were removed using AW1 buffer (500 µL) centrifuged at 6000 x *g* for 1 min followed by AW2 buffer (500 µL) centrifuged at 20,000 x *g* for 3 mins. DNA was eluted with 100 µL of AE buffer, aliquoted (2 x 50 µL) and frozen at -80 ^{o}C until qPCR.

Previously designed primers (Clark et al., 2013b) were used to amplify WSSV DNA. A single qPCR reaction consisted of 12.5 µL of TaqMan® Universal PCR master mix (Applied Biosystems™, CA, USA), 2 µL of DNA extract, 0.75 µL of 10 µM forward primer F1-WSDvp28 (5'GTGACCAACACCATCGAAAC3'), 0.75 µL of 10 µM reverse primer R1-WSDvp28 (5'TGAAGTAGCCTGATCCAACC3'), 0.375 µL of 10 µM TaqMan® probe P1-WSDvp28 (5'CCTCCGCATTCCTGTGACTGC3'-FAM/TAMRA), and 8.6 µL of nuclease-free water (UltraPure™ DNase/RNase-Free Distilled water, Applied Biosystems™, CA, USA) to yield a final reaction volume of 25 µL. Reactions were carried out on a Chromo4™ Real-Time PCR system (Bio-Rad Laboratories, CA, USA) as follows: 50 °C for 2 min, 95 °C for 10 min, 40 cycles of 95 °C for 15 sec, 60 °C for 1 min, plate read, and a final incubation at 20 °C for 5 min. A plasmid standard (10^7 viral copies) was diluted with nuclease-free water and used to quantify WSSV viral titre in samples. Viral copy number and cycle threshold (C_T) value were recorded using Opticon Monitor™ software (Bio-Rad Laboratories, CA, USA).

3.3.5 Histology

Tissues collected for histology (Section 3.3.2) were fixed in 10% neutral buffered formalin (NBF; Sigma-Aldrich, Oakville, ON, Canada) for 24 hours,

decanted and then post fixed in fresh 10% NBF for four weeks. All 12 tissues from one lobster were trimmed into one labeled Surgipath® Multi-cassette (Leica Biosystems, Wetzlar, Germany). Cassettes were submitted to the histology department at the Atlantic Veterinary College (University of Prince Edward Island Charlottetown, PE, Canada) for standard processing. Briefly, tissues were rinsed, dehydrated (using a graded series of ethanol washes), cleared (using a series of xylene washes) and infiltrated with paraffin wax using a Tissue-Tek® vacuum infiltration tissue processor (Somagen Diagnostics Inc., Edmonton, AB, Canada). Serial sections (5 μm) were cut on a rotary microtome (Microm HM 355, Thermo Fisher Scientific, Waltham, MA, USA) and mounted onto glass slides. Slides were stained with haematoxylin and eosin (H&E). Slides were analyzed using a light microscope (Zeiss Axioplan 2, Zeiss, Thornwood, NY, USA) and digital images were captured using an AxioCam HRC camera (Zeiss Microimaging, Thornwood, NY, USA).

3.3.6 Transmission electron microscopy

Only the antennal gland was examined for the present study. The right antennal gland of each lobster was removed using the blunt end of a scalpel blade holder. Tissue was gently placed in a weigh boat where two evenly spaced cuts through the whole gland were made. The central ~1 cm length of tissue containing both the anterior and posterior portion was collected and fixed in 4 mL of 2.5% glutaraldehyde (SPI® Supplies, Toronto, ON, Canada) in 0.1 M phosphate buffer overnight at 4 ^{o}C. The antennal gland from one individual from each sampling period (one-week PI, two-week PI, or control) from each of the four temperatures

was randomly selected for immediate processing to blocks as a representation for the group. Antennal gland of other lobsters remained in 2.5% glutaraldehyde (0.1 M phosphate buffer at 4 ^{o}C) until histology slides were examined. A second individual from each group was processed to blocks following completion of histological analysis to confirm and corroborate findings.

For processing to blocks, tissues were washed twice with ~5 mL of 0.1 M phosphate buffer at room temperature on a rotator (Fisher Hematology Chemistry Mixer, Artisan Technology Group, Champaign, IL, USA) and post fixed with 2 mL of 1% osmium tetroxide EM grade (SPI® Supplies, Toronto, ON, Canada) in 0.2 M phosphate buffer for 1 hour at room temperature. Samples were dehydrated, via a graded series of EtOH washes at concentrations of 50%, 70% 95% and 100%, twice for 10 mins with the exception of the final 100% EtOH wash being overnight at room temperature. Samples were washed twice with 100% propylene oxide (PO; SPI® Supplies, Toronto, ON, Canada) for 10 mins and infiltrated with Epon (SPI® Supplies, Toronto, ON, Canada) at a ratio of Epon:PO of 50:50 and 75:25 for 1 hour each. Tissues were infiltrated with 100% Epon overnight in a vacuum desiccator (Hitachii Hus 5GB, Nissei Sangyo, Rexdale, ON, Canada). Samples were placed in BEEM® capsules (Canemco Inc., Lakefield, QC, Canada) filled with Epon and polymerized overnight at 70 ^{o}C.

Polymerized Epon blocks were trimmed into a trapezoidal shape using a razor blade and dissecting microscope. Thick (0.5 µm) sections were cut on an ultramicrotome (Reichert-Jung Ultracut E, Leica Biosystems, Wetzlar, Germany) using a glass knife (Leica EM KMR2 Knife Maker, Leica Biosystems, Wetzlar,

Germany) and mounted onto a glass slide. Slides were stained with 1% toluidine blue in 1% sodium tetraborate solution. Thick sections were observed under light microscope to select areas for ultrathin sectioning.

Blocks were re-trimmed for ultrathin sectioning. Ultrathin sections (90 nm) were cut with either a glass knife or diamond knife (Pelco® Diamond Knife, Ted Pella Inc., Redding, CA, USA) and collected onto 200 mesh copper Supergrids™ (SPI® Supplies, Toronto, ON, Canada). Sections were stained with uranyl acetate (Thermo Fisher Scientific, Waltham, MA, USA) for 30 mins, followed by lead acetate (JBEM Services Inc., Point-Claire Dorval, QC, Canada) for 2 mins. Grids were triple washed in diH_2O for 30 sec in-between stains and set to dry at room temperature. Grids were examined using a transmission electron microscope (Hitachi H-7500, Nissei Sangyo, Rexdale, ON, Canada) operated at 80 kV and digital images were captured by AMT HR40 side mount digital camera (Advance Microscopy Techniques, Danvers, Ma, USA).

3.4 Results

3.4.1 WSSV Inoculum

WSSV was first passed through *L. vannamei* as a bioassay to assess viability and infectivity of WSSV prior to infection trial with *H. americanus*. All infected *L. vannamei* died within 72 hours post inoculation (PI) and were confirmed WSSV positive via qPCR. Negative staining of tail muscle from *L. vannamei* inoculated with the fresh inoculum (same viral filtrate used for *H. americanus* challenge) revealed the presence of whole viral WSSV particles (Fig. 3.1). Viral particles were preserved in the characteristic rod shape with trilaminar envelope present (Fig. 3.1

A). Viral particles were observed in varying stages of development with the striated nucleocapsid core (Fig. 3.1 A) not yet enveloped. Some virions also contained the distinctive tail-like appendage (Fig. 3.1 B). Virions ranged from 200-350 nm in length, and were confirmed as WSSV based on appropriate size and morphology.

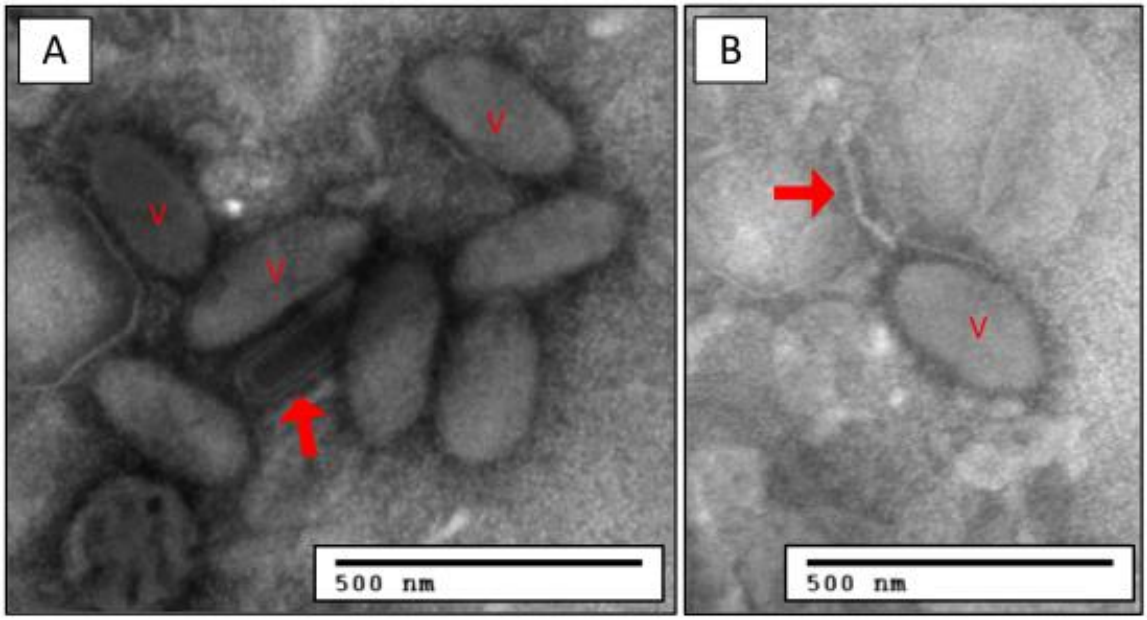

Figure 3.1: Negative stained WSSV virions collected from *Litopenaeus vannamei* tail muscle.

WSSV infection in *L. vannamei* generated using same inoculum used for *H. americanus* challenge. (A) Cluster of WSSV virions with striated nucleocapsid core present (arrow). (B) Single WSSV virion containing tail like projection (arrow). (v) = virions

3.4.2 WSSV Infection challenge

The health of *H. americanus* was monitored closely during the infection trial. Haemolymph cultures, revealed the absence of bacterial or ciliate protist infections in all *H. americanus*. The haemolymph refractive index was not statistically significant between infected and control animals across all four temperatures. At 20 ^{o}C, a single mortality was observed 144 hours PI. Necropsy revealed the cause of death to be a rubber claw band present within the stomach contents of *H. americanus.* At 288 hours PI, total haemocyte concentration (THC) in some of the WSSV infected *H. americanus* at 20 ^{o}C fell below $3.0x10^{9}$/L. The animals appeared moribund so the infection trial (at 20 ^{o}C) was ended one day early (312 hours PI). This group is still referred to as 20 ^{o}C two-week PI.

Results of THC (Section 2.4.2; Fig. 2.2) and WSSV-qPCR viral titre (Section 2.4.3; Fig. 2.3) revealed a decline in clinical condition of WSSV challenged *H. americanus* at 17.5 ^{o}C and 20 ^{o}C but not at 15 ^{o}C and 10 ^{o}C. WSSV-qPCR of haemolymph showed an increase in WSSV viral copy number during the trial at 15 ^{o}C, 17.5 ^{o}C and 20 ^{o}C. At 10 ^{o}C WSSV viral copy number remained at consistently low infection levels throughout the trial. WSSV-qPCR of haemolymph was negative for all control *H. americanus*.

3.4.3 WSSV-qPCR of Tissues

Variation in viral load was observed between the different tissues and between infected *H. americanus* at different temperatures and sampling time points. All tissues collected from control *H. americanus* across all four temperatures were negative for WSSV DNA. All tissues of infected *H. americanus* one-week and two-

weeks PI at 10 ^{o}C were also negative for WSSV DNA (Fig 3.2). Interestingly, all tissues collected from one-week PI infected *H. americanus* at 15 ^{o}C were negative but at two-weeks PI at 15 ^{o}C tissues were positive (Fig 3.2). At 17.5 ^{o}C and 20 ^{o}C all tissues collected from infected animals were positive and viral load in the tissues increased as time progressed (Fig. 3.2). At 17.5 ^{o}C two-weeks PI and 20 ^{o}C one-week and two-weeks PI the antennal gland tissue had the highest viral titre. In WSSV infected *H. americanus* two-weeks PI at 17.5 ^{o}C an average of 1.90E+08 relative WSSV DNA copies/30 mg of antennal gland tissue was detected (Fig. 3.2). At one-week and two-week PI at 20 ^{o}C an average of 2.62E+06 and 4.03E+06 WSSV DNA copies/30 mg of antennal gland tissue was detected, respectively. For the two-weeks PI at 15 ^{o}C and the one-week PI at 17.5 ^{o}C, the antennal gland was among the top 5 tissues with the highest viral titre. Interestingly at two-weeks PI at 15 ^{o}C the tail muscle had the highest viral titre and cuticular epithelium had the lowest (Fig 3.2).

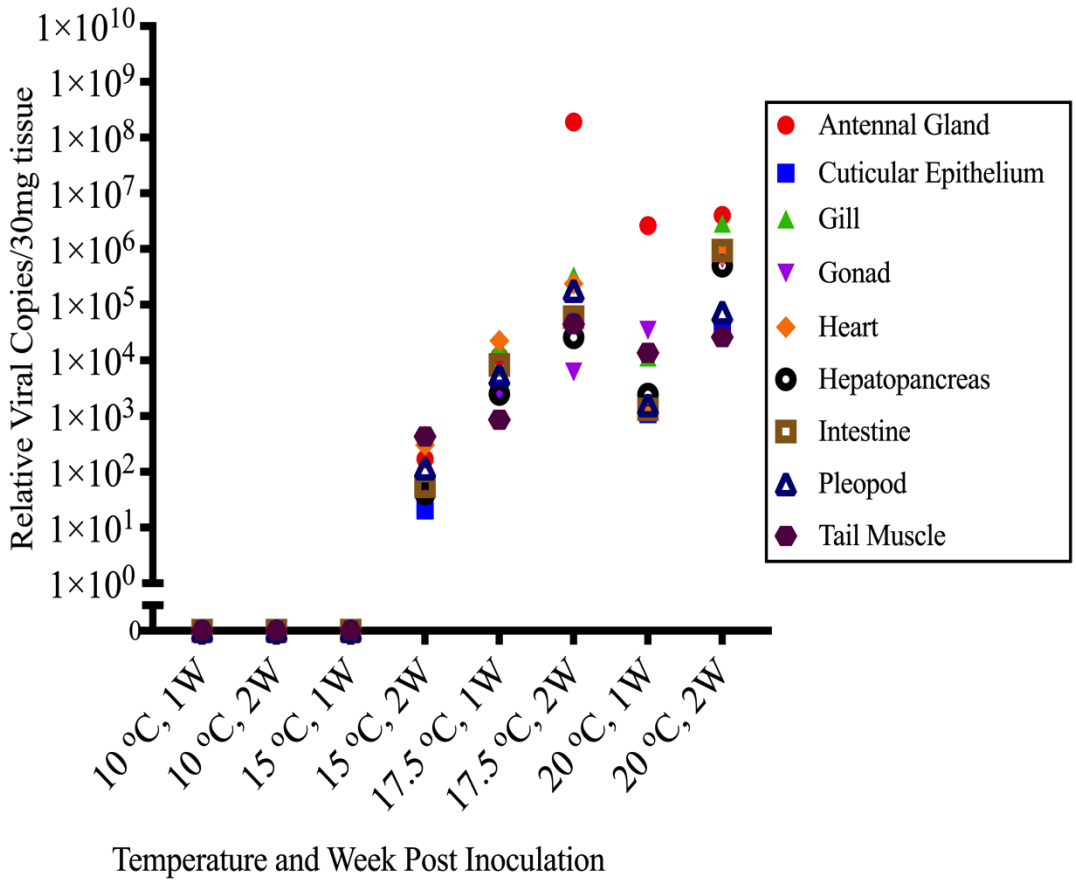

Figure 3.2: Relative WSSV DNA copies per 30 mg of tissue detected using WSSV-qPCR in WSSV infected *Homarus americanus* one and two-weeks post inoculation at the four experimental temperatures.

Data was log transformed. Break in the Y-axis highlights the transition from numerical scale to log scale; required in order to plot true zero values as true zeros. Data points represent the mean of 4 lobsters at each sampling time point.

3.4.4 Histology

Histopathology observed in each tissue collected at the different temperatures and sampling points is summarized (Table 3.1). At 10 ^{o}C one and two-weeks PI and 15 ^{o}C one-week PI no WSSV associated pathology was observed in any of the collected tissues. At 15 ^{o}C two-weeks PI a few candidate nuclei (defined as very mildly hypertrophied or irregularly shaped) were present within the antennal gland, tail muscle and intestine of *H. americanus*. At 17.5 ^{o}C and 20 ^{o}C one and two-weeks PI, large hypertrophied infected nuclei with inclusions were readily identified throughout the antennal gland (Fig. 3.3A) and intestine (Fig. 3.3B). WSSV pathology was more prevalent two-weeks PI at 17.5 ^{o}C and 20 ^{o}C compared to one-week PI at the respective temperatures. Increased WSSV pathology later in the infection trial corroborates WSSV-qPCR tissue data where a higher viral titre was also observed at the two-weeks PI sampling period for 17.5 ^{o}C and 20 ^{o}C compared to the one-week PI sampling period. A few candidate nuclei were also identified within pleopod, stomach, gill and gonad tissue two-weeks PI at 20 ^{o}C.

In WSSV infected *H. americanus* at 17.5 ^{o}C and 20 ^{o}C WSSV associated pathology was not uniformly distributed throughout the antennal gland tissue. Some sections of the tubular labyrinth region of the antennal gland contained apparently healthy nuclei whereas, other sections of the tubular labyrinth region contained many WSSV infected hypertrophied nuclei. The distribution of WSSV infected nuclei appeared random throughout tissue. Interestingly, cuticular epithelium showed no WSSV associated pathology in any of the infected animals across all

temperatures. None of the control animals (across all temperatures) displayed any signs of WSSV infection.

Table 3.1: Summary of histopathology observed in various tissues collected from WSSV experimentally infected *Homarus americanus* one and two-weeks post inoculation at the four experimental temperatures.

H. americanus tissues	10 °C		15 °C		17.5 °C		20 °C	
	1W PI	2W PI	1W PI	2W PI	1W PI	2W PI	1W PI	2W PI
Cuticular Epithelium	-	-	-	-	-	-	-	-
Antennal Gland	-	-	-	*	**	***	**	***
Pleopod	-	-	-	-	-	-	-	*
Heart	-	-	-	-	-	-	-	-
Gill	-	-	-	-	-	-	-	*
Hepatopancreas	-	-	-	-	-	-	-	-
Intestine	-	-	-	*	**	***	**	***
Stomach	-	-	-	-	*	*	*	*
Gonad	-	-	-	-	-	-	-	*
Brain	N/A	-	-	-	-	-	-	-
Nerve Cord	-	-	-	-	-	-	-	-
Tail Muscle	-	-	-	*	*	*	*	*

* A few candidate nuclei (very mildly hypertrophied or irregularly shaped) randomly distributed in tissue
**Infected nuclei (hypertrophied with eosinophilic inclusion bodies and marginated chromatin) randomly distributed in tissue
***Infected nuclei highly prevalent throughout tissue
- WSSV associated histopathology not evident
N/A Tissue was not collected for examination

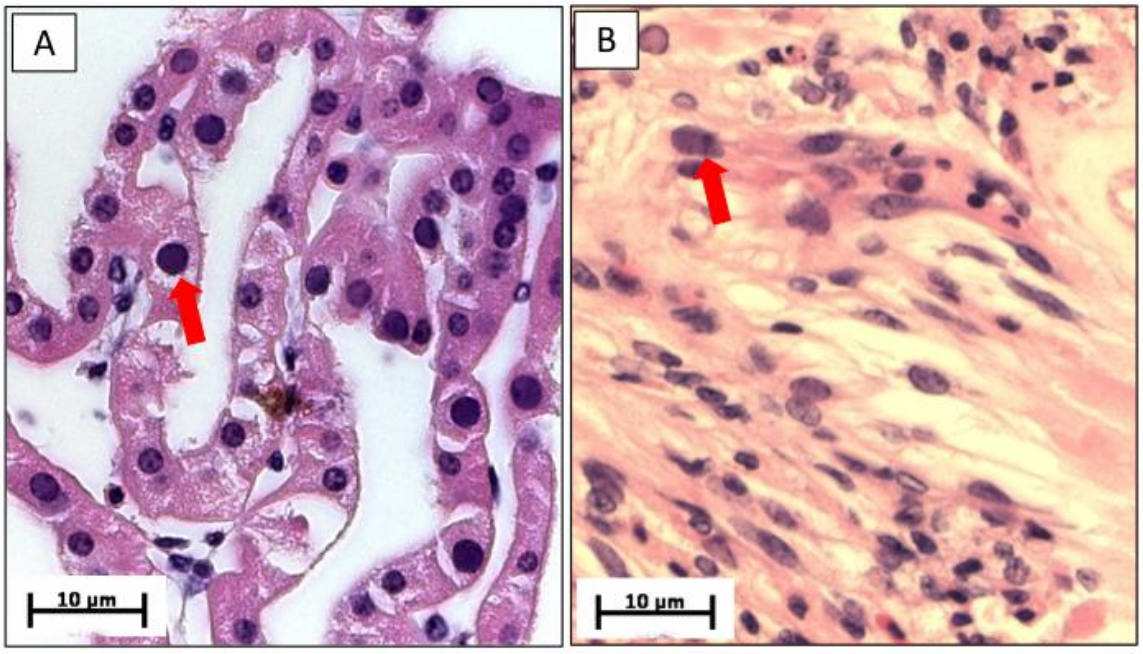

Figure 3.3: Haematoxylin and eosin stained cross section of antennal gland and intestine tissue in WSSV infected *Homarus americanus* two-weeks PI at 20 ^{o}C.

(A) Antennal gland tissue. (B) Intestine tissue. WSSV infected hypertrophied nuclei are highlighted with red arrows in both images.

3.4.5 Transmission electron microscopy and ultrastructure

Transmission electron microscopy and light microscopy (H&E) were both used to further characterize the general ultrastructure of the antennal gland in *H. americanus.* The *H. americanus* antennal gland contained two main cell types, the labyrinth cells and the coelomosac cells (Fig 3.4A). The tubular labyrinth cells interdigitate with the coelomosac cells. (Fig 3.4A) The labyrinth cells were the most prominent; comprising the greatest proportion of the tissue. They contained numerous infoldings on the basal side of the basement membrane and a pronounced brush border of microvilli that extended into the lumen (Fig. 3.4B). Among the control and WSSV-infected animals at the warmer temperatures (17.5 ^{o}C and 20 ^{o}C) the lumen of the labyrinth cells contained lots of cellular debris and blebbing. All labyrinth cells also contained several vacuoles and mitochondria. Coelomosac cells were identified by their columnar shape and absence of apical microvilli (Fig 3.4B). Coelomosac cells also contained mitochondria, numerous vacuoles and voluminous globules that appeared to detach into the lumen.

Transmission electron microscopy was also used to confirm the presence of WSSV in the antennal gland and also to elucidate the general ultrastructure of the antennal gland. WSSV virions were identified in the nucleus of the antennal gland labyrinth cells at 17.5 ^{o}C and 20 ^{o}C one-week and two-week PI (Fig 3.5). At one-week PI at 17.5 ^{o}C and 20 ^{o}C, nuclei were hypertrophied, had marginated nuclear material and virions were present at various stages of viral development within the nuclei (Fig 3.5A). Characteristic rod shaped viral particles with an electron dense centre and a trilaminar envelope were found within the nuclei of labyrinth cells two-

weeks PI at 17.5 ^{o}C and 20 ^{o}C (Fig. 3.5B). Two-weeks PI at 17.5 ^{o}C had the highest WSSV viral titre (detected using qPCR) and was the only group where the nuclear membranes of some infected nuclei appeared to be ruptured potentially releasing WSSV viral particles into the cell cytoplasm (Fig 3.5C). In one individual, at 17.5 ^{o}C, two-weeks PI, viral particles were found free within the luminal space of the labyrinth (Fig 3.5D). Examination of the coelomosac cells of the antennal gland was less comprehensive using electron microscopy due to fewer viewing opportunities as a result of tissue orientation. No viral particles were identified within the limited sections of coelomosac cells viewed using transmission electron microscopy. However, light microscopy of infected tissues at 17.5 ^{o}C and 20 ^{o}C both one and two-weeks PI, revealed the presence of infected hypertrophied nuclei in the coelomosac region, suggesting that WSSV infection in the antennal gland is not limited to a particular cell type. At 15 ^{o}C, two-weeks PI, the nuclei of antennal gland cells appeared slightly hypertrophied and contained areas of suspected WSSV tubular-shaped capsid formation (not pictured), however WSSV virions were never identified at 15 ^{o}C two-weeks PI despite presence of candidate nuclei on light microscopy. No virions were identified in the antennal gland at 10 ^{o}C or 15 ^{o}C one and two-weeks PI or in any of the control *H. americanus* across all temperatures.

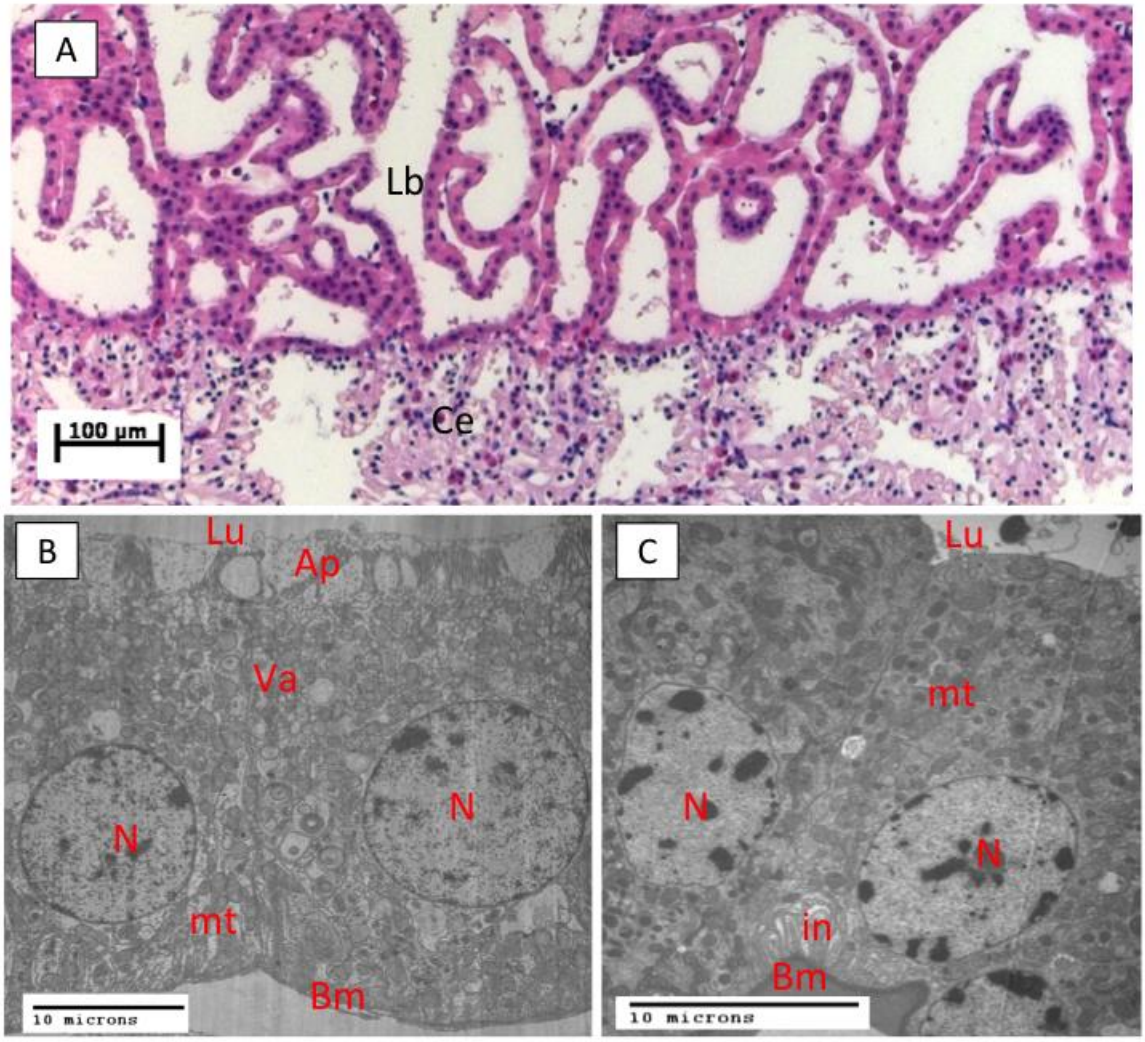

Figure 3.4: Haematoxylin and eosin stained cross section of *Homarus americanus* antennal gland and transmission electron micrographs of labyrinth and coelomosac cells with cellular components identified.

(A) H & E stained cross section. (B) Labyrinth cells. (C) Coelomosac cells. Ultrastructure of antennal gland regions was consistent regardless of temperature or WSSV infection. Images captured at varying temperatures. (A) *H. americanus* at 17.5 ^{o}C (B) 15 ^{o}C and (C) 20 ^{o}C. Lu=Lumen, Ap= Apical microvilli, Va= Vacuole, N=Nucleus, mt= mitochondria, Bm=basement membrane, in=infoldings, Ce= coelomosac, Lb= labyrinth.

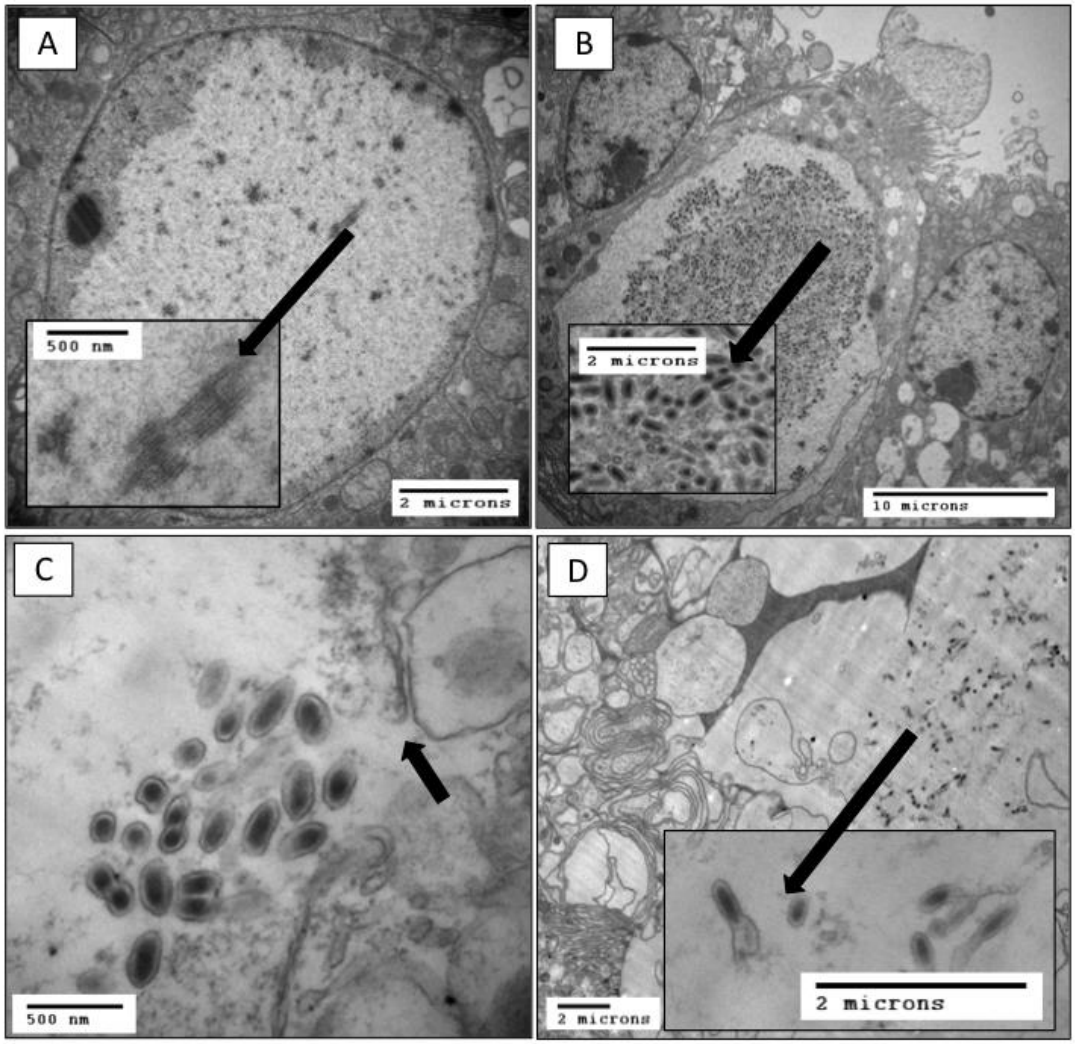

Figure 3.5: Transmission electron micrographs of WSSV infected nuclei in labyrinth cells of the antennal gland in *Homarus americanus*, one-week PI at 20 ^{o}C and two-weeks PI at 17.5 ^{o}C.

(A) One-week PI at 20 ^{o}C. (B, C & D) Two-weeks PI at 17.5 ^{o}C. Representative images of WSSV infected nuclei within the antennal gland tissue of *H. americanus* infected with WSSV. (A) One week PI at 20 ^{o}C with hypertrophied nuclei, marginated host chromatin and WSSV viral particles in early stages of viral development and encapsulation (arrow and increased magnification in box). (B) Two weeks PI at 17.5 ^{o}C with significantly hypertrophied nuclei with multiple WSSV viral particles present inside nucleus. Apparently normal nuclei present on both sides of infected nuclei. (C) Two weeks PI at 17.5 ^{o}C, infected nuclei with disrupted nuclear membranes (arrow) and WSSV virions present within nuclei. (D) Single individual two weeks PI at 17.5 ^{o}C where WSSV virions (arrow) were observed free within the lumen of the antennal gland.

3.5 Discussion

The main goals of this study were to explore the impact of water temperature on WSSV infection in *H. americanus*, confirm the antennal gland as a key target tissue for WSSV replication, and provide an updated ultrastructural review of the antennal gland in adult *Homarus americanus*. Analysis of viral load in the different tissues via WSSV-qPCR was critical for understanding the impact of water temperature and confirming the antennal gland as a key target tissue for WSSV infection. Analysis of the data suggests that at 10 ^{o}C, following intramuscular injection *H. americanus* can be infected with WSSV but does not manifest clinical signs of infection (Table 3.1; Chapter 2, Fig. 2.3). WSSV-qPCR tissue results from the present study further corroborate this hypothesis because at 10 ^{o}C none of the WSSV-qPCR tested tissues were positive. At 15 ^{o}C one-week PI all of the tested tissues were negative, however at two-weeks PI tissues were WSSV positive. Due to the pre-determined one and two-week sampling periods the present study was unable to conclude if at 10 ^{o}C, temperature inhibits the viruses ability to replicate or if cold temperatures simply slow the entire replication process. A longer infection trial (>2 weeks) is required in order to address this. You et al., (2010) found that in WSSV-infected *Marsupenaeus japonicus* increased water temperatures (outside of the thermal preference for WSSV) slowed the onset of disease and reduced mortality rates. Similarly, Sonnenholzner et al., (2002) found that in *L.vannamei*, WSSV is capable of invading all tissues in only 36 hours at 27 ^{o}C but requires four days at 33 ^{o}C (a temperature outside of the thermal range for WSSV). The present results suggest that in WSSV infected *H. americanus* cold temperatures (outside of the

thermal range for WSSV) may also increase the time to onset of disease or prevent disease manifestation with further work needed to confirm the latter.

WSSV-qPCR data in conjunction with histology results highlighted the antennal gland as a key target tissue for WSSV-replication in *H. americanus.* WSSV associated histopathology was most readily identifiable in the antennal gland and intestine of WSSV infected *H. americanus* at 17.5 ^{o}C and 20 ^{o}C. At the warmer temperatures the antennal gland also had the highest viral titre via WSSV-qPCR. Previous research by Escobedo-Bonilla et al., (2007) found that following oral inoculation in *L. vannamei* the primary sites of WSSV replication were the cells of the foregut and gills at low and high dose and the cells of the antennal gland at high dose. The researchers speculated that WSSV infection might target these tissues because they are essential for maintenance of homeostasis and disruption can result in host mortality.

In *Penaeus merguiensis* WSSV virions have been identified in varying stages of replication within both the semi-granular and granular haemocytes (Wang et al., 2002). However, in *L. vannamei* WSSV has been found to spread in a cell-free form via the haemolymph with haemocytes being refractory to WSSV infection (Escobedo-Bonilla et al., 2007). The present study did not examine if replicating WSSV virions were present within *H. americanus* haemocytes however previous work has demonstrated that WSSV viral titre increases within the haemolymph of WSSV infected *H. americanus* over time (Clark et al., 2013c; Chapter 2). In crustaceans, the haemolymph bathes all tissues and thus provides a mechanism by which WSSV virions can disperse to various tissues. The antennal gland is the main

osmoregulatory organ in decapod crustaceans (Khodabandeh et al., 2005b) and plays a crucial role in ion-regulatory and excretory functions in *Homarus* species (Khodabandeh et al., 2005b). Haemolymph (along with the WSSV virions) is filtered through the antennal gland in *H. americanus.* As a result, it is not surprising that the antennal gland would be a prominent site for detecting WSSV. It would be of particular interest to explore if urine output in WSSV-infected *H. americanus* contains WSSV, and whether this may serve as a pathway for horizontal transfer of WSSV. Histology results also confirmed that for the antennal gland and intestine, the virus was directly infecting the cells of the tissues as opposed to just loosely attached to the cells surface, or becoming infected via contamination from the haemolymph.

The final goal of this study was to provide an updated evaluation of the ultrastructure of the antennal gland in *H. americanus*. In 1899 Waite provided the first in-depth assessment of the antennal gland in *H. americanus* highlighting the gross anatomy, finer anatomy, development and general structure. In *H. americanus* the gland is located at the base of the second antenna, and contains three lobes, a median anterior lobe, a lateral anterior lobe and a posterior lobe (Waite, 1899). The authors noted that at a structural level the gland contained two parts, the endsac and the labyrinth (Waite, 1899). Khodabandeh et al. (2005b) conducted an investigation of the antennal gland in *Homarus gammarus* and determined that the gland was composed of a coelomosac, labyrinth divided into two parts (I and II) and a bladder region. More recently, Freire et al. (2008) summarized the structure of the antennal gland in a variety of crustaceans; noting that the general structure varies between

species. In crayfish *Procambarus blandingii*, the gland is comprised of a coelomosac (endsac), labyrinth and nephridial canal region (Peterson and Loizzi, 1973), whereas in *Pacifastacus leniusculus*, the gland is comprised of a coelomosac, proximal nephron tubule, distal nephron tubule and labyrinth (Fuller et al., 1989). The antennal gland in the fiddler crab *Uca modax*, is comprised of only a coelomosac and labyrinth region and no nephridial canal (Schmidt-Nielsen et al., 1968; Tsai and Lin, 2014). Unlike what is reported in the closely related *H. gammarus* (Khodabandeh et al., 2005b), this study was not able to differentiate between distinct regions of labyrinth cells in *H. americanus*. We identified two main regions characterized by two morphological cell types, the coelomosac cells and the labyrinth cells. The epithelium of the tubular labyrinth region had numerous membrane infoldings and a high number of mitochondria characteristic of ion transporting epithelia. The coelomosac cells contained numerous vacuoles and voluminous globules that are characteristic of ultrafiltration and secretory activity similar to that of the vertebrate podocytes (Tsai and Lin, 2014). To our knowledge this is the first study to explore the ultrastructure of the antennal gland in *H. americanus* as well as examine the tissue tropism of WSSV infected *H. americanus* at different temperatures. Results from this study provide further insight into a broader understanding of how temperature and WSSV dynamics interact in an atypical host, *H. americanus*.

3.6 References

Acorn, A.R., Clark, K.F., Jones, S., Després, B.M., Munro, S., Cawthorn, R.J., Greenwood, S.J., 2011. Analysis of expressed sequence tags (ESTs) and gene expression changes under different growth conditions for the ciliate *Anophryoides haemophila*, the causative agent of bumper car disease in the American lobster (*Homarus americanus*). J. Invertebr. Pathol. 107, 146–154.

Aiken, D.E., Waddy, S.L., 1986. Environmental influence on recruitment of the American lobster, *Homarus americanus*: a perspective. Can. J. Fish. Aquat. Sci. 43, 2258–2270.

Bateman, K.S., Tew, I., French, C., Hicks, R.J., Martin, P., Munro, J., Stentiford, G.D., 2012. Susceptibility to infection and pathogenicity of white spot disease (WSD) in non-model crustacean host taxa from temperate regions. J. Invertebr. Pathol. 110, 340–351.

Cameron, J.N., Batterton, C. V., 1978. Antennal gland function in the freshwater blue crab *Callinectes sapidus*: water, electrolyte, acid-base and ammonia excretion. J. Comp. Physiol. 123, 143–148.

CFIA Biohazard Containment and Safety, 2010. Containment standards for facilities handling aquatic animal pathogens., 1st ed. Canadian Food Inspection Agency.

Clark, K.F., Acorn, A.R., Greenwood, S.J., 2013a. A transcriptomic analysis of American lobster (*Homarus americanus*) immune response during infection with the bumper car parasite *Anophryoides haemophila*. Dev. Comp. Immunol. 40, 112–122.

Clark, K.F., Greenwood, S.J., Acorn, A.R., Byrne, P.J., 2013b. Molecular immune response of the American lobster (*Homarus americanus*) to the white spot syndrome virus. J. Invertebr. Pathol. 114, 298–308.

Durand, S., Lightner, D. V., Nunan, L.M., Redman, R.M., Mari, J., Bonami, J.R., 1996. Application of gene probes as diagnostic tools for White Spot Baculovirus (WSBV) of penaeid shrimp. Dis. Aquat. Organ. 27, 59–66.

Escobedo-Bonilla, C.M., Wille, M., Alday Sanz, V., Sorgeloos, P., Pensaert, M.B., Nauwynck, H.J., 2007. Pathogenesis of a Thai strain of white spot syndrome virus (WSSV) in juvenile, specific pathogen-free *Litopenaeus vannamei*. Dis. Aquat. Organ. 74, 85–94.

Freire, C.A., Onken, H., McNamara, J.C., 2008. A structure – function analysis of ion transport in crustacean gills and excretory organs. Comp. Biochem. Physiol. Part A 151, 272–304.

Fuller, E.G., Highison, G.J., Brown, F., Bayer, C., 1989. Ultrastructure of the crayfish antennal gland revealed by scanning and transmission electron microscopy combined with ultrasonic microdissection. J. Morphol. 200, 9–15.

Khodabandeh, S., Charmantier, G., Blasco, C., Grousset, E., Charmantier-Daures, M., 2005a. Ontogeny of the antennal glands in the crayfish *Astacus leptodactylus* (Crustacea, Decapoda): anatomical and cell differentiation. Cell Tissue Res. 319, 153–165.

Khodabandeh, S., Charmantier, G., Charmantier-Daures, M., 2005b. Ultrastructural studies and Na+, K+-ATPase immunolocalization in the antennal urinary

glands of the lobster *Homarus gammarus* (Crustacea, Decapoda). J. Histochem. Cytochem. 53, 1203–1214.
Lawton, P., Lavalli, K.L., 1995. Postlarval, juvenile, adolescent and adult ecology, in: Factor, J.R. (Ed.), Biology of the Lobster *Homarus americanus*. Academic Press, pp. 47–88.
Lua, D.T., Hirono, I., 2015. Effect of low water temperature on the pathogenicity of white spot syndrome virus (WSSV) in Kuruma shrimp (*Marsupenaeus japonicus*). J. Sci. Dev. 13, 1405–1414.
Martin, G.G., Hose, J.E., 1995. Circulation, the blood, and disease, in: Factor, J.R. (Ed.), Biology of the Lobster *Homarus americanus*. Academic Press, pp. 464–495.
McMahon, B.R., 1995. The physiology of gas exchange, circulation, ion regulation and nitrogen excretion: an integrative approach, in: Factor, J.R. (Ed.), Biology of the Lobster *Homarus americanus*. Academic Press, pp. 497–517.
Moser, J.R., Álvarez, D.A.G., Cano, F.M., Garcia, T.E., Molina, D.E.C., Clark, G.P., Marques, M.R.F., Barajas, F.J.M., López, J.H., 2012. Water temperature influences viral load and detection of white spot syndrome virus (WSSV) in *Litopenaeus vannamei* and wild crustaceans. Aquaculture 326–329, 9–14.
Peterson, D.R., Loizzi, R.F., 1973. Regional cytology and cytochemistry of the crayfish kidney tubule. J. Morphol. 141, 133–145.
Pradeep, B., Rai, P., Mohan, S.A., Shekhar, M.S., Karunasagar, I., 2012. Biology, host range, pathogenesis and diagnosis of white spot syndrome virus. Indian J. Virol. 23, 161–174.
Sánchez-Paz, A., 2010. White spot syndrome virus: an overview on an emergent concern. Vet. Res. 41, 43.
Schmidt-Nielsen, B., Gertz, K.H., Davis, L.E., 1968. Excretion and ultrastructure of the antennal gland of the fiddler crab *Uca mordax*. J. Morphol. 125, 473–495.
Söderhäll, I., 2016. Crustacean hematopoiesis. Dev. Comp. Immunol. 58, 129–141.
Sonnenholzner, S., Betancourt, I., Rodríguez, J., Pérez, F., Echeverría, F., Calderón, J., 2002. Supervivencia y respuesta inmune de camarones juveniles *L. vannamei* desafiados por vía oral a WSSV. Manejo Enfermedades en Camarones 8, 50–55.
Tsai, J.-R., Lin, H.-C., 2014. Functional anatomy and ion regulatory mechanisms of the antennal gland in a semi-terrestrial crab, *Ocypode stimpsoni*. Co. Biol. 3, 409–417.
Waite, F., 1899. The structure and development of the antennal glands in *Homarus americanus* Milne-Edwards. Bull. Museum Comp. Zool. 35.
Wang, Y., Liu, W., Seah, J., Lam, C., Xiang, J., Korzh, V., Kwang, J., 2002. White spot syndrome virus (WSSV) infects specific hemocytes of the shrimp *Penaeus merguiensis*. Dis. Aquat. Organ. 52, 249–259.
You, X.X., Su, Y.Q., Mao, Y., Liu, M., Wang, J., Zhang, M., Wu, C., 2010. Effect of high water temperature on mortality, immune response and viral replication of WSSV-infected *Marsupenaeus japonicus* juveniles and adults. Aquaculture 305, 133–137.

4.0 GENERAL DISCUSSION

4.1 Summary

In the experiments described in this thesis we used a range of laboratory techniques (microarray, RT-qPCR, histology, electron microscopy) and experimental temperatures (10 ^{o}C, 15 ^{o}C, 17.5 ^{o}C, 20 ^{o}C) to expand on our understanding of how temperature influences host pathogen interactions in the American lobster *Homarus americanus*. The overall goal of the study was to characterize the effect that temperature can have on clinical presentation of WSSV, tissue, and molecular immune response of *H. americanus* experimentally infected with white spot syndrome virus (WSSV).

Total haemocyte concentration (THC) and WSSV-qPCR testing of haemolymph enabled us to characterize the clinical response of WSSV infected *H. americanus* at different temperatures. Results revealed that warmer temperatures had negative effects on the host's clinical response to WSSV. A statistically significant decline in THC between infected and control *H. americanus* was only observed at 17.5 ^{o}C and 20 ^{o}C and not at 10 ^{o}C and 15 ^{o}C. WSSV viral amplification (detected via WSSV-qPCR testing of haemolymph) increased with increasing water temperature among the infected animals. Interestingly, at the colder temperatures (10 ^{o}C and 15 ^{o}C) WSSV was not completely cleared from the haemolymph of inoculated *H. americanus* despite the absence of any clinical signs of infection. Results from WSSV-qPCR testing of tissues and light and electron microscopy corroborated the clinical results. At the colder temperatures (10 ^{o}C and 15 ^{o}C) little to no WSSV associated histopathology was observed. Our findings from WSSV-

qPCR testing of the tissues and histology highlighted two novel findings. The antennal gland is a key target tissue for WSSV replication, followed by the intestine. The antennal gland had the highest viral titre among the tested tissues at 17.5 ^{o}C and 20 ^{o}C. The second finding was that at 15 ^{o}C, no viral amplification was detected in the tested tissues one-week post inoculation, but was then detected two-weeks post inoculation.

Jiravanichpaisal et al. (2004) noted that at colder temperatures (4 ^{o}C) freshwater crayfish *Pacifastacus leniusculus* can act as subclinical carriers of WSSV. Bateman et al. (2012) more recently presented three categories of relative susceptibility to WSSV infection. Under this criterion, *Homarus americanus* could be classified as type 3 low, with low-level mortality during injected exposure and little or no pathology evident at the colder temperatures (10 ^{o}C and 15 ^{o}C). Interestingly, Bateman et al. (2012) recommended that susceptibility must also be considered on an individual level, where an individual's physiological conditions likely play a part in the progression of infection to disease and likelihood of mortality. Our results support this notion and highlight that increased temperatures in particular play an important role in the progression of WSSV infection in *H. americanus.* These results become increasingly important when one considers the viability of WSSV within the subclinical host. In the study of Bateman et al. (2012), WSSV infected tissue from *Carcinus maenas*, a type 3 low species, was found to provide sufficient dose to cause disease and mortality in other highly susceptible hosts. A passage bioassay of infected *H. americanus* tissue from animals at the different temperatures could provide interesting results.

The present study also used a lobster specific microarray chip and RT-qPCR in order to elucidate the effect of temperature on the molecular immune response of *H. americanus* experimentally infected with WSSV. Host genetic background can significantly influence the outcomes of viral infection (Hsu and Spindler, 2012). Our microarray findings revealed 771 significantly differentiated genes between control and infected *H. americanus* one and two-weeks post inoculation across the different temperatures. Additionally, hierarchical clustering of the significantly differentially expressed genes revealed that at 15 ^{o}C, 17.5 ^{o}C and 20 ^{o}C WSSV infected *H. americanus* demonstrated expression profiles more similar to themselves than to controls. When expression profiles of infected *H. americanus* across the different temperatures were examined a similar pattern was presented. However, of the significantly differentially expressed only 38% of them were functionally annotated. Functional annotation continues to be a limitation of working in a non-model organism, however next-generation sequencing and advances in bioinformatics tools are advancing the field (Clark and Greenwood, 2016). Nonetheless, the annotated genes identified in the present study do provide interesting results. At 10 ^{o}C there was no clear link to primary immune function or immune activation based on available annotated sequence. However at 15 ^{o}C, 17.5 ^{o}C and 20 ^{o}C a variety of immune related genes showed variable expression patterns. At one-week PI across all temperatures acute phase serum amyloid A (SAA) showed a 2.8 fold increase in expression as temperature increased from 10 ^{o}C to 20 ^{o}C, corroborating a role for SAA as an indicator of health in *H. americanus* (Clark et al., 2013a, 2013b, 2013c). At two-weeks PI across all the temperatures crustin-like protein *fc*-1 exhibited a

2.106 fold down-regulation as temperature increased. Christie et al. (2007) previously reported the down-regulation of crustin in correlation with *Penaeus monodon* succumbing to WSSV. Our results support the notion that crustin may be associated with late-stage WSSV infection.

4.2 Future Directions

The present study was successful at highlighting the complexity that temperature can bring to interactions between adult *H. americanus* and WSSV. In order to further our understanding of these interactions, the following areas warrant exploration:

- Assess the viability of WSSV agent isolated from within *H. americanus* infected tissue via a passage bioassay to shrimp.

- Explore whether WSSV viral amplification is halted altogether or simply significantly slowed at colder temperatures by conducting a longer WSSV challenge trial > 2 weeks at colder temperatures (10 ^{o}C and 15 ^{o}C).

- Assess if transferring *H. americanus* infected at 10 ^{o}C to higher temperatures results in an increase in WSSV replication

- Examine the transcriptome of the antennal gland and intestine in WSSV infected *H. americanus*. These two tissues were identified as the most prominent sites of viral replication in WSSV infected *H. americanus* and

could identify host molecular machinery that is being circumvented by the virus.

- Assess the susceptibility of other *H. americanus* life stages such as larvae to WSSV. Larval *H. americanus* are planktonic, free-swimming and inhabit the warmer surface waters before settling to the benthos to continue development. Given that the ideal thermal range for the virus is very similar to the larval *H. americanus* range we are likely to see a considerably different outcome regarding susceptibility and mortality.

- Compile baseline gene expression data for healthy *H. americanus* at different temperatures. Characterize how temperature is influencing the animal on a broad molecular level. Also explore different stressful environmental conditions.

4.3 Conclusion

H. americanus is considered one of Canada's most economically important crustacean species and given the potential monetary significance of WSSV, understanding the relationship between host, pathogen and environment is important. By building on available knowledge regarding lobster immunity we are strengthening our ability to assure the sustainability of the lobster industry in the face of changing environments.

4.4 References

Bateman, K.S., Tew, I., French, C., Hicks, R.J., Martin, P., Munro, J., Stentiford, G.D., 2012. Susceptibility to infection and pathogenicity of white spot disease (WSD) in non-model crustacean host taxa from temperate regions. J. Invertebr. Pathol. 110, 340–351.

Christie, A.E., Rus, S., Goiney, C.C., Smith, C.M., Towle, D.W., Dickinson, P.S., 2007. Identification and characterization of a cDNA encoding a crustin-like, putative antibacterial protein from the American lobster *Homarus americanus*. Mol. Immunol. 44, 3333–3337.

Clark, K.F., Acorn, A.R., Greenwood, S.J., 2013a. A transcriptomic analysis of American lobster (*Homarus americanus*) immune response during infection with the bumper car parasite *Anophryoides haemophila*. Dev. Comp. Immunol. 40, 112–122.

Clark, K.F., Acorn, A.R., Greenwood, S.J., 2013b. Differential expression of American lobster (*Homarus americanus*) immune related genes during infection of *Aerococcus viridans* var. *homari*, the causative agent of Gaffkemia. J. Invertebr. Pathol. 112, 192–202.

Clark, K.F., Greenwood, S.J., 2016. Next-Generation sequencing and the crustacean immune system: The need for alternatives in immune gene annotation. Integr. Comp. Biol. 56, 1113–1130.

Clark, K.F., Greenwood, S.J., Acorn, A.R., Byrne, P.J., 2013c. Molecular immune response of the American lobster (*Homarus americanus*) to the white spot syndrome virus. J. Invertebr. Pathol. 114, 298–308.

Hsu, T.-H., Spindler, K.R., 2012. Identifying host factors that regulate viral infection. PLoS Pathog. 8, e1002772.

Jiravanichpaisal, P., Söderhäll, K., Söderhäll, I., 2004. Effect of water temperature on the immune response and infectivity pattern of white spot syndrome virus (WSSV) in freshwater crayfish. Fish Shellfish Immunol. 17, 265–275.

APPENDIX A

Study:_____ **Lobster ID#:**_____ **Date:** _____

Sex: _____ **BW (g)** _____**CL (mm)** _____ **CS #** _____ **Moult Stage:**_____

RI: _____ **Brix:** _____ **HC:** _____ x 10^9/L **PEA** ___ TSB ___ **Ciliate** ____

tail tone:	excellent _____	good____	moderate _____	poor____
defensive posture:	excellent _____	good____	moderate _____	poor____
eyestalk withdrawl:	excellent _____	good____	moderate _____	poor____
shell hardness:	hard ____	intermediate_____	soft ____	

lesions

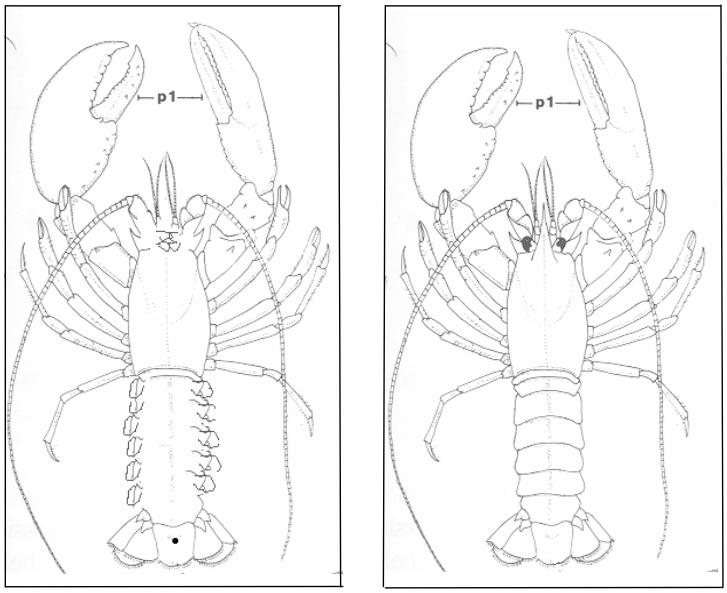

ventral surface **dorsal surface**

Figure A1: *Homarus americanus* health assessment form.

APPENDIX B

Manufacturer's instructions for DNA extraction using a DNeasy® Blood & Tissue Kit

When starting with haemolymph:

1. Pipet 20 µl proteinase K into a 1.5 ml or 2 ml microcentrifuge tube. Add 50–100 µl anticoagulated blood. Adjust the volume to 220 µl with PBS.
2. Add 200 µl Buffer AL. Mix thoroughly by vortexing, and incubate at 56 °C for 10 min. It is essential that the sample and Buffer AL are mixed immediately and thoroughly by vortexing or pipetting to yield a homogeneous solution.
3. Add 200 µl ethanol (96–100%) to the sample and mix thoroughly by vortexing. It is important that the sample and the ethanol are mixed thoroughly to yield a homogeneous solution. Proceed to step 4.

When starting with tissue:

1. Cut up to 30 mg tissue into small pieces, and place in a 1.5 ml microcentrifuge tube. Add 180 µL Buffer ATL
2. Add 20 µl proteinase K. Mix thoroughly by vortexing, and incubate at 56 °C until the tissue is completely lysed. Vortex occasionally during incubation to disperse the sample, or place in a thermomixer, shaking water bath, or on a rocking platform. Lysis time varies depending on the type of tissue processed. Lysis is usually complete in 1–3 h or, for rodent tails, 6–8 h. If it is more convenient, samples can be lysed overnight; this will not affect them adversely.
3. After incubation vortex for 15 s. Add 200 µl Buffer AL to the sample, and mix thoroughly by vortexing. Then add 200 µl ethanol (96–100%), and mix again thoroughly by vortexing. Proceed to step 4.

Spin column protocol:

4. Pipet the mixture from step 3 into the DNeasy Mini spin column placed in a 2 mL collection tube (provided). Centrifuge at 6000 x g (8000 rpm) for 1 min. Discard flow-through and collection tube.
5. Place the DNeasy Mini spin column in a new 2 ml collection tube, add 500 µl Buffer AW1, and centrifuge for 1 min at 6000 x g (8000 rpm). Discard flow-through and collection tube. Note: Buffer AW1 and Buffer AW2 are supplied as concentrates. Before using for the first time, add the appropriate volume of ethanol (96–100%) as indicated on the bottle and shake thoroughly. Buffer AW1 and Buffer AW2 are stable for at least 1 year after the addition of ethanol when stored closed at room temperature (15–25 °C).
6. Place the DNeasy Mini spin column in a new 2 ml collection tube (provided), add 500 µl Buffer AW2, and centrifuge for 3 min at 20,000 x g (14,000 rpm) to dry the DNeasy membrane. Discard flow-through and collection tube. Note: It is important to dry the membrane of the DNeasy Mini spin column, since residual ethanol may interfere with subsequent reactions.

7. Following the centrifugation step, remove the DNeasy Mini spin column carefully so that the column does not come into contact with the flow-through, since this will result in carryover of ethanol. If carryover of ethanol occurs, empty the collection tube, and then reuse it in another centrifugation for 1 min at 20,000 x g (14,000 rpm).
8. Place the DNeasy Mini spin column in a clean 1.5 ml or 2 ml microcentrifuge tube and pipet 100 µl Buffer AE directly onto the DNeasy membrane.
9. Incubate at room temperature for 1 min, and then centrifuge for 1 min at 6000 x g (8000 rpm) to elute.

APPENDIX C

AVC Lobster Science Centre protocol for microarray hybridization

Pre-Hybridization Protocol:

1. Wash: Temp 23 °C; Channel 3; Run: 1, Wash time 30 s, Soak time 30 s
2. Wash: Temp 23 °C; Channel 2; Rim: 1, Wash time 30 s, Soak time 30 s
3. Wash: Temp 37 °C; Channel 2; Run: 1, Wash time 30 s, Soak time 30 s
4. Hybridization: Temp 46 °C; Agitation Frequency: Medium, High Viscosity Mode: Yes, Time: 16 h
5. Wash: Temp 23 °C; Channel 2; Run: 1, Wash time 30 s, Soak time 0 s
6. Wash: Temp 37 °C; Channel 3; Run: 1, Wash time 20 s, Soak time 0 s
7. Slide drying: Temp 30 °C, Time: 2 min, Final Manifold Cleaning: No, Channel: No
8. Place all channels in Milli-Q water and start the rinse and drying cycle

Hybridization protocol:

1. Hybridization: Temp 65 °C, Agitation Frequency: No, High Viscosity Mode: No, Time: 10 min.
2. Wash: Temp 65 °C; Channel 1; Run: 1, Wash time 20 s, Soak time 0 s
3. Wash: Temp 50 °C; Channel 1; Run: 1, Wash time 20 s, Soak time 0 s
4. Hybridization: Temp 50 °C, Agitation Frequency: No, High Viscosity Mode: Yes, Time: 13 min
5. Wash: Temp 50 °C, Channel 1, Run: 1, Wash time: 20 s, Soak Time: 0 s
6. Hybridization: Temp 48 °C, Agitation Frequency: High, High Viscosity Mode: Yes, Time: 13 min
7. Wash: Temp 45 °C, Channel 1, Run: 1, Wash time: 1 min, Soak Time: 0 s
8. Wash: Temp 48 °C, Channel 4, Run: 1, Wash time: l min, Soak Time: l min
9. Sample Injection: Temp 48 °C, Agitation: Yes, BCR: No
10. Hybridization: Temp 48 °C, Agitation Frequency: High, High Viscosity Mode: Yes, Time: 16 h
11. Wash: Temp 41 °C, Channel 2, Run: 1, Wash time: 1 min, Soak Time: 0 s
12. Hybridization: Temp 48 °C, Agitation Frequency: Medium, High Viscosity Mode: No, Time: 2 min
13. Wash: Temp 30 °C, Channel 2, Run: 1, Wash time: 1 min, Soak Time: 0 s
14. Wash: Temp 30 °C, Channel 5, Run: 1, Wash time: 1 min, Soak Time: 0 s
15. Hybridization: Temp 30 °C, Agitation Frequency: Medium, High Viscosity Mode: No, Time: 2 min
16. Wash: Temp 23 °C, Channel 5, Run: 1, Wash time: 1 min, Soak Time: 0 s
17. Wash: Temp 23 °C, Channel 3, Run: 1, Wash time: 1 min, Soak Time: 0 s
18. Hybridization: Temp 23 °C, Agitation Frequency: Medium, High Viscosity Mode: No, Time: 2 min
19. Wash: Temp 23 °C, Channel 3, Run: 1, Wash time: 1 min, Soak Time: 0 s

20. Slide Drying: Temp 30 °C, Time: 3 min, Final Manifold Cleaning: No, Channel: No

APPENDIX D

Table D.1: Significantly differentially expressed genes identified between one-week PI, two-week PI and control *Homarus americanus* at 10 ^{o}C using a one-way ANOVA with α=0.001.

Data are reported as mean $\log_2$ expression ratios of sample/reference. Data are normalized to controls.

Gene Name	Accession #	Controls	1 week PI	2 weeks PI	p-value
NA	FE840841	0	0.777	0.458	0.001
protein O-mannosyl transferase [*Neosartorya fischeri* NRRL 181]	EH116039	0	0.786	-0.344	0.001
glutamate carboxypeptidase [*Tribolium castaneum*]	EX487372	0	0.824	-0.633	0.001
AGAP008106-PA [*Tribolium castaneum*]	CN854225	0	0.526	-0.353	0.001
membrane associated guanylate kinase 2 [*Homo sapiens*]	EY291238	0	-0.801	0.181	0.001
NA	EW997745	0	1.595	-0.531	0.001
NA	FE841066	0	0.657	-0.262	0.001
NA	CN951510	0	-1.037	0.759	0.001
GK20981 [*Drosophila willistoni*]	FD483036	0	-0.511	-0.746	0
NA	CN951021	0	-0.762	0.636	0
NA	EX471330	0	-0.475	-0.166	0.001
rho guanine dissociation factor isoform 1 [*Tribolium castaneum*]	FC556498	0	0.482	0.166	0
predicted protein [*Nematostella vectensis*]	EG949153	0	-0.404	0.223	0.001
NA	DV771472	0	0.743	-0.723	0.001
NA	FE659915	0	0.908	0.236	0
Guanylate kinase [*Bombyx mori*]	EX471111	0	1.127	-0.19	0.001
NA	FC071487	0	0.749	-0.609	0.001
NA	EX567999	0	10.701	0.324	0.001
transposase [*Oryzias latipes*]	DV771133	0	-0.627	0.463	0
oxygenase [*Oplophorus gracilorostri*s]	FD585249	0	-0.426	0.561	0
60S ribosomal protein L27a [*Apis mellifera*]	FD483474	0	-0.653	0.601	0.001
ribosomal protein L13 [*Danio rerio*]	FE535088	0	-0.408	2.294	0.001
ribosomal protein L11 [*Ixodes scapularis*]	CN952190	0	-0.503	0.467	0
ribosomal protein L39 [*Ixodes scapularis*]	GD242090	0	-0.579	1.502	0

Table D.2: Average expression ratio of significantly differentially expressed genes identified between one-week PI, two-week PI and control *Homarus americanus* at 15 °C using a one-way ANOVA with α=0.001.

Data are reported as mean $\log_2$ expression ratios of sample/reference. Data are normalized to controls.

Gene Name	Accession #	Controls	1 week PI	2 weeks PI	p-value
endonuclease\reverse transcriptase [*Strongylocentrotus purpuratus*]	DV774776	0	0.986	1.196	0.001
calponin [*Branchiostoma belcher*i]	FD699000	0	0.58	0.99	0
NA	CN853050	0	0.553	0.341	0.001
Phenylalanyl-tRNA synthetase CG13348-PA [*Acyrthosiphon pisum*]	FD584878	0	0.718	0.28	0.001
NA	CN950226	0	-0.536	-0.937	0
NA	CN950247	0	0.393	0.811	0
solute carrier family 35 member B1 [*Acyrthosiphon pisum*]	FE535241	0	0.596	1.169	0.001
C-type lectin [*Litopenaeus vannamei*]	CN950717	0	-0.374	-0.887	0
GTP-binding protein sar1 [*Aedes aegypti*]	CN951019	0	-0.528	-0.683	0.001
GA17475-PA [*Tribolium castaneum*]	FE841164	0	-0.403	0.711	0.001
NA	CN951603	0	0.483	1.107	0
deiodinase type III [*Neoceratodus forsteri*]	CN951787	0	0.845	0.155	0.001
ubiquitin specific protease 37 isoform 2 [*Canis familiaris*]	FD483281	0	1.419	0.931	0
NA	CN951930	0	0.399	0.588	0
mitogen-activated protein kinase 15 [*Danio rerio*]	CN952022	0	0.556	0.402	0
NA	EX471451	0	1.445	0.837	0
NA	DV771097	0	0.51	1.197	0
NA	DV773163	0	0.898	0.456	0
NA	DV774122	0	-2.56	-3.283	0.001
NA	DV774674	0	-0.791	-1.167	0.001
NA	EH035265	0	-0.767	0.789	0
NA	DV775063	0	0.636	0.912	0
pupal cuticle protein [*Culex quinquefasciatus*]	FE535896	0	-0.09	-0.525	0
NA	EH035207	0	-0.609	-0.884	0.001
DEAD box ATP-dependent R helicase [*Tribolium castaneum*]	EH116182	0	0.68	1.861	0.001
NA	EH116365	0	0.342	0.68	0.001
NA	FD483889	0	0.909	0.567	0.001

signal recognition particle 54 kda protein [*Culex quinquefasciatus*]	EV781629	0	-0.557	-0.358	0.001
cat eye syndrome chromosome region, candidate 1 [*Pongo abelii*]	FD584857	0	-0.282	0.482	0.001
NA	EW702829	0	0.251	0.621	0
seryl-tRNA synthetase [*Tribolium castaneum*]	EW703198	0	0.326	1.229	0.001
transposase [*Pachygrapsus marmoratus*]	EW997859	0	0.447	0.982	0.001
COP9 constitutive photomorphogenic homolog subunit 3 [*Apis mellifera*]	EY116927	0	1.14	0.927	0.001
metastasis associated protein [*Nasonia vitripennis*]	EX568204	0	0.9	0.722	0.001
intraflagellar transport 172 [*Danio rerio*]	EY116788	0	1.613	0.73	0
MIT, microtubule interacting and transport, domain containing 1 [*Equus caballus*]	EY117261	0	-0.894	-0.419	0
NA	EY117425	0	1.06	0.453	0
NA	EY291027	0	0.425	0.775	0
NA	FC556668	0	0.806	0.248	0
NA	FD467682	0	0.32	0.758	0
connectin [*Nasonia vitripennis*]	FD467872	0	0.901	1.141	0.001
NA	FD483001	0	0.741	0.645	0.001
F-box only protein 6 (F-box only protein 6b) [*Apis mellifera*]	FD584589	0	0.596	0.7	0
NA	FD585093	0	0.29	0.909	0.001
NA	FD585129	0	0.653	1.1	0
copper chaperone Atox1 [*Aedes aegypti*]	FE043929	0	0.63	0.788	0.001
NA	FE535449	0	0.359	0.868	0
NA	FE840922	0	0.348	0.694	0
NA	FE841215	0	1.388	0.769	0.001
NA	FF277687	0	0.536	1.035	0
septin 9b [*Danio rerio*]	FF278030	0	1.001	0.543	0.001
NA	DV771783	0	1.627	1.118	0.001
NA	FD699915	0	0.912	0.69	0.001
Keren CG32179-PA [*Tribolium castaneum*]	FD585158	0	-0.557	-0.755	0.001

Table D.3: Significantly differentially expressed genes identified between one-week PI, two-week PI and control *Homarus americanus* at 17.5 ^{o}C using a one-way ANOVA with α=0.001.

Data are reported as mean $\log_2$ expression ratios of sample/reference. Data are normalized to controls.

Gene Name	Accession #	Controls	1 week PI	2 weeks PI	p-value
NA	CN949900	0	-2.356	-0.506	0.001
NA	DV773782	0	-1.763	-1.314	0.001
NA	EH035711	0	-10.933	-10.449	0
mitogen-activated protein kinase organizer 1 [*Canis familiaris*]	EV781809	0	-13.406	-13.823	0.001
prolyl-4-hydroxylase-alpha EFB CG31022-PA [*Apis mellifera*]	EW997795	0	-1.695	-1.141	0.001
NA	EX487455	0	-0.889	-1.365	0.001
NA	FC555994	0	-1.305	-1.012	0.001
NA	FD483867	0	-2.302	-1.819	0.001
NA	FD585390	0	-1.09	-0.873	0.001
Dpol- CG7602-PA, isoform A [*Apis mellifera*]	FE535196	0	-1.265	-0.616	0.001
NA	FE659761	0	0.603	1.501	0.001

Table D.4: Significantly differentially expressed genes identified between one-week PI, two-week PI and control *Homarus americanus* at 20 ^{o}C using a one-way ANOVA with α=0.001.

Data are reported as mean $\log_2$ expression ratios of sample/reference. Data are normalized to controls.

Gene Name	Accession #	Controls	1 week PI	2 weeks PI	p-value
NA	CN852749	0	1.08	-0.412	0
NA	CN853321	0	0.911	-1.005	0
PAR-domain protein 1 CG17888-PE, isoform E [*Drosophila melanogaster*]	CN853480	0	1.692	-0.565	0.001
conserved hypothetical protein [*Culex quinquefasciatus*]	CN853638	0	1.68	-0.179	0.001
NA	CN854010	0	1.772	-0.253	0.001
NA	EH035670	0	0.934	-0.737	0
NA	CN951512	0	-0.904	-1.038	0.001
short-chain dehydrogenase [*Aedes aegypti*]	FD585222	0	2.061	-1.957	0.001
NA	DV772731	0	1.771	-0.814	0
NA	CN951967	0	0.863	-2.307	0
NA	DV771228	0	-2.45	1.751	0.001
NA	DV771364	0	1.476	-1.287	0.001
linker histone H1M [*Danio rerio*]	EY117116	0	-2.348	-0.784	0.001
dynein light intermediate chain [*Tribolium castaneum*]	EY290773	0	0.522	-1.13	0
NA	DV773779	0	1.255	-0.683	0
NA	DV774264	0	2.383	-1.051	0
NA	DV774341	0	1.382	-0.822	0
NA	DV774923	0	1.01	-0.248	0.001
NA	EG948697	0	0.41	-1.047	0
SH2 domain containing 4B [*Gallus gallus*]	EH034887	0	-1.014	-1.246	0.001
testis expressed gene 10 [*Rattus norvegicus*]	FD699046	0	0.329	3.183	0
ribbon [*Tribolium castaneum*]	EH035752	0	0.925	-0.672	0.001
NA	EH116070	0	-0.462	-1.242	0.001
sidestep protein [*Aedes aegypti*]	EH116264	0	1.446	-0.625	0
NA	EH116432	0	-0.671	-5.796	0
NA	FD585012	0	0.375	-2.213	0
NA	EW702779	0	0.755	-3.487	0
transmembrane and tetratricopeptide repeat containing 4 [*Equus caballus*]	EW702817	0	0.34	-1.761	0
NA	EW997769	0	0.745	-0.725	0.001
amyotrophic lateral sclerosis 2 (juvenile) chromosome region, candidate 8 [*Bos taurus*]	EW997950	0	0.524	-1.675	0

Pol [*Drosophila melanogaster*]	FD467286	0	1.326	-0.878	0
NA	EX471122	0	1.466	-0.931	0
NA	EX486852	0	-0.699	3.244	0
NA	EX568399	0	-0.813	-0.927	0.001
NA	EX827373	0	0.848	-0.798	0.001
NA	EX827414	0	0.672	-2.963	0
NA	EY116996	0	0.694	-0.738	0
sterile alpha motif domain containing 4 isoform 1 [*Monodelphis domestica*]	EY291033	0	-0.398	-8.099	0
NA	EY291364	0	0.249	-0.901	0
laminin subunit gamma-3 [*Culex quinquefasciatus*]	FC071527	0	0.535	-0.495	0
NA	FD483491	0	0.775	-0.61	0.001
NA	FD483740	0	1.797	-0.158	0
NA	FD483742	0	0.378	-0.949	0
NA	FD699408	0	0.371	-0.971	0
NA	FD699544	0	0.726	-1.423	0.001
NA	FE043644	0	1.225	-0.362	0.001
NA	FE044013	0	-1.537	-0.658	0
Zinc finger protein 84 (Zinc finger protein HPF2) [*Apis mellifera*]	FE535551	0	-1.562	-0.661	0
NA	FE535752	0	0.866	-0.728	0
NA	FE659417	0	0.564	-0.93	0.001
NA	FE659659	0	0.355	2.138	0
NA	FE660003	0	0.293	-0.752	0.001
NA	FE841298	0	1.319	-1.227	0
NA	FF277877	0	-1.494	-0.753	0
jaguar CG5695-PB, isoform B, partial [*Apis mellifera*]	FF278082	0	-0.815	-2.107	0
pre-mRNA cleavage complex II protein Clp1 [*Culex quinquefasciatus*]	FE044187	0	0.866	-0.657	0

Table D.5: : Significantly differentially expressed genes identified between WSSV infected *Homarus americanus* at each temperature one-week PI using a one-way ANOVA with α=0.001.

Data are reported as mean $\log_2$ expression ratios of sample/reference.

Gene Name	Accession #	10 °C	15 °C	17.5 °C	20 °C	p-value
NA	CN852484	1.106	1.236	1.866	2.697	0.001
NA	CN852496	1.402	1.457	1.989	4.032	0.001
Sjogren's syndrome\scleroderma autoantigen 1 homolog [*Xenopus (Silurana) tropicalis*]	CN852522	-0.814	-0.676	1.551	2.511	0.001
camp and camp-inhibited cgmp 3,5-cyclic phosphodiesterase [*Strongylocentrotus purpuratus*]	CN852573	-3.302	-3.221	-0.921	0.601	0.001
NA	CN852528	0.693	1.505	2.245	3.575	0
NA	CN951275	0.479	1.000	2.234	2.732	0.001
clathrin coat assembly protein [*Nasonia vitripennis*]	CN852555	-0.748	-0.376	1.791	2.198	0
NA	CN852587	0.405	0.111	0.129	5.022	0.001
NA	CN852610	-0.139	0.582	2.421	3.996	0.001
NA	CN852616	3.110	2.292	2.773	4.392	0
cop9 complex subunit 7a [*Culex quinquefasciatus*]	FE841297	0.845	1.385	3.210	3.868	0.001
chromatin modifying protein 1b [*Bombyx mori*]	FE659428	-2.502	-2.282	-0.839	-0.020	0
NA	CN852648	-0.484	-0.885	0.062	1.516	0.001
NA	CN852663	1.057	1.670	2.985	4.232	0.001
c-Jun protein [*Acyrthosiphon pisum*]	FE659630	-0.365	0.407	1.851	3.888	0.001
NA	CN852680	-1.895	-1.049	1.738	1.946	0.001
NA	CN852712	-2.082	-2.131	-0.816	1.047	0.001
NA	CN852724	0.895	0.336	0.915	2.707	0.001
NA	CN852729	-1.184	-1.136	-0.107	1.683	0.001
NA	CN852747	-0.981	-0.944	1.280	0.481	0.001
cytochrome c oxidase polypeptide IV [*Bombyx mori*]	CN852766	-0.282	-0.537	0.720	1.477	0
calponin [*Branchiostoma belcheri*]	FD699000	0.407	-0.095	0.447	3.052	0
DNA directed RNA polymerase II polypeptide G [*Homo sapiens*]	EX487405	-0.290	0.037	1.259	1.461	0.001
NA	FF278071	2.014	2.582	3.180	5.388	0
NA	CN852833	-0.576	-0.627	0.171	8.257	0.001
NA	CN852931	-1.671	-1.899	-0.924	0.566	0.001
NA	CN852938	0.122	0.725	1.953	3.298	0.001
NA	EX486518	0.706	0.193	1.275	2.757	0.001
ATP-binding cassette, sub-family C, member 11 isoform a isoform 2 [*Macaca mulatta*]	CN852984	-0.700	-0.722	0.334	1.644	0
General transcription factor 3C polypeptide 5 (Transcription factor IIIC-epsilon subunit) [*Apis mellifera*]	CN853031	0.575	1.643	2.547	4.069	0.001
tricarboxylate carrier protein [*Monodelphis domestica*]	FE535882	-0.635	-0.569	1.239	1.673	0
NA	EY117156	-0.554	-0.066	1.611	1.886	0.001
NA	CN853040	-2.047	-1.201	0.614	1.152	0.001
NA	CN853117	1.958	1.673	2.434	3.642	0.001
NA	FF277894	-0.229	-0.856	0.878	2.684	0.001
predicted protein [*Nematostella vectensis*]	CN950219	-0.106	-0.064	1.568	2.204	0.001
mucin-like protein 1 [*Ctenocephalides felis*]	EY290801	-0.988	-0.879	0.928	1.363	0.001
fibropellin Ia, partial [*Strongylocentrotus purpuratus*]	CN853164	-1.726	-0.837	1.274	0.983	0.001
NA	CN853169	1.585	1.561	2.577	7.703	0.001
NA	EH117102	0.635	0.705	1.526	2.491	0.001
multidrug resistance-associated protein 14 [*Culex quinquefasciatus*]	CN853190	-3.366	-3.329	-1.787	-1.354	0.001
inorganic pyrophosphatase [*Nasonia vitripennis*]	FE659972	-1.796	-1.701	-0.159	0.753	0.001
NA	CN853200	-0.922	-1.678	0.515	1.608	0.001
NA	FF277383	-0.263	-0.649	0.846	2.362	0.001
hypothetical protein TRIADDRAFT_29295 [*Trichoplax adhaerens*]	CN853390	4.839	3.902	2.459	3.692	0

NA	CN853287	-0.401	-0.604	1.448	1.856	0.001
NA	EX487479	-0.263	-0.118	1.555	2.015	0.001
collagen pro alpha-chain [*Haliotis discus*]	CN853303	-0.215	0.293	2.496	2.781	0.001
NA	CN853305	-0.646	-1.524	1.141	1.364	0
NA	CN952118	-1.115	-0.841	1.293	2.823	0.001
NA	CN853344	0.622	1.089	1.640	2.512	0.001
NA	CN853348	-1.313	-0.162	1.121	1.358	0.001
oxidase\peroxidase [*Tribolium castaneum*]	CN952081	1.128	0.858	1.187	2.574	0.001
NA	CN854473	2.206	2.135	2.631	4.502	0.001
NA	EW702735	0.574	0.529	-0.992	1.201	0
polyglutamine binding protein 1 [*Tribolium castaneum*]	FD584522	-1.273	-0.594	0.951	1.400	0.001
NA	CN853466	-0.985	-0.342	1.407	3.108	0
phospholipase A2, group IVB [*Bos taurus*]	CN853551	-0.295	-0.248	0.109	2.190	0.001
NA	CN853557	0.661	0.470	1.334	3.708	0.001
nephrin [*Tribolium castaneum*]	CN853558	-0.426	-0.124	0.380	1.944	0
NA	CN853573	-0.222	-0.247	0.716	2.652	0.001
NA	CN853591	-2.539	-2.609	-0.688	-0.198	0
proteasome (prosome, macropain) 26S subunit, ATPase 2 [*Mus musculus*]	FF277794	-3.006	-3.388	-2.547	-1.076	0
NA	CN853643	0.416	0.962	1.790	2.684	0.001
NA	CN853658	-1.429	-2.141	-3.522	-3.442	0
26S protease (S4) regulatory subunit, [*Nasonia vitripennis*]	CN853687	-0.755	0.271	2.356	2.670	0
NA	FE535748	-3.825	-2.202	-0.237	0.193	0.001
dehydrodolichyl diphosphate synthase [*Danio rerio*]	EY117248	-1.996	-2.364	-0.629	-1.244	0.001
Fkbp13 CG9847-PA, isoform A [*Drosophila melanogaster*]	CN853780	1.041	1.379	1.354	2.077	0.001
NA	CN853787	2.333	2.090	2.141	3.760	0
flotillin-1 [*Aedes aegypti*]	CN853805	0.634	1.128	2.398	2.209	0
4-coumarate-CoA ligase-like protein [*Arabidopsis thaliana*]	EH116951	0.570	1.397	1.539	2.594	0
NA	FC071313	1.110	1.785	2.258	2.631	0
NA	CN853885	-3.489	-3.418	-4.808	-4.932	0.001
NA	EW997983	-1.375	-0.167	-0.062	1.196	0
NA	FE535715	0.858	0.739	1.532	2.984	0.001
NA	CN854000	-0.912	-1.119	0.197	2.134	0.001
GA11814-PA [*Tribolium castaneum*]	FD483297	1.888	2.234	2.437	9.511	0
pyruvate dehydrogenase [*Culex quinquefasciatus*]	EH116673	0.641	0.576	1.494	2.730	0
NA	CN854084	3.354	2.390	1.399	4.459	0.001
integrin beta-PS [*Culex quinquefasciatus*]	FD585331	-0.187	-0.999	0.689	3.506	0
NA	EH034911	0.558	0.107	0.369	3.902	0
NA	FD699101	0.806	1.384	3.578	4.074	0.001
NA	CN854214	1.391	1.613	2.383	1.856	0
NA	CN854234	-1.324	-0.712	0.812	1.376	0.001
Protein Star [*Acyrthosiphon pisum*]	EH116645	-1.550	-1.157	-0.036	1.187	0.001
WD repeat protein 34 [*Gallus gallus*]	FE535157	-0.235	0.727	2.217	1.976	0
chitinase [*Araneus ventricosus]*	FD467301	-2.789	-2.420	-1.145	0.120	0.001
Mediator complex subunit 31 CG1057-PA, isoform A [*Drosophila melanogaster*]	EH401684	-2.859	-1.737	0.623	0.719	0.001
acute phase serum amyloid A (SAA) [*Oncorhynchus mykiss*]	CN949986	-2.687	-2.328	-0.306	0.201	0
NA	EH034778	0.408	0.798	1.867	3.212	0
NA	CN854407	-1.590	-1.566	0.658	0.856	0.001
NA	CN854414	-0.919	0.351	0.411	1.360	0
beta1,4 mannosyltransferase [*Nasonia vitripennis*]	CN854471	-0.608	-0.916	0.733	1.944	0
CG4630 CG4630-PA [*Drosophila melanogaster*]	CN854472	-0.544	0.558	0.499	2.731	0
thioredoxin-related protein 14 [*Branchiostoma belcheri tsingtaunese*]	FF277519	0.863	0.327	0.266	1.830	0
NA	CN949883	-0.449	-2.614	-3.809	-2.767	0
elongation of very long chain fatty acids-like protein [Marsupenaeus japonicus]	EX827272	-1.268	-0.680	0.512	1.046	0
NA	CN949992	-1.347	-0.631	0.657	1.642	0.001
cellular repressor of E1A-stimulated genes [*Apis mellifera*]	FE043722	-0.246	0.521	2.317	2.367	0
immature colon carcinoma [*Acyrthosiphon pisum]*	CN950033	1.596	2.097	2.396	3.688	0.001

periplasmic copper-binding [*Acidovorax sp*. JS42]	CN950044	-0.650	-0.727	0.536	1.886	0.001
survival of motor neuron 1, telomeric [*Nasonia vitripennis*]	EH035333	-0.215	-0.014	1.838	3.131	0.001
protein tyrosine phosphatase-like (proline instead of catalytic arginine), member b [*Equus caballus*]	CN950074	-1.076	-0.592	0.706	1.431	0
NA	FE535104	-0.663	-1.559	-0.144	1.423	0.001
NA	CN950120	1.403	0.489	0.977	2.224	0.001
NA	CN950229	2.465	2.138	0.677	0.262	0.001
NA	CN950264	-1.147	-0.253	0.771	1.950	0
NA	CN950320	-0.039	-0.463	0.990	1.882	0.001
NA	CN950323	-2.025	-2.587	-3.062	-3.527	0.001
NA	FE659461	0.308	-0.056	0.461	1.705	0
Troponin I (TnI)	FD699253	-0.392	0.111	2.302	2.838	0
Profilin	FD467456	-2.812	-2.839	-0.768	-0.242	0
NA	CN951216	-0.026	-0.754	0.379	6.552	0.001
NA	CN950478	-0.079	-0.837	1.675	2.575	0.001
NA	CN950504	0.400	0.593	2.388	3.858	0.001
NA	FD483929	-0.669	-0.923	-0.444	0.880	0.001
CGI-140 protein [*Monodelphis domestica*]	CN950521	0.409	0.304	0.741	2.242	0
cryptochrome 2 [*Antheraea pernyi*]	CN950567	0.580	0.553	1.603	2.664	0.001
NA	FD585382	3.180	0.813	-0.671	-0.887	0
Angiotensin converting enzyme CG8827-PA, isoform A [*Apis mellifera*]	CN950641	-3.849	-4.208	-2.587	-1.434	0
Organic cation transporter 2 CG13610-PA [*Drosophila melanogaster*]	CN950642	0.625	0.956	1.705	2.928	0
NA	EX486876	-0.645	-0.527	1.070	0.971	0.001
NA	FD467584	1.229	1.355	1.590	2.632	0.001
methylosome protein 50 [*Rattus norvegicus*]	FD584739	1.175	1.206	2.265	4.179	0.001
NA	CN950719	-0.173	-0.054	-1.384	-0.881	0
NA	CN950726	2.245	1.507	1.421	3.849	0.001
AGAP007607-PA [*Anopheles gambiae* str. PEST]	EY290669	1.432	1.229	2.343	3.739	0.001
NA	FD467842	2.058	1.919	2.081	3.944	0
NA	FC556564	0.192	0.018	0.637	2.086	0.001
basophilic leukemia expressed protein [*Canis familiaris*]	FD468089	-0.998	-1.755	-0.476	0.558	0.001
NA	EH116329	-0.191	0.147	0.968	2.128	0.001
CG3032 CG3032-PA [*Drosophila melanogaster*]	CN950984	0.860	0.851	0.658	7.280	0.001
NA	CN951103	-1.822	-1.619	-0.567	0.312	0.001
cAMP specific phosphodiesterase [*Drosophila melanogaster*]	DV771769	1.640	1.700	2.243	2.900	0.001
tRNA methyltransferase [*Culex quinquefasciatus*]	CN951201	-0.199	0.599	0.887	1.838	0.001
NA	CN951222	1.031	1.166	1.494	2.663	0.001
Plenty of SH3s CG4909-PA [*Apis mellifera*]	EX471742	-2.983	-3.349	-1.865	-1.027	0.001
NA	FE044104	0.879	1.153	1.437	2.960	0
ribosomal protein L39 [*Ixodes scapularis*]	GD242090	-4.980	-4.474	-3.627	-4.011	0
dynein heavy chain [*Aedes aegypti*]	CN951373	0.012	0.455	2.003	2.081	0.001
pre-mRNA processing factor 8 [*Strongylocentrotus purpuratus*]	CN951379	0.746	-0.323	1.300	1.136	0.001
NA	CN951447	-0.472	-0.227	0.663	1.326	0
NA	FD467591	-0.127	-0.542	0.873	1.553	0
NA	FE841231	-3.836	-3.384	-4.676	-4.159	0
sugar transporter [*Nasonia vitripennis*]	EH116637	-1.041	-0.076	2.405	2.210	0.001
NA	EY117324	-0.620	-1.097	0.755	2.769	0
NA	CN951512	-2.036	-2.130	-2.964	-3.165	0.001
NA	CN951540	-2.881	-3.305	-4.268	-5.079	0
beta-1,4-endoglucanase 2 [*Panesthia cribrata*]	CN951583	-1.306	-0.335	1.308	1.305	0.001
NA	CN951647	-2.800	-3.050	-4.472	-4.524	0.001
replication factor C\activator 1 subunit, partial [*Ornithorhynchus anatinus*]	CN951653	-1.025	-0.947	-2.686	-3.113	0.001
pre-mRNA-splicing factor cwc15 [*Acyrthosiphon pisum*]	CN951668	-1.012	-0.831	0.783	1.824	0.001
Nascent polypeptide associated complex protein alpha subunit [*Apis mellifera*]	CN951682	-1.733	-2.342	-0.519	0.521	0
hypothetical protein AaeL_AAEL010556 [*Aedes aegypti*]	CN951717	0.754	1.210	1.465	2.055	0
NA	CN951726	-0.266	-0.491	0.349	3.453	0.001
NA	CN951825	-0.387	-0.208	0.137	2.005	0

Nuclear transcription factor Y subunit beta (CAAT-box DNA-binding protein subunit B) [*Apis mellifera*]	FD699580	-0.122	0.264	0.446	1.634	0.001
NA	CN951982	-0.338	-0.487	0.156	7.909	0.001
NA	CN951998	-2.239	-1.675	-0.302	1.435	0
Histone-lysine N-methyltransferase SETD8 (SET domain-containing protein 8)	CN952033	1.633	2.948	2.638	2.879	0.001
26S proteasome regulatory complex ATPase RPT4 [*Nasonia vitripennis*]	FD699258	-1.434	-1.567	-1.164	0.125	0.001
Cysteine string protein [*Apis mellifera*]	CN952127	-0.615	-1.030	0.388	0.890	0.001
NA	FE535510	1.498	0.901	0.781	2.048	0
NA	CN952149	1.472	1.176	2.005	4.443	0.001
NA	CN952183	1.267	0.815	0.393	1.812	0
alpha-2-macroglobulin [*Macrobrachium rosenbergii*]	CN952197	1.573	0.715	0.622	-0.102	0.001
NA	EY116689	-1.760	-1.981	-3.568	-3.897	0.001
choline transporter-like protein 2 [*Danio rerio*]	CN952251	-2.495	-2.228	-1.201	-0.205	0
NA	CN952282	-0.190	-0.276	0.380	1.360	0.001
NA	CN952310	3.412	2.163	0.539	3.506	0.001
ATP-dependent RNA helicase A (DEAH-box protein 9) isoform 2 [*Canis familiaris*]	CN952319	0.918	0.005	-0.568	0.197	0
Ankyrin repeat and SOCS box-containing protein 13 isoform 1 [*Bos taurus*]	EH401492	0.656	-0.223	-0.014	1.769	0
zinc finger protein 3 [*Macaca mulatta*]	DV771099	-0.570	-1.745	-0.188	1.188	0.001
NA	DV772815	-0.929	-0.395	0.968	1.303	0.001
receptor expression enhancing protein 5 [*Monodelphis domestica*]	DV771130	-2.931	-3.040	-4.307	-4.521	0.001
NA	DV774720	-0.228	0.569	2.782	3.934	0
NA	DV771250	-2.177	-2.127	-4.055	-2.743	0
hypothetical protein AaeL_AAEL005383 [*Aedes aegypti*]	DV771253	-1.221	-1.684	-0.401	0.555	0.001
NA	DV771258	3.209	3.529	3.452	4.830	0
NA	DV771280	0.709	0.733	-0.584	0.164	0
DEAD box ATP-dependent RNA helicase [*Nasonia vitripennis*]	DV774250	0.420	0.147	1.525	2.384	0
NA	FC556348	1.737	1.767	2.516	3.328	0
NA	DV771371	1.203	0.838	1.161	2.795	0
NA	DV771387	-2.106	-2.119	-3.283	-3.020	0.001
NA	FE535523	-0.744	-1.557	-0.027	1.032	0.001
NA	DV771427	-0.045	-0.160	1.594	2.188	0.001
NA	DV771443	-0.908	-1.349	0.650	1.816	0.001
NA	DV771475	2.625	2.890	2.791	16.474	0.001
NA	DV771536	-1.325	-1.862	-3.530	-3.411	0.001
NA	DV771626	1.492	1.413	1.230	4.341	0.001
NA	DV774850	1.587	0.731	1.627	4.472	0
chaperonin subunit 6a zeta [*Tribolium castaneum*]	DV773788	-2.453	-3.021	-1.245	-1.924	0.001
reductase-related protein [*Aplysia californica*]	DV771931	-2.012	-2.790	-1.933	0.139	0.001
NA	CN852603	0.057	0.369	2.764	3.823	0
NA	DV771990	-0.504	-0.837	-0.878	-0.147	0
hypothetical protein PGUG_01276 [*Pichia guilliermondii* ATCC 6260]	DV775002	-2.086	-2.484	-0.660	-0.180	0.001
NA	DV772045	3.397	2.479	2.989	4.152	0.001
NA	DV772053	1.325	1.710	1.947	5.185	0.001
NA	DV772129	-0.001	-0.930	-0.415	9.284	0.001
NA	DV772189	1.467	0.948	2.672	3.026	0.001
NA	DV772264	1.098	0.978	0.908	2.088	0
ribosomal protein rps21 [*Arenicola marina*]	EY116908	-3.753	-3.643	-2.102	-1.396	0.001
NA	DV773730	-1.384	-0.955	1.270	1.542	0.001
NA	FD585041	1.782	1.551	0.814	2.720	0
TFIIH basal transcription factor complex helicase subunit (DNA excision repair protein ERCC-2)	FE535432	-1.665	-2.089	-3.210	-3.303	0
acyl-Coenzyme A dehydrogenase family, member 8 [*Danio rerio*]	FE660196	-0.010	-0.813	-2.271	-2.288	0
UDP-glucose pyrophosphorylase [*Nasonia vitripennis*]	FD584962	1.504	0.685	1.098	2.298	0.001
NA	DV773050	-0.373	0.069	0.927	1.813	0
NA	DV773060	0.559	0.222	2.068	2.562	0
NA	FF277939	0.122	-0.055	0.425	1.833	0.001
quinolinate synthetase [*Oceanospirillum sp.*	DV773121	3.445	3.077	1.495	2.983	0.001

MED92]						
NA	DV773160	1.027	1.414	2.129	3.639	0
NA	DV773300	1.135	0.667	-0.101	1.761	0.001
NA	DV773402	-2.329	-3.223	-0.128	2.162	0
NA	DV773449	2.699	1.817	2.539	12.241	0.001
NA	DV773609	2.319	1.963	1.712	3.431	0
NA	DV773674	-1.356	-0.215	1.258	2.209	0
NA	EW703103	0.462	0.631	1.038	3.130	0
NA	DV773779	0.782	0.471	0.999	1.964	0
NA	DV773782	1.856	0.767	0.733	2.375	0
NA	CN852898	-2.159	-2.983	-0.436	1.976	0.001
NA	EX471541	-2.991	-3.140	-4.395	-4.638	0.001
NA	DV774065	-1.867	-2.450	-0.931	-1.431	0.001
NA	DV774072	-3.035	-2.429	-1.209	-1.170	0.001
NA	EX827394	0.723	0.104	0.369	2.589	0.001
NA	FD467698	1.401	1.473	1.521	2.869	0.001
NA	DV774242	1.438	2.297	2.730	4.200	0
NA	DV774306	0.922	0.128	0.411	1.278	0.001
CG2852 CG2852-PA, isoform A [*Drosophila melanogaster*]	FE659628	-3.067	-3.174	-1.157	-0.956	0.001
NA	DV774430	1.804	1.160	1.599	3.541	0
NA	DV774615	-1.554	-1.750	-0.843	0.714	0.001
GG19893 [*Drosophila erecta*]	DV774660	-0.450	0.553	-0.113	-1.171	0
NA	DV774846	-1.491	-1.491	0.076	0.791	0.001
NA	DV774879	-5.636	-6.501	-8.289	-8.632	0
DNA photolyase [*Nasonia vitripennis*]	DV774883	0.405	0.331	1.122	1.963	0.001
NA	DV774915	-3.149	-3.393	-4.636	-4.307	0.001
NA	DV774929	3.636	2.790	1.903	2.087	0
NA	DV775066	0.014	0.629	0.809	2.632	0.001
hypothetical protein [*Tribolium castaneum*]	FF277324	3.281	2.342	1.556	2.584	0
NA	EG948624	3.207	3.346	2.548	4.418	0
clotting protein precursor [*Pacifastacus leniusculus*]	FE044029	-0.504	-0.591	1.186	1.729	0.001
FUN14 family protein [*Ixodes scapularis*]	FE841492	2.008	0.773	1.373	2.462	0.001
NA	EG948713	-1.095	-0.151	1.460	1.228	0
NA	EG948731	0.617	0.710	1.521	2.906	0.001
NA	EG948742	2.039	1.440	0.287	1.776	0
NA	EG948814	2.734	1.786	2.168	6.091	0.001
ribosomal protein S25 [*Ixodes scapularis*]	FC556272	-4.760	-4.099	-3.158	-2.538	0
NA	EG948889	0.457	0.252	1.169	2.276	0.001
ferredoxin-NADP reductase [*Ornithorhynchus anatinus*]	EG949165	-0.289	-0.161	0.180	2.496	0
NA	FD467988	-3.990	-3.679	-5.418	-5.455	0
NA	EG949035	0.040	-0.164	-0.857	0.550	0.001
NA	EG949155	5.124	4.135	1.773	3.045	0
NA	EG949353	1.753	1.293	-0.294	4.700	0
NA	EG949428	0.558	0.234	1.405	10.292	0.001
NA	EG949470	-0.056	-0.208	1.425	2.524	0.001
DNA methyltransferase [*Danio rerio*]	EG949465	-1.755	-1.768	-2.980	-2.730	0.001
NA	EG949556	1.805	0.996	1.404	2.536	0
NA	EY116674	-1.343	-1.741	-2.880	-2.887	0.001
ribosomal protein S5 isoform 1 [*Apis mellifera*]	FD467527	-4.051	-4.047	-3.535	-2.882	0
Endonuclease G like 1 (Endo G like) [*Canis familiaris*]	FE043954	2.429	1.331	0.314	2.135	0.001
NA	EH034703	1.338	1.531	1.699	3.762	0.001
NA	EH034826	-0.099	-0.659	-0.077	1.541	0.001
hypothetical protein AaeL_AAEL009759 [*Aedes aegypti*]	EH034863	2.363	0.211	0.010	0.138	0.001
uroporphyrinogen decarboxylase isoform 9 [*Pan troglodytes*]	FF277645	-0.970	-0.991	-2.608	-2.810	0
NA	EH034955	-0.157	-0.329	-1.537	-1.376	0
NA	EH035000	0.557	0.485	1.774	0.957	0
NA	FC071715	1.201	0.719	1.225	3.316	0.001
NA	EH035204	0.407	-0.364	-0.103	2.140	0
missing oocyte CG7074-PA [*Tribolium castaneum*]	EH035322	3.968	2.481	2.047	3.274	0.001
NA	FE535190	1.184	-0.039	1.624	2.620	0
NA	FE535238	-0.223	-0.475	-0.791	1.453	0.001
NA	EH035393	-1.543	-1.044	-2.475	-1.945	0.001
reticulocalbin [*Aedes aegypti*]	EH035407	1.184	1.672	3.516	2.994	0.001

NA	EH035639	-0.660	-1.129	-2.208	-2.359	0
NA	FC071384	0.494	0.039	0.605	1.447	0
NA	EH115974	3.802	1.783	-0.557	0.197	0
NA	EH116110	4.330	2.524	1.462	1.700	0
predicted protein [Nematostella vectensis]	EH116277	-0.241	0.186	2.924	2.610	0.001
inosine monophosphate dehydrogenase 1 isoform b [Homo sapiens]	EH116330	-0.422	-0.721	-0.736	0.775	0
NA	EH116364	-3.522	-2.958	-4.825	-4.568	0.001
NA	EH116481	-1.478	-2.036	-3.066	-3.607	0
ubiquitin carboxyl-terminal hydrolase FAF-X (Ubiquitin thioesterase FAF-X) (Ubiquitin-specific-processing protease FAF-X) (Deubiquitinating enzyme FAF-X) (Fat facets protein-related, X-linked) (Ubiquitin-specific protease 9, X chromosome)	FF277155	0.637	1.578	2.078	2.102	0
NA	EH116502	1.506	1.484	0.290	1.149	0
NA	EH116621	0.772	1.177	1.788	2.876	0.001
4-nitrophenylphosphatase [*Tribolium castaneum*]	EH116640	1.329	1.383	2.530	3.596	0
uty-prov protein [*Tribolium castaneum*]	EH116641	0.854	1.488	1.541	5.398	0
NA	EH116668	-0.539	-0.460	-0.090	1.569	0.001
cyclin J [*Culex quinquefasciatus*]	FE535347	0.561	0.875	2.182	2.886	0.001
NA	FD468205	1.988	1.960	2.454	4.082	0
NA	FD585193	1.277	0.920	1.156	2.931	0
NA	EH117190	1.358	2.645	2.933	16.649	0.001
PEST-containing nuclear protein (PCNP) [*Apis mellifera*]	FD483617	1.797	1.318	0.556	1.785	0
btb poz domain containing protein 9 OR CG7102 CG7102-PA [*Acyrthosiphon pisum*]	EH401283	-0.961	-1.422	-0.214	1.159	0.001
Coatomer subunit alpha (Alpha-coat protein) (Alpha-COP) [Contains: Xenin (Xenopsin-related peptide); Proxenin]	FD699435	2.743	1.950	1.449	2.649	0.001
NA	EH401378	-0.045	-0.024	1.125	1.103	0.001
NA	EH401482	-1.467	-2.091	-3.874	-3.693	0.001
NA	EH401537	-0.955	-0.421	-0.059	-0.061	0
gamma-glutamyl hydrolase, [*Nasonia vitripennis*]	FE535936	2.013	1.518	1.826	3.006	0
myostatin [*Gecarcinus lateralis*]	EH401678	2.199	2.361	0.983	3.182	0
NA	EH401828	-2.599	-2.023	-1.771	-1.290	0
NA	EH401830	2.245	2.905	3.135	3.596	0.001
NA	EX568243	-0.965	-0.466	0.739	1.324	0
unknown [*Branchiostoma belcheri tsingtaunese*]	EX568289	-4.189	-3.639	-5.521	-5.325	0.001
tubulointerstitial nephritis antigen [*Tribolium castaneum*]	EV781623	2.956	2.657	2.069	2.821	0.001
exonuclease domain containing 1 [*Macaca mulatta*]	EV781701	-1.894	-2.195	-3.627	-3.559	0.001
NA	EV781703	-1.420	-1.320	-2.898	-2.606	0.001
NA	EV781863	0.123	-0.392	-0.257	0.953	0.001
NA	EV782038	-0.639	-0.959	-0.876	0.069	0
60S ribosomal protein L27a [*Apis mellifera*]	FD483474	-4.054	-3.615	-2.955	-3.101	0.001
CG8320-PA [*Apis mellifera*]	EX486490	-0.576	-0.180	-1.751	-0.675	0.001
NA	EV782090	-1.985	-1.820	-3.364	-3.760	0.001
ankyrin repeat-rich membrane-spanning protein [*Aedes aegypti*]	EV782122	-0.990	-1.036	1.130	2.502	0.001
NA	EV782127	-1.337	-2.049	-3.236	-2.769	0.001
Metalloreductase STEAP3 (Six-transmembrane epithelial antigen of prostate 3) (pHyde)	EW702569	2.631	1.172	2.597	4.909	0
NA	EW702600	0.105	0.376	0.659	1.975	0
ubiquitin-activating enzyme E1C isoform 2 [*Monodelphis domestica*]	EW702602	4.101	3.021	2.363	3.053	0
NA	EY116834	1.126	0.717	1.523	2.767	0.001
NA	FE659968	-3.550	-3.948	-1.994	-1.701	0
NA	EW702753	2.306	1.497	-0.205	1.895	0
NA	EW702922	0.601	0.095	0.881	1.759	0.001
NA	EW702961	2.825	3.084	2.281	3.515	0
NA	EX827419	-2.702	-0.896	-1.978	-1.811	0
IP15312p [*Tribolium castaneum*]	EW702980	-0.353	-0.483	0.046	1.620	0
NA	EW703042	2.458	1.705	1.124	2.568	0
NA	FE535184	2.009	1.740	0.469	1.066	0.001
NA	EW703143	1.175	1.408	1.722	5.277	0.001
X-prolyl aminopeptidase (aminopeptidase P) 3, [*Bos taurus*]	FE660125	0.439	0.472	1.419	3.073	0.001

NA	EW997693	-1.908	-1.454	-0.996	-0.043	0.001
tigger transposable element derived 2 [*Equus caballus*]	FE535051	-1.723	-1.640	-0.871	0.604	0.001
Mitochondrial import inner membrane translocase subunit Tim9 [*Apis mellifera*]	EW997727	-0.554	-0.780	-1.819	-1.235	0
glycerate kinase [*Danio rerio*]	EW997728	0.919	1.101	0.894	4.100	0.001
NA	EW997871	0.111	0.794	1.819	2.028	0.001
NA	FE659594	0.330	0.538	-0.729	-0.842	0.001
NA	EW997956	-3.302	-3.589	-5.314	-4.385	0
congenital dyserythropoietic anemia type I (human) [*Nasonia vitripennis*]	FC071666	-0.008	-0.547	0.786	1.660	0.001
NA	EX487656	0.192	-0.087	0.057	1.790	0
Nitrilase homolog 2 [*Equus caballus*]	EW998098	-1.567	-1.694	-0.702	0.284	0
NA	EW998109	1.155	1.088	0.814	2.305	0.001
NA	EW998158	-1.457	-2.500	-4.049	-4.567	0
CG3726 CG3726-PA [*Drosophila melanogaster*]	EX471042	2.184	1.993	1.204	2.078	0
conserved hypothetical protein [*Culex quinquefasciatus*]	EX568171	-3.854	-3.956	-5.049	-4.837	0.001
alanine racemase [Clostridium cellulolyticum H10]	EX471545	5.096	3.635	2.455	3.529	0.001
GF12962 [*Drosophila ananassae*]	EX471753	1.932	1.550	0.385	2.334	0
regulator of g protein signaling [*Aedes aegypti*]	EX486591	1.888	2.094	2.287	3.514	0.001
NA	FC556342	-1.187	-1.195	0.454	27.802	0
NA	EX486741	-2.184	-3.051	-3.827	-3.635	0.001
mitochondrial ribosomal protein S2 CG2937-PA [*Drosophila melanogaster*]	EX486758	-0.751	-1.946	-1.420	-1.160	0
NA	EX486849	-1.981	-1.670	-3.014	-3.056	0
NA	EX487561	2.272	1.337	0.957	1.822	0
Epac CG34392-PD, isoform D [*Drosophila melanogaster*]	EX487042	0.651	-0.620	1.496	1.375	0
NA	EX487073	-0.241	-0.267	-1.528	-1.349	0.001
ribosomal protein L28-like protein [*Maconellicoccus hirsutus]*	FE841076	-4.742	-4.329	-3.840	-3.521	0
NA	EX487218	3.493	2.229	1.383	2.183	0
"SAM domain, SH3 domain and nuclear localization signals, 1 [*Mus musculus*]"	EX487280	0.878	1.566	2.176	2.965	0
NA	EX487365	-1.596	-1.834	-0.534	0.163	0
NA	EX487400	0.325	1.098	0.645	1.181	0.001
NA	EX487486	-0.400	-0.175	0.361	1.611	0
ADP-ribosylation-like factor 6 interacting protein 5 [*Bos taurus*]	GE298727	-2.858	-3.401	-4.222	-4.084	0
hypothetical protein, conserved [*Entamoeba histolytica* HM-1:IMSS]	EX487689	-0.772	-0.771	0.406	0.828	0
NA	EX487814	0.746	0.920	0.149	0.002	0.001
NA	EX568071	-3.050	-5.801	-2.155	-0.901	0
NA	EX568572	-2.599	-3.079	-3.936	-4.221	0.001
NA	EX568495	-0.509	-0.953	-2.304	-1.958	0
NA	EX568544	0.366	-0.904	-1.245	1.533	0.001
aquaporin [*Culex quinquefasciatus*]	EX568605	-1.265	-1.570	-2.314	-1.943	0
NA	FE660178	1.619	1.605	2.123	5.534	0.001
NA	FE535799	0.739	1.119	1.136	2.922	0.001
zinc\iron transporter [*Culex quinquefasciatus*]	EX827171	-2.827	-2.629	-1.371	-0.053	0
MGC84305 protein [*Strongylocentrotus purpuratus*]	EX827221	-2.333	-1.705	-1.071	-0.549	0
NA	EX827277	1.253	1.119	-0.177	1.526	0.001
NA	EX827382	-1.738	-2.707	-3.781	-3.793	0.001
NA	EX827475	1.938	1.222	0.887	0.606	0
NA	EY116749	3.341	2.483	2.415	1.966	0
NA	EY116891	1.359	1.690	0.795	0.865	0
NA	EY116914	0.086	0.439	0.859	3.400	0
MRP-like ABC transporter [*Arabidopsis thaliana*]	EY116994	5.180	3.209	1.424	3.392	0
lens epithelium-derived growth factor [*Mus musculus*]	FF277208	0.509	0.525	-0.082	0.872	0
novel protein [*Danio rerio*]	EY117070	0.953	0.400	0.240	1.209	0.001
NA	FD699114	-1.371	-1.668	-0.537	0.619	0.001
NA	EY117182	-0.275	-0.686	-0.357	0.383	0
Chitobiase, di-N-acetyl- [*Danio rerio*]	FD699488	2.955	1.900	0.790	0.897	0.001
GG10667 [*Drosophila erecta*]	EY117228	-1.475	-0.995	0.263	-0.551	0
NA	EY117286	1.104	0.460	1.838	0.975	0

NA	EY117307	-2.541	-2.907	-4.215	-4.164	0
ribosomal protein rpl17 [*Arenicola marina*]	EY117358	-4.242	-3.928	-3.511	-3.305	0.001
NA	EY290738	2.282	1.225	0.756	2.141	0.001
barrier-to-autointegration factor B [*Tribolium castaneum*]	EY290876	-6.430	-6.461	-7.410	-7.021	0.001
tRNA phosphotransferase 1 [*Danio rerio*]	FF277106	0.906	0.122	-1.678	-1.259	0.001
NA	EY291089	2.158	2.514	1.508	2.352	0.001
NA	EY291124	1.431	1.165	1.766	2.587	0
NA	EY291187	4.674	1.963	1.463	1.937	0.001
NA	FD467315	-1.910	-2.220	-1.533	-0.664	0.001
NA	FF277409	1.608	0.923	2.051	2.757	0.001
gamma-butyrobetaine hydroxylase [*Danio rerio*]	EY291424	4.077	3.475	1.862	2.707	0.001
ATP-binding cassette, sub-family A (ABC1), member 5 [*Apis mellifera*]	EY291425	1.216	0.360	0.303	0.884	0.001
NA	FC071259	-1.710	-1.407	-0.536	0.808	0.001
NA	FC071357	4.093	3.479	2.564	3.867	0
dynein heavy chain [*Aedes aegypti*]	FC071365	0.552	0.776	1.081	2.326	0
NA	FC071415	-2.584	-2.728	-4.393	-3.568	0
NA	FC071485	0.217	0.196	-1.558	-2.035	0
NA	FC071740	-1.191	-1.762	-3.176	-2.595	0
broad [*Oncopeltus fasciatus*]	FF278034	0.440	0.771	1.252	1.898	0.001
NA	FC071953	1.540	0.653	0.624	2.259	0.001
NA	FC555990	-2.334	-3.149	-4.524	-4.658	0.001
ADP-ribosylation factor-like 2 binding protein isoform 1 [*Canis familiaris*]	FC556116	2.556	2.563	1.587	25.604	0
beclin-1 *[Acyrthosiphon pisum*]	FC556268	0.481	-0.140	1.028	0.276	0
NA	FC556301	-2.250	-2.597	-3.127	-3.618	0.001
NA	FC556329	3.865	2.950	2.081	3.483	0
cysteine dioxygenase [*Tribolium castaneum*]	FC556339	3.745	3.221	2.528	2.391	0.001
NA	FC556393	-0.927	-1.836	-0.238	0.022	0.001
NA	FE841266	-2.657	-2.972	-1.782	-1.187	0
NA	FC556505	2.998	2.714	2.207	3.576	0.001
NA	FC556519	-0.849	-1.621	-3.035	-2.800	0.001
NA	FC556556	0.913	1.700	1.922	1.806	0.001
NA	FC556730	-0.487	-0.854	-2.128	-2.158	0.001
NA	FD425469	3.017	2.599	1.654	3.048	0
NA	FD467432	-3.506	-3.785	-5.590	-5.590	0
NA	FD467548	0.516	0.297	-0.715	0.061	0
NA	FD467794	0.511	-1.230	-0.932	-0.587	0
NA	FD467905	-2.000	-2.413	-4.143	-4.034	0
NA	FD467941	-1.494	-1.764	-0.869	-0.380	0.001
NA	FD467945	-0.037	-0.858	-0.417	0.722	0
ubiquitin-protein ligase [*Nasonia vitripennis*]	FD585166	-0.736	-1.563	0.109	1.646	0.001
CG14972-PA [*Apis mellifera*]	FD467977	0.736	0.530	1.417	8.868	0.001
NA	FD483724	-1.830	-1.285	-3.485	-3.412	0.001
CCAAT\enhancer-binding protein gamma (C\EBP gamma) (Immunoglobulin enhancer-binding protein 1) (IG\EBP-1) (Granulocyte colony-stimulating factor promoter element 1-binding protein) (GPE1-binding protein) (GPE1-BP) [*Apis mellifera*]	FD468001	0.999	0.639	-0.489	0.411	0
NA	FD468008	-0.386	0.493	0.526	2.113	0
NA	FD468066	-1.203	-0.007	0.660	1.082	0.001
f-spondin [*Tribolium castaneum*]	FD468074	3.511	3.282	2.259	2.257	0.001
NA	FD468137	1.548	-0.368	-0.677	0.171	0
cytoplasmic carbonic anydrase [*Callinectes sapidus*]	FE043957	-1.466	-1.022	0.520	0.499	0.001
NA	FD468174	-0.778	-0.591	-2.768	-2.432	0
transcription factor Elk [*Strongylocentrotus purpuratus*]	FD483016	2.579	1.960	1.482	2.771	0.001
NA	FD483025	-1.874	-2.311	-3.297	-3.519	0.001
NA	FD483046	-3.172	-3.266	-5.147	-4.925	0.001
NA	FD483062	-3.023	-3.022	-1.515	-1.202	0.001
NA	FD483072	-1.407	-0.848	-0.476	-0.146	0.001
hypothetical protein AaeL_AAEL001300 [*Aedes aegypti*]	FD483184	-0.147	-0.630	0.386	1.452	0
NA	FD483203	1.813	1.580	1.568	5.873	0.001
Titin (Connectin) (Rhabdomyosarcoma antigen MU-RMS-40.14) [*Danio rerio*]	FD483354	-1.043	-1.374	0.028	1.757	0
solute carrier family 5 (sodium\glucose	FD483413	-3.686	-3.297	-4.378	-4.096	0.001

cotransporter), member 9 [*Strongylocentrotus purpuratus*]						
NA	FD584637	2.109	1.419	0.461	2.464	0
cytochrome P450 1C2 [*Strongylocentrotus purpuratus*]	FD483465	2.155	1.301	0.402	1.067	0
NA	FD483503	2.433	2.770	2.511	3.806	0.001
NA	FD483573	-0.493	-0.576	-2.298	-2.244	0.001
pyruvate dehydrogenase [*Tribolium castaneum*]	FD483648	-0.403	0.699	1.242	2.209	0.001
NA	FD483728	0.532	0.757	1.199	1.777	0
NA	FD483738	-1.630	-1.439	-3.492	-3.288	0
NA	FD483764	-2.611	-3.440	-4.370	-4.807	0
NA	FD483765	1.040	0.977	0.043	0.817	0
NA	FE535232	2.387	1.739	0.844	1.793	0
NA	FE044167	1.866	2.122	1.092	9.160	0
NA	FD584926	2.981	2.329	1.190	2.284	0
NA	FD584983	-3.795	-3.471	-4.853	-4.549	0
NA	FD585035	-0.412	-1.037	-2.235	-2.279	0
NA	FD585062	0.280	-0.612	-0.640	1.401	0
NA	FD585073	-1.629	-1.458	-0.418	0.296	0
NA	FD585074	3.166	1.230	0.566	1.797	0.001
NA	FD585080	2.161	1.906	-0.242	1.294	0
NA	FD585096	-1.633	-1.521	-3.195	-2.312	0
NA	FD585310	3.162	0.421	-0.150	1.066	0.001
NA	FD585379	-1.790	-2.085	-3.498	-2.661	0
CG3308-PA [*Apis mellifera*]	FD585426	2.156	2.095	1.377	2.608	0.001
NA	FD585440	-1.313	-1.753	-0.704	0.003	0.001
unkempt homolog-like [*Acyrthosiphon pisum*]	FD699065	3.477	2.231	1.683	1.400	0.001
mitochondrial ribosomal protein L37 CG6547-PA [*Drosophila melanogaster*]	FD699222	0.954	-0.813	-1.326	-0.424	0
synaptic vesicle glycoprotein 2 a [*Mus musculus*]	FD699238	0.308	0.108	-0.418	17.177	0.001
NA	FD699255	0.182	-0.158	0.626	2.046	0.001
NA	FD699344	1.485	1.570	1.411	2.757	0.001
NA	FD699556	1.754	0.777	1.592	3.184	0
NA	FD699563	-0.940	-0.730	-0.259	0.219	0.001
Trifunctional purine biosynthetic protein adenosine-3	FE659479	2.027	1.115	0.822	1.991	0.001
NA	FD699775	2.601	1.648	0.687	1.569	0.001
NA	FD699809	-1.926	-2.015	-1.183	0.967	0.001
NA	FD699911	0.916	0.531	0.092	1.378	0
NA	FD699929	2.495	1.255	0.634	0.579	0
NA	FE043534	0.976	0.982	0.063	-0.138	0
NA	FE043577	-1.401	-1.421	-2.368	-2.417	0.001
N(2),N(2)-dimethylguanosine tRNA methyltransferase (tRNA(guanine-26,N(2)-N(2)) methyltransferase) (tRNA 2,2-dimethylguanosine-26 methyltransferase) (tRNA(m(2,2)G26)dimethyltransferase) [*Acyrthosiphon pisum*]	FE043626	-1.120	-1.446	-2.200	-0.578	0
NA	FE043691	0.211	-0.552	-0.480	0.356	0.001
Ubiquitin thiolesterase protein OTUB1 (Otubain 1) (OTU domain-containing ubiquitin aldehyde-binding protein 1) (Ubiquitin-specific processing protease OTUB1) (Deubiquitinating enzyme OTUB1) [*Canis familiaris*]	FE043713	2.931	2.249	1.624	1.975	0
NA	FE043896	-1.610	-2.070	-3.422	-3.288	0.001
NA	FE043907	-2.214	-3.321	-4.028	-4.777	0
NA	FE043940	-1.780	-1.311	-2.652	-2.812	0.001
NA	FE043974	3.155	2.448	1.263	2.167	0
CG4768-PA [*Apis mellifera*]	FE044198	0.809	0.206	0.371	1.666	0.001
NA	FE044235	-0.456	1.330	1.055	-0.191	0.001
NA	FE044267	-2.216	-2.840	-3.643	-3.792	0.001
NA	FE535136	2.739	1.975	0.384	1.022	0
NA	FE535257	-0.604	-0.676	-1.017	-2.242	0
NA	FE535268	3.027	2.717	1.659	2.467	0.001
NA	FE535434	1.452	0.941	-0.698	-0.787	0
Zinc finger protein 84 (Zinc finger protein HPF2) [*Apis mellifera*]	FE535551	2.006	1.611	1.071	0.693	0
NA	FE535647	-5.622	-4.592	-4.219	-3.578	0.001
NA	FE535795	3.223	3.378	2.165	3.082	0.001
angiomotin [*Tribolium castaneum*]	FE535796	-4.690	-4.497	-5.437	-5.774	0

prostaglandin E synthase 2 [*Tribolium castaneum*]	FE535887	2.662	1.506	0.680	2.216	0
asparagine-linked glycosylation 10 homolog B (yeast, alpha-1,2-glucosyltransferase) [*Rattus norvegicus*]	FE535905	-0.322	-1.176	-1.968	-1.011	0
NA	FE535920	5.116	3.464	2.531	3.517	0
oxysterol binding protein-like 1A [*Danio rerio*]	FE659606	-3.562	-2.815	-1.450	-1.326	0
Replication protein A1, 70kDa [*Ornithorhynchus anatinus*]	FE659616	-2.448	-2.245	-3.658	-4.218	0
NA	FE659700	-0.268	0.315	0.962	1.568	0.001
NA	FE659705	-0.725	-0.903	-0.537	0.418	0.001
NA	FE659910	5.671	2.746	-2.332	2.002	0.001
NA	FE659947	0.373	0.048	0.338	1.000	0
NA	FE659949	0.910	0.797	0.045	0.960	0
NA	FE840828	-1.381	-1.449	-1.053	-0.211	0.001
NA	FE840841	4.005	3.258	2.144	3.002	0
NA	FE840972	-0.321	-0.250	-1.278	-0.931	0
NA	FE841036	-0.321	0.081	0.639	1.790	0
NA	FE841041	2.208	1.606	1.184	2.341	0
DNA-directed RNA polymerases I, II, and III subunit RPABC5 (RNA polymerases I, II, and III subunit ABC5) (RPB10) [*Acyrthosiphon pisum*]	FE841044	-0.460	-1.027	-1.411	-0.572	0.001
NA	FE841238	3.217	2.638	1.022	3.583	0
GM14540 [*Drosophila sechellia*]	FE841445	0.897	1.524	1.587	2.266	0
CG30118-PA [*Apis mellifera*]	FE841484	-0.777	-0.590	0.449	1.093	0
six transmembrane epithelial antigen of the prostate 2 [*Danio rerio*]	FE841506	-0.991	-1.755	-2.774	-3.224	0
myosin heavy chain kinase [*Dictyostelium discoideum* AX4]	FF277133	-0.702	-0.346	-1.941	-1.625	0
NA	FF277313	-1.421	-1.270	-2.732	-2.425	0
delta-9 desaturase 1 [*Nasonia vitripennis*]	FF277319	1.830	1.602	0.684	1.445	0
acheron [*Manduca sexta*]	FF277338	0.134	-0.688	0.150	1.751	0
NA	FF277340	2.974	1.948	0.624	3.011	0
NA	FF277855	2.663	2.067	0.601	1.498	0
NA	FF277875	3.241	2.539	2.175	2.830	0.001
NA	FF277877	4.669	3.864	2.626	2.460	0
NA	FF278041	2.339	2.242	1.421	0.876	0.001
Deoxycytidylate deaminase (dCMP deaminase) [*Strongylocentrotus purpuratus*]	CN852918	1.297	1.673	2.141	3.840	0.001
NA	FE841384	-1.872	-2.107	-0.521	0.516	0.001
CG9987-PA [*Apis mellifera*]	CN854044	0.558	0.406	1.246	1.990	0
Rpl23a protein [*Pan troglodytes*]	FF278016	-3.705	-3.805	-2.907	-1.896	0.001
ENSANGP00000025789 [*Anopheles gambiae* str. PEST]	CN951259	2.140	2.479	4.020	4.924	0.001
hypothetical protein XP_425606 [*Gallus gallus*]	CN951549	-0.144	-0.272	1.272	1.864	0.001
histidine ammonia lyase [*Mus musculus*]	CN951708	1.060	1.446	2.613	3.206	0.001
general transcription factor IIH, polypeptide 2, partial [*Strongylocentrotus purpuratus*]	CN951116	2.599	3.045	2.840	4.135	0
hypothetical protein RUMGNA_02189 [*Ruminococcus gnavus* ATCC 29149]	CN949905	-1.194	-0.392	0.183	1.401	0.001
minor ampullate silk protein MiSp1 [*Nephila clavipes*]	DV773512	1.337	2.195	3.231	4.598	0.001
NA	DV774469	-0.200	0.779	2.363	3.268	0.001
ribosomal protein, large P2 [*Danio rerio*]	CN950042	-4.216	-3.694	-2.633	-2.550	0
hypothetical protein LOC507035 [*Bos taurus*]	EH035144	-1.630	-1.922	-0.106	0.718	0
NA	CN853291	-2.302	-1.805	-0.449	0.059	0.001
jerky homolog-like isoform 2 [*Bos taurus*]	FE043863	1.128	-0.018	1.705	2.719	0
superkiller viralicidic activity 2 (S. cerevisiae homolog)-like [*Danio rerio*]	EX486661	0.254	1.839	2.989	4.491	0
NA	DV771822	-1.041	-0.051	1.162	1.719	0
DIS3 mitotic control homolog (S. cerevisiae)-like 2 [*Equus caballus*]	FE660033	0.984	0.959	2.192	2.110	0.001
negative elongation factor B [*Culex quinquefasciatus*]	FE840893	0.678	-0.422	0.079	2.142	0
NA	FD585206	-0.652	-0.266	1.016	2.099	0
G protein beta subunit-like [*Danio rerio*]	FE841302	1.459	1.646	1.637	3.523	0.001
prophenoloxidase [*Homarus americanus*]	CN952203	0.782	2.042	1.990	4.004	0.001
hypothetical protein TRIADDRAFT_55610 [*Trichoplax adhaerens*]	FE043581	2.620	1.736	1.985	3.281	0
Glyoxylase 1 [*Gallus gallus*]	FF277579	-0.137	0.569	1.271	2.828	0

NA	FC071644	1.573	1.100	1.440	3.380	0.001

Table D.6: Significantly differentially expressed genes identified in WSSV infected *Homarus americanus* at each temperature two-weeks PI using a one-way ANOVA with α=0.001.

Data are reported as mean $\log_2$ expression ratios of sample/reference.

Gene Name	Accession #	10 °C	15 °C	17.5 °C	20 °C	p-value
amyotrophic lateral sclerosis 2 (juvenile) chromosome region, candidate 8 [*Bos taurus*]	EW997950	0.999	1.140	2.039	-0.597	0.001
metallo-beta-lactamase, [*Aedes aegypti*]	FE660133	0.433	0.493	-0.201	2.302	0
protein phosphatase 2a, regulatory subunit [*Aedes aegypti*]	FD584510	1.058	0.477	0.825	-0.569	0.001
UNC93A protein [*Aedes aegypti*]	EH117134	0.240	-0.855	0.148	-1.253	0.001
beta-N-acetylglucosaminidase [*Fenneropenaeus chinensis*]	EW998213	-3.496	-3.799	-5.218	-4.664	0.001
crustin-like protein fc-1 [*Fenneropenaeus chinensis*]	EY291018	-1.079	-1.156	-1.630	-3.185	0
defective in cullin neddylation protein [*Tribolium castaneum*]	FD585354	-0.408	0.607	-2.284	2.505	0.001
DH dehydrogenase [*Culex quinquefasciatus*]	DV774383	-1.646	-2.079	-2.454	-3.061	0.001
DH dehydrogenase subunit 5 [*Pseudocarcinus gigas]*	FF277865	-1.699	-1.224	-2.569	-3.118	0
endomembrane protein emp70 [*Tribolium castaneum*]	EX487295	-3.657	-3.895	-4.363	-4.709	0
f-spondin [*Tribolium castaneum*]	FD468074	3.908	3.777	2.315	3.345	0
glutamate dehydrogenase [*Litopenaeus vannamei*]	EX471784	2.950	3.070	2.904	4.991	0
golgi-specific brefeldin A-resistance guanine nucleotide exchange factor 1 [*Strongylocentrotus purpuratus]*	FD585004	-0.084	0.362	-0.011	6.042	0
hypothetical protein CBG22962 [*Caenorhabditis briggsae AF16*]	FE659717	-2.478	-2.555	-3.160	-3.626	0.001
hypothetical protein NEMVEDRAFT_v1g7830 [*Nematostella vectensis*]	FD699418	-0.286	0.202	0.266	1.523	0
LanC lantibiotic synthetase component C-like 2 [*Rattus norvegicus]*	FD584785	-0.325	-0.416	-1.787	-0.836	0.001
membrane associated guanylate kinase 2 [*Homo sapiens*]	EY291238	1.582	1.527	1.122	-2.001	0
membrane-associated ring finger (C3HC4) 3 *[Xenopus tropicalis]*	EH116299	-0.989	-1.153	-2.448	-2.990	0
mitochondrial ATP synthase alpha subunit precursor [*Toxoptera citricida*]	FD699788	-0.756	-1.202	-1.323	-2.281	0
N-6 adenine-specific D methyltransferase 2 [N*asonia vitripennis*]	CN852906	-1.166	-0.930	-0.002	9.490	0
NA	DV772530	-0.661	0.122	-0.269	-5.605	0.001
NA	FD483511	-1.662	-2.375	-3.009	-2.995	0.001
NA	FD584508	0.062	-0.026	-0.574	-1.510	0.001
NA	EY116689	-1.518	-1.509	-3.893	-3.854	0.001
NA	EY116674	-1.449	-1.688	-3.131	-2.454	0
NA	EX471451	1.219	0.961	1.296	-0.640	0
NA	FE841303	-1.750	-2.104	-2.352	-2.697	0
NA	FE535406	-1.586	-1.970	-2.988	-4.345	0.001
NA	EX827414	3.351	2.685	2.901	-0.323	0
NA	EH116687	1.735	1.785	-1.354	0.186	0
NA	EV781700	-0.887	-1.396	-1.378	-2.458	0.001
NA	FE043534	1.115	0.609	0.114	-0.219	0
NA	EY290613	0.770	0.164	0.241	-0.433	0
NA	EX487869	-2.512	-2.769	-3.663	-3.249	0.001
NA	EY291364	0.936	0.487	1.245	-0.386	0.001
NA	EX471122	-0.085	-0.695	-0.106	-1.288	0
NA	FE659740	0.446	-0.073	0.394	-0.693	0.001
NA	EH401783	0.957	0.097	0.181	-1.093	0
NA	EH116342	1.037	0.608	0.566	-0.259	0
NA	EX487073	0.110	-0.473	-1.516	-1.799	0
NA	CN950229	2.776	2.108	0.232	0.097	0
NA	CN951967	-0.986	-0.419	0.278	-3.034	0
NA	EG948737	1.443	0.548	-1.048	-1.986	0.001

NA	FD483046	-3.157	-3.645	-5.227	-4.602	0
NA	EH116110	3.170	3.058	1.278	1.636	0
NA	FC071758	-1.054	-1.165	-2.859	-3.335	0
NA	FC071225	-0.481	-0.118	-2.095	-1.286	0
NA	EH035207	-2.465	-2.991	-4.300	-4.081	0.001
NA	EH116317	-2.193	-2.473	-3.845	-3.870	0
NA	EY117133	-3.226	-3.467	-4.836	-4.838	0
NA	EY290828	1.626	0.478	0.969	-2.219	0
NA	EX471625	2.143	1.438	-0.494	-0.865	0.001
NA	CN951543	1.461	2.196	2.678	3.304	0.001
NA	EX486852	1.403	1.657	1.465	5.191	0
NA	EY290958	-2.634	-3.277	-3.110	-3.385	0.001
NA	EH035642	-2.363	-2.524	-3.519	-8.431	0
NA	CN854448	-0.831	-1.265	-0.432	4.188	0.001
NA	DV774072	-3.073	-2.769	-1.662	-0.937	0.001
NA	FD699846	-0.312	0.088	0.500	3.922	0.001
NA	DV774419	-0.646	-0.894	-1.836	-0.463	0.001
NA	FE043732	-0.654	-0.872	-0.841	-2.097	0
NA	EW702888	2.114	2.193	1.272	1.557	0.001
NA	DV773202	-0.413	-0.750	-1.598	-1.963	0
NA	EX486992	4.379	4.422	4.162	17.685	0.001
Negative elongation factor E	FE535654	0.058	-0.621	-0.751	-1.204	0
pontin [*Tribolium castaneum*]	FD483812	-1.324	-1.483	-0.818	-2.113	0.001
pontin [*Tribolium castaneum*]	FD467494	2.502	3.135	3.443	6.833	0
predicted protein [*Nematostella vectensis*]	FF277649	-0.642	-0.677	-1.231	-1.868	0
rho-type GTPase activating protein [*Tribolium castaneum*]	FD584832	2.902	3.125	0.814	1.313	0.001
ribosomal protein S24 [*Marsupenaeus japonicus*]	EX827155	-2.972	-2.570	-2.528	0.091	0
sec1 family domain containing 2 [*Danio rerio*]	FE044283	1.068	1.265	1.314	5.897	0
sterile alpha motif domain containing 4 isoform 1 [*Monodelphis domestica]*	EY291033	0.250	0.563	0.467	-6.789	0
transmembrane domain protein regulated in adipocytes [*Apis mellifera*]	FD467407	-0.231	-0.624	-0.433	5.401	0
Ubiquinol-cytochrome c reductase complex chaperone CBP3 homolog	EH034842	0.458	0.783	0.277	2.694	0.001
ubiquitin [*Monodelphis domestica*]	DV771037	-1.968	-2.017	-1.666	1.310	0.001

APPENDIX E

Table E.1: K-means cluster 1 containing significantly differentially expressed genes for infected *Homarus americanus* sampled two-weeks PI across all four experimental temperatures (10 °C, 15 °C, 17.5 °C, 20 °C)

Significantly differentially expressed genes identified via one-way ANOVA with α=0.001. Fold change in expression represents average $\log_2$ expression ratios of sample/ref. Data are normalized to 10 °C.

Gene name	Accession #	10 °C	15 °C	17.5 °C	20 °C	p-value
NA	FC071225	0	0.363	-1.614	-0.804	0.001
NA	EH035207	0	-0.526	-1.836	-1.616	0.001
NA	EH116110	0	-0.113	-1.892	-1.534	0.001
NA	EX487869	0	-0.258	-1.152	-0.737	0.001
NA	FD483046	0	-0.488	-2.069	-1.445	0.001
NA	EH116317	0	-0.280	-1.652	-1.677	0.001
NA	EX487073	0	-0.583	-1.627	-1.909	0.001
NA	FE043534	0	-0.505	-1.000	-1.334	0.001
NA	EY117133	0	-0.241	-1.610	-1.613	0.001
NA	FD483511	0	-0.713	-1.347	-1.333	0.001
NA	DV773202	0	-0.336	-1.184	-1.550	0.001
NA	EY116689	0	0.009	-2.375	-2.336	0.001
NA	EW702888	0	0.079	-0.841	-0.557	0.001
NA	EY116674	0	-0.239	-1.682	-1.004	0.001
LanC lantibiotic synthetase component C-like 2 [*Rattus norvegicus*]	FD584785	0	-0.092	-1.463	-0.511	0.001
beta-N-acetylglucosaminidase [*Fenneropenaeus chinensis*]	EW998213	0	-0.303	-1.722	-1.168	0.001
NA	EH116687	0	0.050	-3.089	-1.549	0.001
NA	FE841303	0	-0.354	-0.602	-0.947	0.001
rho-type GTPase activating protein [*Tribolium castaneum*]	FD584832	0	0.223	-2.088	-1.590	0.001
f-spondin [*Tribolium castaneum*]	FD468074	0	-0.131	-1.593	-0.563	0.001

Table E.2: K-mean cluster 2 containing significantly differentially expressed genes for infected *Homarus americanus* sampled two-weeks PI across all four experimental temperatures (10 ^{o}C, 15 ^{o}C, 17.5 ^{o}C, 20 ^{o}C).

Significantly differentially expressed genes identified via one-way ANOVA with α=0.001. Fold change in expression represents average $\log_2$ expression ratios of sample/ref. Data are normalized to 10 ^{o}C.

Gene Name	Accession #	10 ^{o}C	15 ^{o}C	17.5 ^{o}C	20 ^{o}C	p-value
NA	EX471451	0	-0.258	0.077	-1.859	0.001
NA	EX827414	0	-0.666	-0.451	-3.674	0.001
protein phosphatase 2a, regulatory subunit [*Aedes aegypti*]	FD584510	0	-0.580	-0.233	-1.627	0.001
NA	EY290613	0	-0.606	-0.528	-1.202	0.001
UNC93A protein, [*Aedes aegypti*]	EH117134	0	-1.095	-0.091	-1.492	0.001
NA	EX471122	0	-0.611	-0.022	-1.203	0.001
NA	FE659740	0	-0.519	-0.052	-1.139	0.001
NA	EH401783	0	-0.860	-0.776	-2.050	0.001
NA	EH116342	0	-0.429	-0.471	-1.297	0.001
NA	CN951967	0	0.567	1.264	-2.048	0.001
Membrane associated guanylate kinase 2 [*Homo sapiens*]	EY291238	0	-0.055	-0.461	-3.584	0.001
NA	FE043732	0	-0.218	-0.188	-1.443	0.001
Pontin [*Tribolium castaneum*]	FD483812	0	-0.159	0.506	-0.789	0.001
amyotrophic lateral sclerosis 2 (juvenile) chromosome region, candidate 8 [*Bos taurus*]	EW997950	0	0.140	1.040	-1.596	0.001
NA	EY291364	0	-0.449	0.309	-1.322	0.001
NADH dehydrogenase [*Culex quinquefasciatus*]	DV774383	0	-0.434	-0.808	-1.415	0.001

Table E.3: K-means cluster 3 containing significantly differentially expressed genes identified for infected *Homarus americanus* sampled two-weeks PI across all four experimental temperatures (10 °C, 15 °C, 17.5 °C, 20 °C).

Significantly differentially expressed genes identified via one-way ANOVA with α=0.001. Fold change in expression represents average $\log_2$ expression ratios of sample/ref. Data are normalized to 10 °C.

Gene Name	Accession #	10 °C	15 °C	17.5 °C	20 °C	p-value
Golgi-specific brefeldin A-resistance guanine nucleotide exchange factor 1 [*Strongylocentrotus purpuratus*]	FD585004	0	0.447	0.074	6.126	0.001
Pontin [*Tribolium castaneum*]	FD467494	0	0.633	0.941	4.331	0.001
Ubiquinol-cytochrome c reductase complex chaperone CBP3 homolog	EH034842	0	0.326	-0.181	2.237	0.001
NA	EX486852	0	0.254	0.062	3.788	0.001
Metallo-beta-lactamase [*Aedes aegypti*]	FE660133	0	0.061	-0.633	1.870	0.001
N-6 adenine-specific DNA methyltransferase 2 [*Nasonia vitripennis*]	CN852906	0	0.236	1.164	10.656	0.001
Glutamate dehydrogenase [*Litopenaeus vannamei*]	EX471784	0	0.120	-0.045	2.041	0.001
sec1 family domain containing 2 [*Danio rerio*]	FE044283	0	0.197	0.246	4.830	0.001
NA	DV774072	0	0.304	1.411	2.136	0.001
NA	FD699846	0	0.401	0.812	4.234	0.001
Transmembrane domain protein regulated in adipocytes [*Apis mellifera*]	FD467407	0	-0.393	-0.202	5.632	0.001
NA	EX486992	0	0.043	-0.217	13.307	0.001
NA	CN951543	0	0.735	1.216	1.843	0.001
NA	CN854448	0	-0.434	0.399	5.019	0.001

Table E.4: K-means cluster 4 containing significantly differentially expressed genes identified for infected *Homarus americanus* sampled two-weeks PI across all four experimental temperatures (10 ^{o}C, 15 ^{o}C, 17.5 ^{o}C, 20 ^{o}C).

Significantly differentially expressed genes identified via one-way ANOVA with α=0.001. Fold change in expression represents average $\log_2$ expression ratios of sample/ref. Data are normalized to 10 ^{o}C

Gene Name	Accession #	10 ^{o}C	15 ^{o}C	17.5 ^{o}C	20 ^{o}C	p-value
NA	DV772530	0	0.782	0.392	-4.944	0.001
NA	FD584508	0	-0.088	-0.636	-1.572	0.001
sterile alpha motif domain containing 4 isoform 1 [*Monodelphis domestica*]	EY291033	0	0.312	0.216	-7.040	0.001
NA	EX471625	0	-0.705	-2.637	-3.009	0.001
NA	FE535406	0	-0.384	-1.401	-2.759	0.001
NA	EV781700	0	-0.509	-0.491	-1.570	0.001
NA	CN950229	0	-0.669	-2.544	-2.679	0.001
NA	EG948737	0	-0.895	-2.491	-3.429	0.001
NA	FC071758	0	-0.111	-1.805	-2.281	0.001
Membrane-associated ring finger (C3HC4) 3 [*Xenopus tropicalis*]	EH116299	0	-0.164	-1.459	-2.002	0.001
NA	EH035642	0	-0.161	-1.156	-6.068	0.001
NADH dehydrogenase subunit 5 [*Pseudocarcinus gigas*]	FF277865	0	0.476	-0.869	-1.418	0.001
Crustin-like protein fc-1 [*Fenneropenaeus chinensis*]	EY291018	0	-0.078	-0.551	-2.107	0.001

Table E. 5: K-means cluster 5 containing significantly differentially expressed genes identified for infected *Homarus americanus* sampled two-weeks PI across all four experimental temperatures (10 ^{o}C, 15 ^{o}C, 17.5 ^{o}C, 20 ^{o}C).

Significantly differentially expressed genes identified via one-way ANOVA with α=0.001. Fold change in expression represents average $\log_2$ expression ratios of sample/ref. Data are normalized to 10 ^{o}C

Gene Name	Accession #	10 ^{o}C	15 ^{o}C	17.5 ^{o}C	20 ^{o}C	p-value
Negative elongation factor E	FE535654	0	-0.678	-0.808	-1.261	0.001
Mitochondrial ATP synthase alpha subunit precursor [*Toxoptera citricida]*	FD699788	0	-0.446	-0.566	-1.524	0.001
Endomembrane protein emp70 [*Tribolium castaneum*]	EX487295	0	-0.238	-0.706	-1.052	0.001
Predicted protein [*Nematostella vectensis*]	FF277649	0	-0.035	-0.589	-1.226	0.001
Hypothetical protein CBG22962 [*Caenorhabditis briggsae*]	FE659717	0	-0.077	-0.682	-1.148	0.001
NA	EY290828	0	-1.148	-0.657	-3.845	0.001
NA	EY290958	0	-0.643	-0.476	-0.751	0.001

Table E. 6: K-means cluster 6 containing significantly differentially expressed genes identified for infected *Homarus americanus* sampled two-weeks PI across all four experimental temperatures (10 °C, 15 °C, 17.5 °C, 20 °C).

Significantly differentially expressed genes identified via one-way ANOVA with α=0.001. Fold change in expression represents average $\log_2$ expression ratios of sample/ref. Data are normalized to 10 °C

Gene Name	Accession #	10 °C	15 °C	17.5 °C	20 °C	p-value
Hypothetical protein NEMVEDRAFT_v1g7830 [*Nematostella vectensis*]	FD699418	0	0.488	0.552	1.809	0.001
Ribosomal protein S24 [*Marsupenaeus japonicus*]	EX827155	0	0.403	0.445	3.063	0.001
Ubiquitin [*Monodelphis domestica*]	DV771037	0	-0.049	0.301	3.278	0.001
NA	DV774419	0	-0.249	-1.190	0.183	0.001
Defective in cullin neddylation protein [*Tribolium castaneum*]	FD585354	0	1.015	-1.876	2.912	0.001